University of Thessaly

Master Thesis

Power Flow Models for Smart Grids

State of the Art

Author:
Dimitris Zimeris

Supervisor:
Manolis Vavalis

A thesis submitted in fulfilment of the requirements
for the degree of Master in Engineering

in the

Department of Electrical and Computer Engineering

October 2015

Declaration of Authorship

I, Dimitris Zimeris, declare that this thesis titled, 'Power Flow Models for Smart Grids

State of the Art' and the work presented in it are my own. I confirm that:

- This work was done wholly or mainly while in candidature for a research degree at this University.
- Where any part of this thesis has previously been submitted for a degree or any other qualification at this University or any other institution, this has been clearly stated.
- Where I have consulted the published work of others, this is always clearly attributed.
- Where I have quoted from the work of others, the source is always given. With the exception of such quotations, this thesis is entirely my own work.
- I have acknowledged all main sources of help.
- Where the thesis is based on work done by myself jointly with others, I have made clear exactly what was done by others and what I have contributed myself.

Signed: _____

Date: _____

"Thanks to my solid academic training, today I can write hundreds of words on virtually any topic without possessing a shred of information, which is how I got a good job in journalism."

Dave Barry

UNIVERSITY OF THESSALY

Abstract

School of Engineering
Department of Electrical and Computer Engineering

Master in Engineering

Power Flow Models for Smart Grids

State of the Art

by Dimitris Zimeris

The Thesis Abstract is written here (and usually kept to just this page). The page is kept centered vertically so can expand into the blank space above the title too...

Acknowledgements

The present Thesis has been co-financed by the European Union (European Social Fund ESF) and Greek national funds through the Operational Program *Education and Lifelong Learning* of the National Strategic Reference Framework (NSRF) - Research Funding Program: THALIS. Investing in knowledge society through the European Social Fund the KRIPIS project and the HEPHAESTUS Excellence Project. ...

Contents

List of Figures

List of Tables

Abbreviations

LAH **L**ist **A**bbreviations **H**ere

Physical Constants

$$\text{Speed of Light} \quad c \quad = \quad 2.997\ 924\ 58 \times 10^{8}\ \text{ms}^{-\text{S}}\ \text{(exact)}$$

Symbols

a	distance	m
P	power	W (Js^{-1})
ω	angular frequency	rads^{-1}

Dedicated to my

family

for the great support and understanding

Chapter 1

Introduction

1.1 Prologue

The electrical power system is one of the most complicated man-made systems ever developed, since it involves the participants of electric energy generation, transmission, distribution and end-using. Its scientific area, consists of a number of different sciences, physics, electrical systems analysis, stability analysis, electromagnetism, mathematics, etc. In that sense, different research issues have come apart, in an attempt to give answers about electric systems operation, analysis and control.

Electric power systems can be viewed as the expansion of electric networks described in general by R,L,C basic elements. The expansion has the meaning of the large scale nature of electric grids compared to simple electric networks. Power system analysis is an area of great importance since it concerns the daily normal, as well as, abnormal in special circumstances, operation of electric power system. This analysis aims at computing all the variables incorporated, in order to identify the system operation. Power flow analysis is the tool that offers the ability for small to large scale calculations of the involved variables. From a simple literature search this is obvious, since anyone easily realizes that power flow is the most analyzed and researched topic of electric power systems.

Power Flow Problems are not new. They have been commonly used for more than a century to operate power grids around the world and a significant amount of effort has been developed in associated research and development. Since its first appearance in the early 60's the power flow has been modified, simplified and extended in order to solve realistic world's electric systems. It's introduction was about the so called AC full power flow based on power mismatches, formulated by polar coordinates. During

the last decades, alternative formulations like the rectangular form power mismatch and more recently the current mismatch have been implemented in commercial software electric system analysis tools. Simplifications of the full AC power flow towards the fast decoupled and the DC load flow have been proved extremely helpful for implementing algorithms involving the power flow model. In the past decades conventional electric power systems utilized power flow, as a powerful tool for systems analysis. Although, recently, a new restructured electric power system has arisen, in the form of distributed generation, microgrids and finally smartgrids, the power flow problem is still there, modified even reconstructed but capable of providing all the information needed for a secure and reliable system operation.

Our efforts are surely not complete.

1.2 Thesis contribution to power flow research field

This initial version of our review effort originated from the need of our research team for solid research background on the power flow problem. Our team consists of experienced electrical engineers, computer scientists, numerical analysts and undergraduate and graduate students working on their theses. We believe that the interdisciplinarity of our team, which is in accordance with the interdisciplinarity inherent in the modern power flow analysis, pose enough challenge when trying to develop any broad and comprehensive review on the subject.

Although its importance had been recognized since the early years, when calculations were executed at hand, its major contribution has been carried out when computers took the advantage of speeding up calculations. Mathematical analysis found a very appealing research area, while numerical analysis has dominated in recent years offering great improvement in solving power flow algorithms.

Until recently the electric power grid was constructed in a way that a small number of large suppliers (that is generation plants) were delivering energy to consumers with high demand during the day and low demand during the night, were demand under a certain profile was established. However, the electric grid deregulation has changed the well-established consumer profiles, in a way that a large number of small scale generation (and storage) of power, the distributed generators, even the households themselves, typically through solar cells or batteries will be interchanging power and energy with the main electrical grid under uncertain consumer profile, due to price responsive control of electric energy, and with a larger night interaction due the charging of electric vehicles. Recently, the aforementioned reformulation of the conventional power grid, has been achieved, by

the introduction, design and implementation of the so-called microgrids leading to a new more attractive form of the smartgrid.

Our study is focused on power flow models, as they have evolved during the last twenty to thirty years. Since a large number of different power flow models, alternatives, simplifications, modifications and extensions are already established not only theoretically but as real industrial implementations, a review process obviously helps as a systematic study of the power flow phenomenon. This effort is based on the fact that the power flow model is in no sense a "terminated case", on the contrary it is our belief that it can be evolved for future use on more complex power systems.

There have been enough power flow review studies over the last years. Studies similar to ours have already appeared [1]. However, we believe that, the ne presented in this thesis is quite analytical, in an attempt to provide extended information for the majority of different alternatives. The main objective however, is the challenge of engaging power flow to modern power system analysis consisting of microgrids, smartgrids, and extended distribution systems. An approach is carried out to present the power flow problem both from the power engineering as well as the mathematical analysis viewpoint, in order to emphasize that there is a strong belief that both sides can be further researched.

This study is extended up to a point in order to serve the needs of this master thesis. However, since this study aims at presenting new numerical methods for improved power flow computations, which can not be discussed here, future expansion of this study will be presented hereafter.

1.3 Thesis Organization

The material in this thesis is organized as follows. In Chapter 2.1 we give the necessary background required and derive the basic Power Flow Problem. The first sections carry out basic characteristics of electric power systems. More specifically 2.2 gives the basic definitions of terminology commonly used for power flow analysis, while 2.3 introduces the basic laws of physics inherent to power system analysis. Section 2.4.1 initializes the power flow formulation. The various variations of the Power Flow Problem, as those originate from the different representations of the basic variables, are presented in several further subsections. In Section 2.4.2 the basic formula of the power flow is introduced, as it is the most widely used technique found in the literature. A basic alternative in terms of variables representation is next presented in 2.4.3. The above formulations constitute the basic power flow modelling procedure. Recent research efforts have proposed new power flow algorithms like the one introduced in 2.4.5 while 2.4.5.1 alternative modelling

and analysis of the typical form are given as incentives for. further reading. In the same way, subsection 2.4.6 offers the reader with interesting approaches of the power flow problem, which could be viewed as extension to new research fields relative to the main problem. In subsections 2.4.7 and 2.4.8 two of the major simplifications of the full AC NRPF are illustrated. These simplified terms, especially DC load flow, play a dominant role in power flow solvers always incorporated in industrial software tools. Both methods are also accompanied by attractive alternatives as well as, by comparisons with the full AC NRPF of others as shown in district subsections 2.4.9. Continuation power flow is presented in 2.4.12, while a new optimization approach of the power flow is introduced in subsection 2.4.13. The following sections of the specific chapter are dedicated to electric power systems issues closely related to the power flow model. In subsections 2.4.10 and 2.4.11 sensitivity as well as, contingency analysis are discussed as power flow features, crucial for power systems analysis. Finally in subsection 2.4.14 the optimal power flow theory and applications are presented in such a detail, such that the reader can approximate the basic concept and the way power flow equations approach the PF algorithm.

In Chapter 3 attractive issues arisen recently, as a consequence of the reformulation of the electric grid are discussed and related to the basic power flow problem. The size increase of electric grids is firstly presented in 3.1. Distribution systems and the related power flow models are illustrated in 3.1.1, while subsections 3.1.1.1. and 3.1.1.2. are concerned with Forward/Backward Sweep method, one of the leading algorithms for radial systems solving. Subsections 3.1.2 and 3.1.3 introduce the basic concepts of microgrids and smartgrids, two of the main new ideas of the reformed electric grid, while the power flow problem in a new advanced form is discussed. A new idea of improving electric grid performance, that is, the distributed slack bus model and its application to the power flow algorithm is presented in 3.2. Finally, in 3.3 basic concepts of daily operation of the transmission system in normal as well as abnormal conditions (congestion) are introduced and further approximated in 3.3.1 and 3.3.2, with subsection 3.3.3 giving the basic idea of a financial tool able to provide an improvement in grid operation.

Finally in chapter 4 a synopsis is illustrated with the highilights and the future research work that we intend to focus on.

recently new improved DC load flow method is

Chapter 2

The Power Flow Equations

2.1 Introduction

The power generation, transmission and distribution system has been widely recognized as one of the most complex man-made systems and the related power flow analysis as the main ingredient of many related studies of the power systems. In this chapter we present the basics of the Power Flow Problems (PFPs), the ones that we will enable us to derive, analyze and implement numerical schemes for the solution of the Power Flow Equations (PFEs).

Surely there are several recent review studies concerning PFP problems. Each one of them considers these problems focusing on specific issues as those reflected from their particular view point which in turn originated from the interdisciplinarity inherent to PFP and the related problems.

In this study a review of the power flow problem is presented, focusing on its typical, conventional as well as, its extended, modified or simplified, formulations. This may be considered as an attempt to make the reader familiar with waht is widely considered as the most powerful tool in electric power systems analysis.

In a future study (that is beyond the scope of this review), we will further consider the problem from a deaper numerical analysis viewpoint and with the assumption that the reader has the required basic Numerical Analysis and Scientific Computing background.

More specifically, for the needs of the subsequent chapters we next view the theory, the practice and the technology involved in PFP from a review viewpoint. That is we assume some basic knowledge in Electrical Engineering in particular from the areas of circuits, electronics and electromagnetism. Readers with limited knowledge on basic

Electric Power Systems are referred to these excellent basic books [2] and courses [3] where several perhaps elementary but important issues and concepts not covered here in detail, are elucidated.

Electrical power systems concern with the generation, transmission, distribution and utilization of electrical energy. They are networks composed of components, mainly buses and lines that connect them, which operate under certain laws of Physics. The importance of the electrical PFP is that it provides us with the ability to predict voltages and flows on the network components.

PFP is a traditional scientific and engineering problem with a long history. Since the electrical networks evolve in several respects, the need for dynamic critical information keeps increasing. Even in the early days of power systems analysis this information needed to be delivered as soon as possible. Therefore, the history of power flow is strongly connected to the history of computing systems and it was common for a utility to spend huge budgets on the development of computing hardware and software.

Power flow analysis is the primary tool for investigating the normal operation state and for planning the evolution of real electric power systems [2]. It consists, together with the static security analysis, the stability analysis, the economic dispatch and other components, the overall power system steady state analysis. Based on a specified generating as wellas demand load state and transmission network topology, load flow analysis calculates the steady operation state in the power system with node voltages and branch power flow. This means that given an initial power plan for supply (generation) and demand (consuming load) the power flow study computes the bus voltages that must be known for the forthcoming calculation of power, and at the same time checks if the computed voltages exceed some limits that lead to system abnormal conditions.

The power flow (also known as load flow) is a set of nonlinear algebraic equations that relate the basic variables involved in the line flow of electric power systems. In other words, it gives an electrical response of the transmission and distribution system to a particular set of loads and generated power outputs. More specifically, for a power system operation, the bus voltages and the system frequency need to be within prescribed limits the same time that the active and reactive power balance in the system are imposed.

A power system is obviously a dynamic system. The system load varies continuously in time and hence, in order to ensure satisfactory system the PFPs need to be solved at a particular time-scale of operation. However, dynamic analysis is based on load flow analysis. This is clearly explained in one-machine and multi-machine stability analysis [4].

It is apparent and widely accepted that the load flow analysis is essential to understand the methodology of modern power system analysis. Planning for future grid extension, economic scheduling (also known as economic dispatch), mainly, as well as real time operation and control area purposes, are the main electric grid features that show load flow analysis importance. For example, whenever power system components have to be maintained during normal operation, it is crucial to know whether the power system will still function within system limits, or what additional measures have to be taken. Moreover, in the case of system malfunctions, also known as system contingencies, like a line outage or a fault on the system, load flow analysis is the basic analysis tool. In principle static security analysis can be replaced by a series of load flow analyses. However, usually there are many contingency states to be checked and the computation burden is quite large if a rigorous load flow calculation method is used. Hence, more effective load flow methods have to be developed to meet the requirement of efficient calculation.

The power flow problem is modelled through a system of non-linear equations that relate the bus voltages to the power generation and consumption. Its solution is used to asses the stability of the power system and to perform contingency analysis. It is also required by other related and relatively new problems, for example the optimal power flow problem, the financial transmission rights mechanisms and many others.

It is known that the power flow problem was first introduced for the transmission system operation, that is, for the part of the electricity grid that starts at the exit of the generation units where supply is first delivered and ends at the next lower level namely the distribution system. However, since distributed systems are also very crucial for the total grid operation, the power flow problem has been one of their most powerful analysis tools. Furthermore, several recent advances (for example the liberalization of the energy markets, the emerging of smart grid technologies, the increasing stochasticity in the power production due to utilization of renewable energy sources, the decentralization of the energy production) have recently increased the complexity of the power flow problems significantly.

The envisioned interconnection of national power systems with global energy markets will be based on truly large scale, continent-wide power flow simulations where the efficiency of the numerical solution of the power flow equations is expected to be a vital requirement.

This study may also be considered as an up-to-day review of the various numerical methods that have been very recently proposed for the solution of power flow equations and

several other related problems. These methods are examined from both the theoretical (convergence analysis) and the practical (efficiency, robustness, numerical stability, implementation) viewpoint.

We also propose several new research directions which, we believe, have the potential to lead us to the next generation power grid simulation engines. Engines that are capable to support operational large scale modern power grid systems associated with open energy markets, paying special attention to the information flow in addition to the power flow.

The rest of this review is organized as follows. A major part of this chapter is dedicated to the power flow equations setting, their formulation and their implementation. Both their conventional polar and the rectangular formulations are presented. The solution process through utilization of widely used iterative techniques like Newton-Raphson, is also presented. In the second part of the chapter is focused on recent modelling methodologies for the power flow problem, like current mismatch versions and their alternatives. The conventional power flow simplifications, like Fast Decoupled Load Flow and DC load flow are analytically discussed, since these are techniques attempting to mitigate computational burden of the conventional AC full power flow. Several alternatives of each of the basic types of power flow are throughtly reviewed. A brief description of optimal power flow and machine stability ends this chapter.

In Chapter 3 we present and discuss several issues that motivate our review. Our objective here is to exhibit that recent theoretical models and advances, emerging enabling technologies and drastic paradigm shifts leave several important issues in a state that needs further elucidation and analysis. The power flow algorithm application in new areas of electric power systems, like distributed generation, renewable resources, microgrids and smartgrids is presented in order to emphasize its necessity as well as its suitability in a variety of recent power systems analysis. Therefore, we believe that an increase on the need for further research on the century old problem of power flow is well justyfied.

2.2 Characteristics

The basic element of a power flow study of electric power grids is the node, also called bus [5]. It is widely known as node since it is analogous to a node in the electric circuit theory. Buses are used in practice in order for the basic electric variables, namely the active and reactive power of the generators, to meet the demand load of the consumers. In order to keep the balance between supply and demand, the main variables of the electric network, namely the voltage phasor, as well as the currents must be calculated

during normal operation. Buses are interconnected by means of interconnecting lines (transmission and distribution lines) which have characteristics, like the impedance, similar to the notion of resistance to AC networks, and is thus a measure of opposition to a sinusoidal current. The reciprocal of the impedance is called the admittance and is the main element describing the geometry and the physics of the line's cables. Obviously, energy losses are are very crucial so that the associated variable must be computed during power flow calculations.

The network buses [6] are coded depending on which variables are known and which are not, so they must be calculated. This is the key point for the forthcoming formulation of the power flow equations. It is stated that complex power seperated in active and reactive part forms the controlled variables of the system. At the same time, complex voltage seperated in voltage magnitude and phase angle is the state variable that has to be calculated first, so that the controlled variables be calculated afterwards. This flexibility offered by the above observation shows the importance of bus distinction into generator buses, load buses and one generator bus as the slack or swing bus. This importance will become apparent by the related discussions that will follow.

The main characteristics of each of the three group of buses are the following:

Load buses also known as PQ buses, can be seen as the buses where load demand in the form of the power vector, is aggregated. The great majority of buses in the transmission network belong to this category. This is expected, since load buses are the aggregated node points of the distribution network that constitutes the system that handles the end-users of electric energy. If one considers how meshed and extended the distribution system is, then can understand why it needs so many aggregated points, that is the transmission load buses. The elements that are considered as the aggregated points are always the transformers that perform the reduction from a higher to a lower voltage level. Since transformers are the core of the substation units, usually substation nodes are taken as load buses. Load buses are defined as the buses where both active and reactive power are known while voltage magnitude and phase angle are unknown. The following are the load bus constraints for bus j for the active and reactive case respectively.

$$P_j = P_j^{sp} = -P_{D_J}^{sp} \tag{2.1}$$

$$Q_J = Q_J^{sp} = -Q_{D_J}^{sp}. \tag{2.2}$$

where, P_j, Q_j are the active and reactive power at bus j which are considered equal to P_j^{sp} and Q_j^{sp}, that is the specified active and reactive power at bus j, where specified has the meaning of initially known and used as that, while, $P_{D_j}^{sp}$ and $Q_{D_j}^{sp}$ denote that these powers have the meaning of load demand (this explains the letter D in notation), at bus j.

The schematic description of a load - PQ bus is given in the following figure 2.1

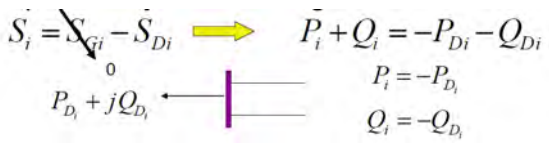

FIGURE 2.1: Schematic description of a load bus

Generator buses are the nodes that are connected to generation stations, so they are the first in which generation power output is delivered. In these buses the voltage regulator of a local interconnected generator keeps the voltage magnitude at a specified value. More generally the buses in which there can be a voltage control with reactive power capacity are taken as generator buses. This means that not only power plants, but substations having enough reactive power compensation to control voltage can be considered as generator buses. Furthermore the active generated power is also specified according to the economic planning by the system operator, meaning that the generator output is available under certain financial criteria. So, a generator bus has the active power and voltage magnitude known while reactive power and voltage phase angle are unknown. The following are the generator bus constraints at bus j.

$$P_j = P_j^{sp} = P_{G_j}^{sp} - P_{D_j}^{sp} \tag{2.3}$$

$$V_j = V_j^{sp}. \tag{2.4}$$

where

P_j is the active power at bus j, which is the subtraction between, $P_{G_j}^{sp}$ which is the specified generator active power (the real power produced by the machine), initially known and used that way (that is the meaning of specified), and P_{D_j} which is the initially specified load demand active power, and finally V_j is the known (controlled to be constant) voltage which equals V_j^{sp} which is the initially specified bus voltage that will be used in calculations.

In other words, a generator bus is described by a power injected to it by the producer (generator) and a power that is withdrawn from it by the load consumer (customer). Generator buses are also known as PV buses.

The schematic description of a generator - PV bus is given in the following figure 2.2

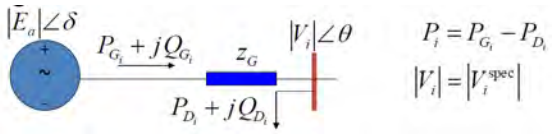

FIGURE 2.2: Schematic description of a generator bus

Slack or swing bus is the unique generator bus that takes into consideration the imbalance in power flow and makes the corrective actions needed for the steady-state stable operation. The effective generator at this node supplies the losses to the network. This is necessary because the magnitude of losses will not be known until the calculation of currents is complete and this can not be achieved unless one node has no power constraint and can feed the required losses into the system. The selection of the swing bus is a crucial issue and usually the slack bus is chosen among those generating buses with largest capacity, frequently being in charge of frequency regulation duties (automatic generation control or frequency control are the basic tasks of the slack bus). The unique slack bus has the voltage magnitude and angle known and the active as well as reactive power unknown, thus they have to be solved. The slack or swing bus is also known as the $V\delta$ bus.

The schematic description of a slack (swing) - $V\delta$ bus is given in the following figure 2.3

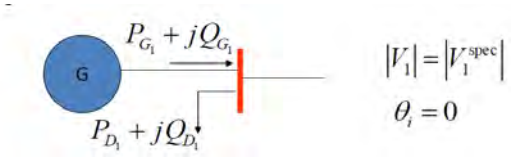

FIGURE 2.3: Schematic description of a slack (swing) bus

For better capturing the idea and significance of the slack-reference bus the following figures 2.4 and 2.5 are representative. The notion of slack bus will be discussed later on when the distributed slack bus technique is referred.

At each bus, two out of the four above mentioned variables are known and the remaining two are obtained by solving a set of nonlinear power flow equations. The above discussion can be summarized in the following table, 2.1

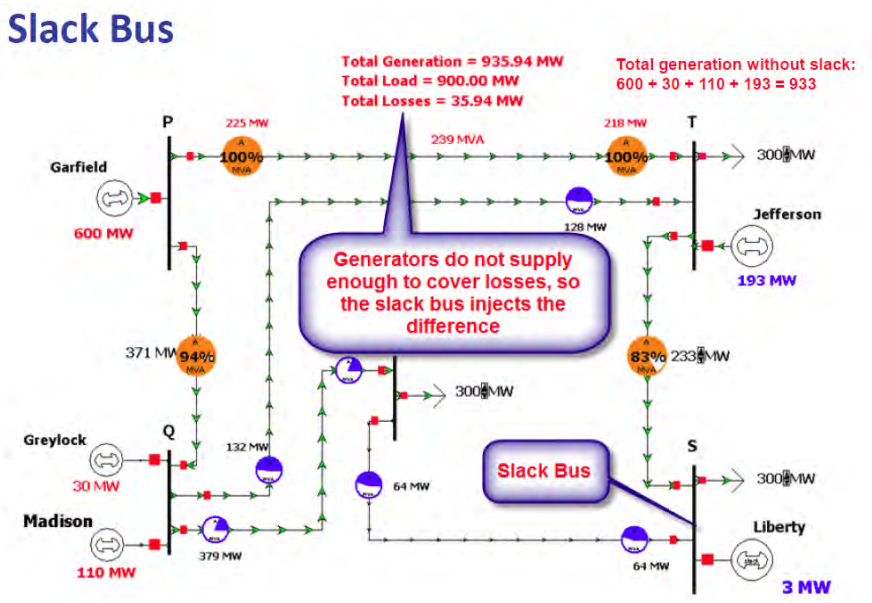

FIGURE 2.4: Slack-reference bus operation in case of losses management

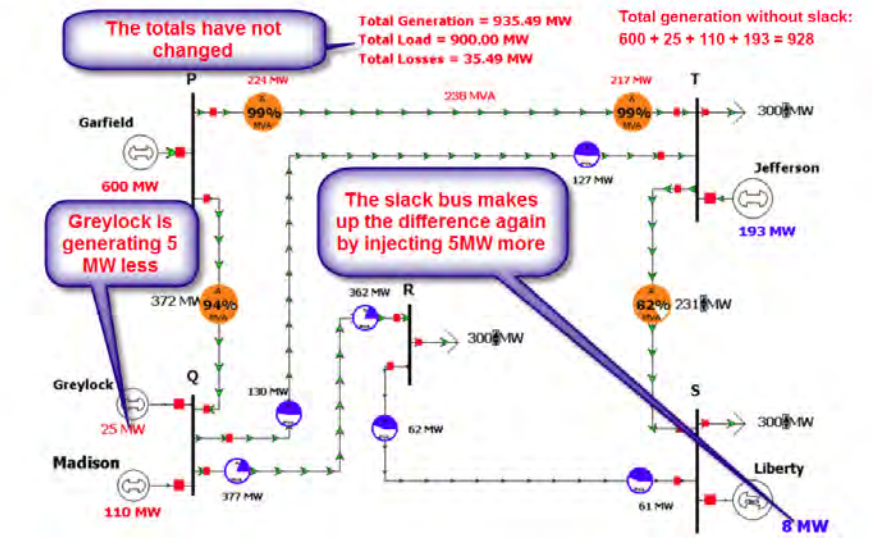

FIGURE 2.5: Slack-reference bus operation in case of generator management

The rest of the basic elements of the power grid are transformers, phase shifters, shunt capacitors, reactors, etc.. Transformers are the mechanisms for either raising or reducing or even regulating voltage. They allow the relative low voltage from generators to be initially raised to high or extra high levels (meaning 150KV-400KV) in order to be transferred by the transmission system by using relative small diameter cables. In a next level, namely the distribution system, they reduce high voltages to medium voltages (20KV) and finally at the end-user level (i.e., the residence) they execute another reduction from medium to low voltage (20KV to 0.4KV) a value more suitable for

Buses	real power	reactive power	voltage magnitude	voltage angle
Load	known	known	unknown	unknown
Generator	known	uknown	known	unknown
Swing	uknown	uknown	known	known

TABLE 2.1: The three types of buses according to their known and unknown variables

consuming utilization. During regulation, transformers are used to change the voltage magnitude or phase angle at a certain point of the system by a small amount. All the accompanying network elements are represented by their equivalent circuits consisting of R (resistive), L (inductive), and C (capacitive) elements. Therefore, the network formed by static components can be considered as a linear network and is represented by the corresponding admittance matrix or the associated impedance matrix (see below). Generators and loads are the basic components and are treated as nonlinear elements.

Electric power grid may be thought as a very large electric network consisting of the basic elements that are already well studied and understood from the electric circuits theory and some additional elements necessary for its operation. A high level abstract diagram of a generic power system is given in Figure 2.6. It consists of various elements (generators, transmission and distribution lines, buses, ...) as well as variables (voltage, current, power ...). These elements and variables are interrelated through laws of physics as well as other expressions that originate from technical requirements.

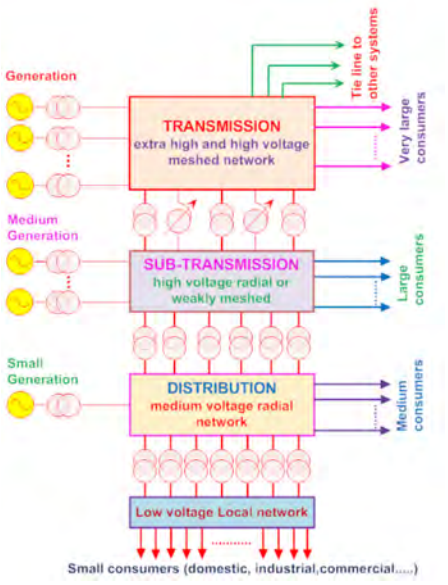

FIGURE 2.6: Structure of a generic power system

A real power system of the US electricity grid is presented is fig. 2.7 and concerns the east coast Pensylvania-Jersey-Meryland (PJM) as it is shown in it's internet site

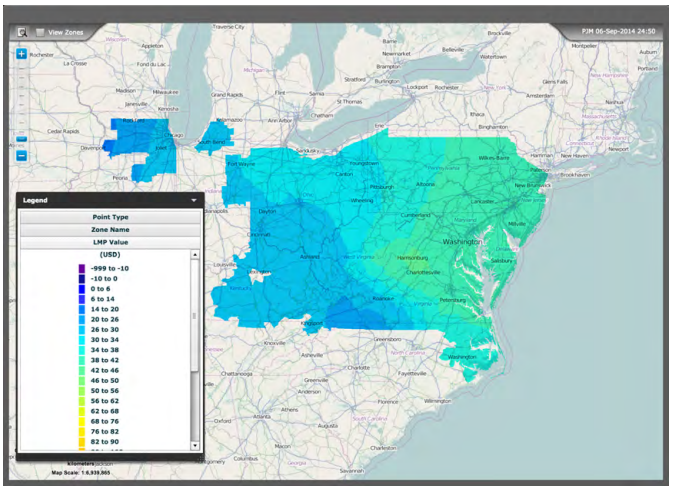

FIGURE 2.7: Structure of a real US power system (Courtesy of http://nptel.ac.in)

One of the major characteristics of electrical grids is their topology. Two kinds of networks are common, namely meshed and radial. Meshed networks are always apparent in the transmission power networks and they are characterized by more than one interconnection of all or a number of buses to adjacent nodes, that is, almost each of the network nodes is connected to two or even more neighbouring nodes. A meshed network is demonstrated in the following figure 2.8

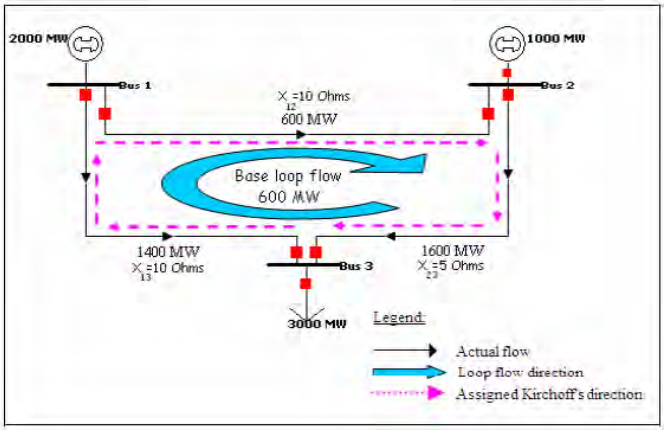

FIGURE 2.8: Meshed electrical power network

The above figure 2.8 introduces the idea of looped networks which is known as the meshed transmission grid. This is because, as one can see, each bus can be connected to more than one adjacent bus (in our case a bus is connected to two other buses), thus creating a closed loop. Before closing this section we should mention that a closed-loop transmission network that interconnects with other systems will experience a phenomenon called loop flow. This happens as power flow is governed by the physical Kirchhoffs law and not

by contractual financial arrangements between the participants of the electric power system. More detailed information on loop flows will be provided in subsection 3.3.2..

On the other hand distribution systems, namely the systems in which the voltage is lower compared to transmission systems and are more close to the end users, that is the consumers, are characterized by a radial topology, which means that almost every node is connected to adjacent nodes radially and not in a looped layout. This formation looks like a tree in which the high level node has the higher voltage level, while lower levels involve lower voltages to the extent of the low voltage that is 230V or 400V. A radial distribution system is presented in figure 2.9

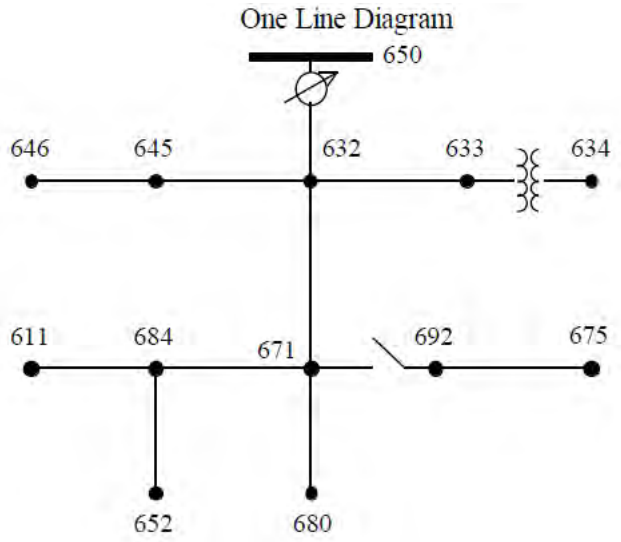

FIGURE 2.9: Radial electrical power network

2.3 Laws of Physics

Ohms law as well as Kirchhoffs laws may be considered as the cornerstones of the mathematical formulation of the equations that describe the electric power grid operation problem. Specifically, according to Kirchhoffs current law, the sum of the currents flowing towards at any point in a circuit is equal to the sum of currents flowing away from that point. Kirchhoffs voltage law states that the directed sum of the electrical potential differences around any closed circuit is zero.

The following figure 2.10 illustrates Kirchhoff's law. Kirchhoff's law is also true for any closed area of the network as shown in figure 2.11

Finally Kirchhoff's law is true for the whole control area, that is, sum of all generation, loads and inter-tie flows equals 0 as shown in figure 2.12

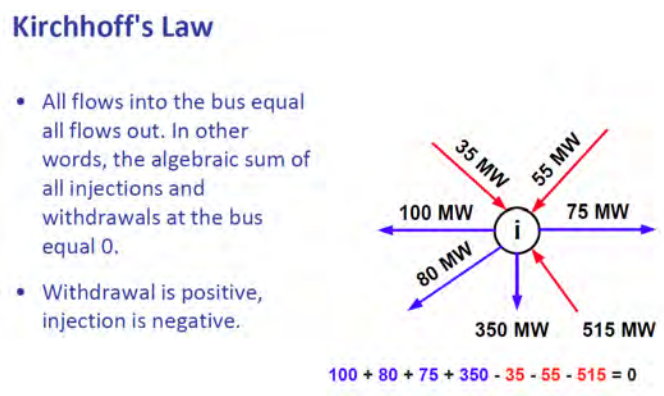

FIGURE 2.10: Kirchhoff's law

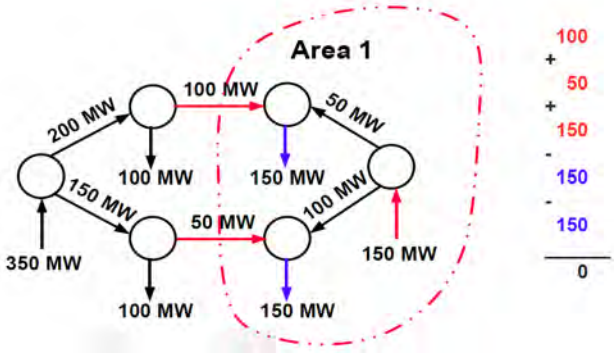

FIGURE 2.11: Kirchhoff's law for closed area of a network

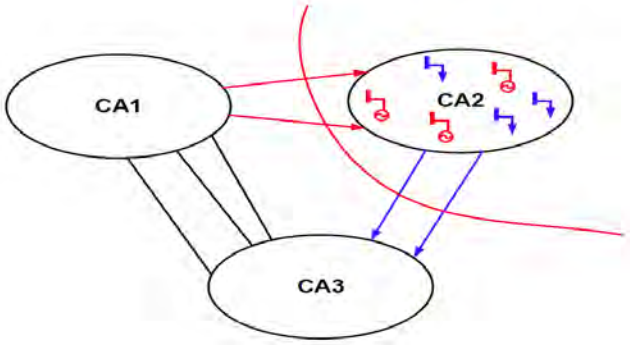

FIGURE 2.12: Kirchhoff's law for control area

The classic power flow problem has the form of the so-called AC power flow and can be formulated based on Kirchhoffs circuit laws in electric power networks. The basic variables involved in AC power flow equations are active and reactive power and nodal voltage that accounts to voltage magnitude and angle. It is proved that these four variables can describe any kind of electric power system. Applying basic Ohms law, which relates current to voltage and the Kirchhoffs current law, to each node and its interconnections with adjacent nodes, we obtain a set of nonlinear equations connecting

each bus real and reactive power to voltage magnitude and angle in a generic form. Since bus variables are known, the interconnected lines (line that structurally, connect flows) can also be calculated, as well as the line flow losses, which depend to voltage drop, as well as due to line cables structural characteristics and geometry. Line flows and relevant losses will be discussed shortly in next paragraphs.

Consider figure 2.13 presenting a schematic description of a bus operation at a time instant where the power flow problem takes place.

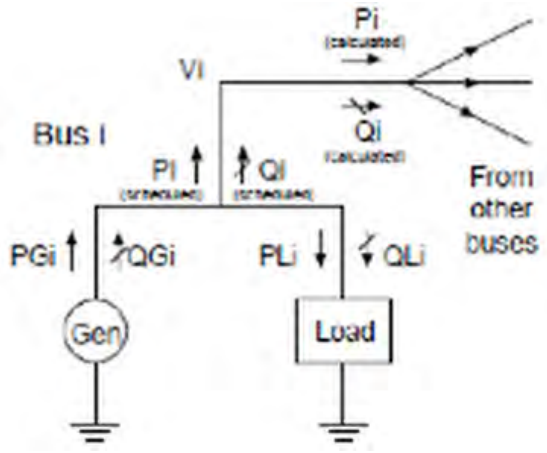

FIGURE 2.13: Power mismatch

bus bar voltage $V_i = |V_i|\angle\delta_i$

net scheduled real power $P_{i(scheduled)} = P_{G_i} - P_{L_i}$

net scheduled reactive power $Q_{i(scheduled)} = Q_{G_i} - Q_{L_i}$

with P_{G_i} and Q_{G_i} representing generator powers and P_{L_i} and Q_{L_i} representing load powers. $P_{i(scheduled)}$ and $Q_{i(scheduled)}$ are the determined by the system operator powers taking into account the supply and demand at a particular time of the system operation, finally $P_{i(calculated)}$, and $Q_{i(calculated)}$ are the active and reactive power flows obtained as a result of the power flow solution. Then the power mismatch $(\Delta P_i, \Delta Q_i)$ is given as follows

$$\Delta P_i = P_{i(scheduled)} - P_{i(calculated)} \tag{2.5}$$

$$\Delta Q_i = Q_{i(scheduled)} - Q_{i(calculated)} \tag{2.6}$$

The meaning of the above equations is as simple as significant can be. It describes the conservation of energy, that is, the balance between supply and demand as presented

initially in the terms $P_{i(scheduled)}$ and $Q_{i(scheduled)}$ and finally in the terms of ΔP_i and ΔQ_i after the solution of the power flow problem and the re evaluation of the the power balance.

To better understand the meaning of bus power injections the following figure 2.14 shows a schematic representation

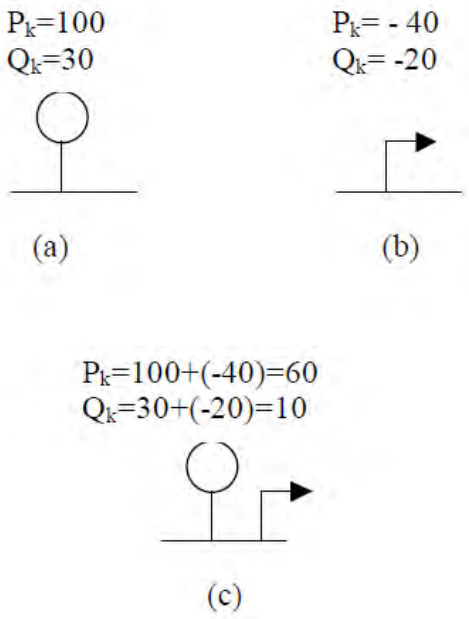

FIGURE 2.14: Illustration of a) a positive injection, b) a negative injection and c) net injection

We start deriving the basic Power Flow Equations (PFEs) by stating that given specific values on the loads, the generation and the network, a power flow study determines the complex voltage

$$V_i = V' + jV'' = |V_i|\angle\delta_i = |V_i|(\cos\delta_i + \mathrm{j}\sin\delta_i), \quad i = 1, \ldots, n_b \tag{2.7}$$

at each bus i in the system, where δ_i is the voltage phase angle at the node, n_b the number of buses in the network and $\mathrm{j} \equiv \sqrt{-1}$.

The following figure 2.15 shows a schematic representation of complex voltage and the significance of the phase angle

A power system of n_b buses is defined by a $n_b \times n_b$ admittance matrix Y. The current injected into the network at bus j is given by

$$I_i = \sum_{j=1}^{nb} Y_{ij} V_j \tag{2.8}$$

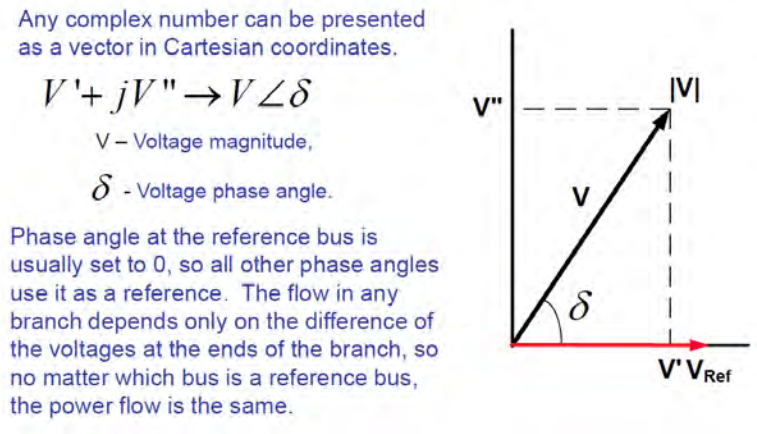

FIGURE 2.15: Complex voltage and phase angle

where $Y_{ij} = |Y_{ij}|\angle\theta_{ij}$ element on the i^{th} row and the j^{th} column of the so-called bus admittance matrix Y and V_j is voltage at bus j. Admittance is the reciprocal of impedance and is given by

$$Y_i = G_i + jB_i \tag{2.9}$$

where G_i is the conductance given by

$$G_i = \frac{R^2}{R^2 + X^2} \tag{2.10}$$

while B_i is the susceptance given by

$$B_i = \frac{-X^2}{R^2 + X^2} \tag{2.11}$$

The bus admittance matrix plays a significant role since it relates current to voltage according to the Ohms law [7]. Its elements, line admittances represent the cabling geometrical characteristic, so in that sense they are constant, and their values are used as input information for load flow analysis. The admittance matrix is usually a very sparse matrix, meaning that it commonly has very few non-zero elements per row (or column). The zero elements of the matrix corresponds to non interconnected buses. In summary, the diagonal elements of the bus admittance matrix are obtained by adding all admittance connected to the respective bus, whereas the off-diagonal elements are simply the negative admittance interconnecting the involved buses, leading therefore to a symmetric matrix. The great majority of the off-diagonal elements will be null because a bus is directly connected typically to just a few buses. The above mentioned

properties, the matrix symmetricity and sparsity, are very important for the calculations during the power flow model study. Another useful power system property is the quite large reactance to resistance ratio of the transmission lines. This property will allow us to perform useful simplifications on the original AC power flow problem equations.

Let us now consider an example of three bus network system as this is depicted in Figure 2.16. For the nodal current at node 1 we have

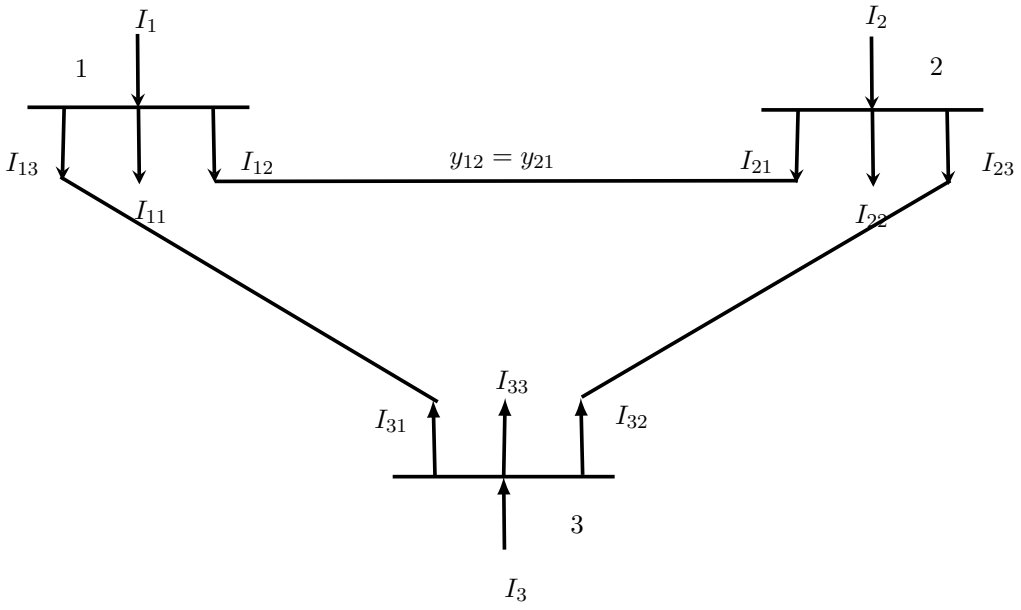

FIGURE 2.16: A three bus system

$$\begin{aligned} I_1 &= I_{11} + I_{12} + I_{13} \\ &= V_1 y_{11} + (V_1 - V_2) y_{12} + (V_1 - V_3) y_{13} \\ &= V_1 (y_{11} + y_{12} + y_{13}) - V_2 y_{12} - V_3 y_{13} \\ &= V_1 Y_{11} + V_2 Y_{12} + V_3 Y_{13} \end{aligned} \tag{2.12}$$

where y_{11} is the shunt charging admittance at bus 1, that is, the admittance on the line-cable connecting the bus to the ground, y_{12} is the series admittance between bus 1 and 2 and where

$$Y_{11} = y_{11} + y_{12} + y_{13} \tag{2.13}$$

$$Y_{12} = -y_{12} \tag{2.14}$$

$$Y_{13} = -y_{13}. \tag{2.15}$$

Similarly for nodes 2 and 3 we have

$$I_2 = V_1Y_{21} + V_2Y_{22} + V_3Y_{23} \tag{2.16}$$

$$I_3 = V_1Y_{31} + V_2Y_{32} + V_3Y_{33}. \tag{2.17}$$

Equations (2.12) and (2.16) can be written in matrix form as follows

$$\begin{bmatrix} I_1 \\ I_2 \\ I_3 \end{bmatrix} = \begin{bmatrix} Y_{11} & Y_{12} & Y_{13} \\ Y_{21} & Y_{22} & Y_{23} \\ Y_{31} & Y_{32} & Y_{33} \end{bmatrix} \begin{bmatrix} V_1 \\ V_2 \\ V_3 \end{bmatrix} \tag{2.18}$$

The above matrix form for a network of $n_b = 3$ buses is given by the matrix equation $I = YV$ where $I, V \in \mathbb{R}^{n_b}$ and $Y \in \mathbb{R}^{n_b \times n_b}$. It can be also presented in summation form as it is shown in 2.8.

To avoid misunderstanding, what is denoted by a lower letter as y_{ij} refers to an individual line admittance, while the capital letter for Y_{ij} denotes the final admittance created by the summation of individual admittances in order to form the bus admittance matrix.

2.4 Categorization

2.4.1 Formulation of the basic power flow problem

The main purpose of an electric power system is to deliver the power that the end-users, that is the customers, require on demand, in real time within acceptable voltage and frequency limits, in a reliable and economic manner. This procedure is complex since it involves many variables that have to be calculated in almost real time for a network that is extended and meshed too. In order to succeed its operation, a power system needs powerful tools in the form of models and algorithms that can compute every complex variable within minutes or even seconds. The most powerful of these tools, has already been proved to be the power flow analysis. Its importance comes from real life. Whenever a load (residential, commercial, industrial) is required by an end users demand, a load flow model must run by the system operator in order to evaluate all the involved variables and check for their limits satisfaction. This is the steady state operation of the system. Almost the same procedure has to be considered when abnormal conditions occur in the network, like line overloading or outage, faults, generation outage, etc. In other words the power flow model, no matter what algorithm engages as a solver, is the most widely used application for operating and planning in electric power systems. It can be

utilized either as a stand-alone algorithm or as a subroutine algorithm in more complex processes such as stability analysis and optimization models like the optimal power flow that will described later on.

The power flow study can be considered as a two basic steps procedure. In the first and most critical one, the complex voltages at all buses of a system are calculated. If all these voltages satisfy the limit conditions initially specified by the system operator, then the second much easier step follows in which the remaining variables of interest like complex power (active and reactive) ohmic losses etc, are computed.

The classical form of the power flow problem consists of a set of nonlinear algebraic equations relating the active and reactive power to the voltage magnitude and angle respectively, which will next be presented in detail.

Practically the number of equations to be solved depends on the number of the unknown variables concerning voltage magnitude and angle. If the values of these variables are determined then the analogous equations of the powers with respect to the unknown variables (complex voltage) are formulated. For each load (PQ) bus with active and reactive power known (specified as already mentioned) and the other two variables (the state variables in the form of voltage magnitude and angle) unknown, two such equations are formulated. They relate the two known variables to the two unknown variables. For generator (PV) buses only one equation is applied for active power only, since reactive power is unknown. So, reactive power can not be considered in the first step of the solution process, but it will be calculated afterwards. Similarly, since the voltage magnitude and angle of the slack bus are specified, the related power equations do not appear in the first step of the solution process. When this step of solution process has ended, the active and reactive power of the slack bus can be calculated by using the power flow equations. The equations are expressed as a set of power mismatch equations between the net scheduled power (also mentioned as specified) coordinated by the system operator, and the injected power that is to be calculated during the solution process. Net power is described as the balance between generation power and load demand power. These information will be valuable when the mathematical and matrix formulations of the power flow algorithms will be presented.

AC power flow [8], [9], is the total analytic formulation of power flow analysis. Since it is described by a set of nonlinear algebraic equations (they will be presented shortly), that can not be easily solved or are even unsolved, a reasonable solution practice involves the use of iterative techniques like Newton-Raphson method which is proved to be the most powerful algorithm using a linearizing technique or the Gauss-Seidel method.

In the following, different expressions of the power flow equations will be presented. The differences are based on the definition of the conjugate terms. If the definition is given in terms of exponents or even trigonometrical terms, then the formulation will be defined as polar. On the other hand, if the definitions are given in terms of real and imaginary part of the conjugate, then the formulation is considered as rectangular.

The NR method is a typical method used to solve non linear equations in mathematics by using the Taylor series expansion, with very favorable convergence if a good initial estimate is given. The NR method uses the Jacobian matrix (which is obtained by the Taylor expansion) as the linearization tool. The elements of the Jacobian are the first order partial derivatives of the active and reactive power (the controlled variables) with respect to voltage magnitude and angle (the state variables), respectively if the polar form of the voltage phasor representation is adopted. For each bus, a 2×2 block submatrix is formulated relating power, active and reactive, with voltage magnitude and phase angle. If the number of system buses is n_b and $r \leq n_b$ is assumed the number of PV (generator) buses, while the last n_b bus is assumed the slack bus, then $n_b - 1$ active power equations and $n_b - r - 1$ reactive power equations are formulated. The number of voltage angle unknowns is therefore, $n_b - 1$ while the number of voltage magnitude unknowns is $n_b - r - 1$. This results in $2n_b - r - 2$ unknown variables that have to be solved by the equivalent $2n_b - r - 2$ power flow equations.

If the rectangular form is adopted then the Jacobian matrix is formulated with elements as the partial derivatives of active and reactive power with respect to real and imaginary part of the voltage phasor. The difference between the two expressions is that with rectangular coordinates the calculation of trigonometric functions (cos, sin) is avoided. However, due to non linear equations inherent characteristics, the AC model has convergence difficulties and is time consuming especially when contingency analysis is considered.

The difference between two formulations consists of the different generators (PV) bus modelling, in which reactive power is unknown. In the AC NR polar form all buses are modeled the same way, as load (PQ) buses while in the rectangular AC NRPF there is a different modelling for generator (PV) buses. An additional equation relating the voltage phasor with the real and imaginary part of voltage assists in the PV bus equation formulation.

Either way, the conventional NR is a set of non-linear algebraic equations with an advantage of being accurate but with the disadvantage of being time-consuming due to the iterative calculation of the whole Jacobian matrix which results in huge dimensions, considering the power grid topology. In either formulation the number of unknown variables matches the set of equations, resulting in a linear system that has to be solved.

After the initial solution (the phase angle at every bus in the system except, the one reference slack bus, and the voltage magnitude at every load bus in the system) is performed, one then can solve for every other derived quantity of interest in the system. Having calculated all derived quantities one can then verify whether they are within their acceptable range of values.

Since, the power flow algorithms are well established and presented in the majority of power systems analysis literature, the authors have made a selection of the most citated publications so as to present the power flow formulations.

2.4.2 AC Power Mismatch Flow in Polar Coordinates

For the polar formulation of the NRPF algorithm the authors refer to [2], [10], [8], [11] in which the polar formulation is expressed in trigonometric terms (sin, cos) while the bus admittance in terms of the rectangular form, involving conductance (real part) and susceptance (imaginary part).

As already mentioned the Kirchhoff's current law applied to the electric grid between interconnected buses results is the following matrix formulation relating bus current to bus voltage through the bus admittance matrix

$$I = YV \tag{2.19}$$

where I is the bus current matrix, Y is the bus admittance matrix and V is the voltage phasor matrix.

By applying the Ohm's law the bus complex power is expressed in relation to bus voltage and bus current as follows

$$S_i = V_i I_i^* = V_i(\sum_{j=1}^{n} V_j Y_{ij})^* = V_i \sum_{j=1}^{n} V_j^* Y_{ij}^* \tag{2.20}$$

where V_j^* is the transpose of the voltage vector and Y_{ij}^* is the conjugate of the bus admittance vector.

By solving the above equation with respect to bus current the following equation is obtained

$$I_i = \frac{S_i^*}{V_i^*} = \frac{S_{Gi}^* - S_{Di}^*}{V_i^*} = \frac{(P_{Gi} - P_{Di}) - j(Q_{Gi} - Q_{Di})}{V_i} \tag{2.21}$$

where

S_i: the complex power at bus i, and S_i^* is the conjugate of it

S_{Gi}^*, S_{Di}^* are the conjugate vectors of generation as well as load demand complex vectors

P_{Gi} : the active power output of the generator connected to bus i

Q_{Gi}: the reactive power output of the generator connected to bus i

P_{Di}: the active power load demand of the connected to bus i

Q_{Di}: the reactive load demand connected to bus i

From the above two equations of the bus current the former relating it to the voltage and the latter relating it to power and by substitution the following expression is derived

$$\frac{(P_{Gi} - P_{Di}) - j(Q_{Gi} - Q_{Di})}{V_i} = Y_{i1}V_1 + Y_{i2}V_2 + \dots Y_{in}V_n \tag{2.22}$$

where n is the number of buses connected to bus i.

In the power flow problem the generation outputs and the load demands are initially known as they are scheduled by the system operator according to the plan of power distribution. It is then easy to define these scheduled powers as

$$P_i = P_{Gi} - P_{Di} \tag{2.23}$$

$$Q_i = Q_{Gi} - Q_{Di} \tag{2.24}$$

Substituting the above equations to eq. 2.22 we can derive the general form of the power flow equation as

$$\frac{P_i - jQ_i}{V_i^*} = \sum_{j=1}^{n} V_j Y_{ij} \tag{2.25}$$

or

$$P_i + jQ_i = V_i \sum_{j=1}^{n} V_j^* Y_{ij}^* \tag{2.26}$$

where P_i, Q_i are the injected active and reactive power at bus i respectively, V_i is the voltage vector (phasor) of the bus under study, V_j is the voltage vector (phasor)

representing all the buses interconnected to bus i and Y_{ij} is the bus admittance of the line interconnecting buses i and j.

This latter equation is very important since it relates each bus complex power to the voltage phasors of not only the same bus but of the adjacent interconnected buses too. This equation will lead to the power flow equations final formulation.

In order to derive the final expression of the power flow equations some basic definitions are given. So, the bus admittance is defined by the equation

$$Y_{ij} = G_{ij} + jB_{ij} \tag{2.27}$$

where G_{ij} is the bus conductance (real part) and B_{ij} is the bus susceptance (reactive part).

The phasor form of the voltage consists of the voltage magnitude as well as the voltage angle and is expressed as

$$V_i = |V_i|e^{j\delta_i} \tag{2.28}$$

Hence the power flow equation can be rewritten as

$$P_i + jQ_i = |V_i|e^{j\delta_i} \sum_{j=0}^{n_{bs}} |V_j|e^{-j\delta_j}(G_{ij} - jB_{ij}) \tag{2.29}$$

where n_{bs} is the number of buses, the power flow study is applied.

The exponential term can be expressed as follows

$$e^{j\delta} = \cos\delta + j\sin\delta \tag{2.30}$$

Utilizing equation 2.30 in equation 2.29

$$P_i + jQ_i = |V_i| \sum_{j=0}^{n_{bs}} |V_j|(G_{ij} - jB_{ij})(\cos\delta_{ij} + j\sin\delta_{ij}) \tag{2.31}$$

where $\delta_{ij} = \delta_i$-δ_j is the voltage phase angle difference between interconnected buses i and j.

Separating the above equation into real and imaginary part leads to the final two equations of the power flow problem consisting the active and reactive power formulation.

$$P_i = |V_i| \sum_{j=0}^{n_{act}} |V_j|(G_{ij} \cos \delta_{ij} + B_{ij} \sin \delta_{ij}) \tag{2.32}$$

$$Q_i = |V_i| \sum_{j=0}^{n_{react}} |V_j|(G_{ij} \sin \delta_{ij} - B_{ij} \cos \delta_{ij}) \tag{2.33}$$

It is worth noting that the number of buses, for the application of power flow study, is now different, concerning the separation between active and reactive power flow. For active power flow the term n_{act} is going to be used, while for reactive power flow the term n_{react} denotes the number of buses.

The above expression of the two equations, is considered as the polar form of the power flow equations, since it involves trigonometric terms. The bus admittance matrix, however, has a rectangular form. As is already mentioned, what matters the power flow computations is the power mismatch in each node, consisting of the difference between the scheduled power (the initially specified by the coordinator, that is the system operator) and the calculated power by the power flow study.

Considering the power mismatch equations 2.32 and 2.33 are expressed as follows:

$$\Delta P_i = P_i^{sp} - |V_i| \sum_{j=0}^{n_{act}} |V_j|(G_{ij} \cos \delta_{ij} + B_{ij} \sin \delta_{ij}) = 0 \tag{2.34}$$

$$\Delta Q_i = Q_i^{sp} - |V_i| \sum_{j=0}^{n_{react}} |V_j|(G_{ij} \sin \delta_{ij} - B_{ij} \cos \delta_{ij}) = 0 \tag{2.35}$$

Based on the above two equations the load flow problem can be described as follows: for specified powers P_i^{sp}, Q_i^{sp} $(i = 1, 2, \ldots, n_b - 1 = n_{act})$, find voltage vector (magnitude V_i and angle phase δ_i) such that the power mismatch (errors) ΔP_i and ΔQ_i $(i = 1, 2, \ldots, n_b - 1 = n_{act})$ are less than an acceptable tolerance.

Another slightly different polar formulation with a polar form of bus admittance, can be found in [3], [6], [9].

For this formulation to be derived all the variables are expressed in exponential terms. Since for the voltage phasor this expression already exists, it is the bus admittance that has to be expressed also in its polar form as follows

$$Y_{ij} = |Y_{ij}|e^{j\theta_{ij}} \tag{2.36}$$

By incorporating trigonometric terms the power flow equation of the complex power has the form

$$P_i - jQ_i = |V_i|e^{-j\delta_i} \sum_{j=0}^{n_{bs}} |V_j|e^{j\delta_j}|Y_{ij}|e^{j\theta_{ij}} \tag{2.37}$$

where n_{bs} denotes the last bus index used for calculation purposes. Remark: In this power flow formulation the conjugate vectors are the complex power $P_i - jQ_i$ as well as the voltage under study, i, i.e., $|V_i|e^{-j\delta_i}$

Separating again into real and imaginary parts the active and reactive power flow equations are

$$P_i = \sum_{j=0}^{n_{act}} |V_i||V_j||Y_{ij}| \cos(\theta_{ij} - \delta_i + \delta_j) \tag{2.38}$$

$$Q_i = -\sum_{j=0}^{n_{react}} |V_i||V_j||Y_{ij}| \sin(\theta_{ij} - \delta_i + \delta_j) \tag{2.39}$$

where n_{act}, n_{react} denote the last bus index for active and reactive power flow calculations respectively.

Thus, the power mismatch equations are expressed as

$$\Delta P_i = P_i^{sp} - P_i = P_i^{sp} - \sum_{j=0}^{n_{act}} |V_i||V_j||Y_{ij}| \cos(\theta_{ij} - \delta_i + \delta_j) = 0 \tag{2.40}$$

$$\Delta Q_i = Q_i^{sp} - Q_i = Q_i^{sp} - \sum_{j=1}^{n_{react}} |V_i||V_j||Y_{ij}| \sin(\theta_{ij} - \delta_i + \delta_j) = 0 \tag{2.41}$$

Let's now assume that the total number of buses is n_b and the number of PV buses is r. For convenience the slack bus is the last bus numbered n_b. Then, $n_b - 1 = n_{act}$ active power equations concerning both PQ and PV buses have the expressions

$$\begin{aligned}
\Delta P_1 &= P_1^{sp} - |V_1| \sum_{j=1}^{n_{act}} |V_j|(G_{1j}\cos\delta_{1j} + B_{1j}\sin\delta_{1j}) = 0 \\
\Delta P_2 &= P_2^{sp} - |V_2| \sum_{j=1}^{n_{act}} |V_j|(G_{2j}\cos\delta_{2j} + B_{2j}\sin\delta_{2j}) = 0 \\
&\vdots \\
\Delta P_{n_{act}} &= P_{n_{act}}^{sp} - |V_{n_{act}}| \sum_{j=0}^{n_{act}} |V_j|(G_{n_{act},j}\cos\delta_{n_{act},j} + B_{n_{act},j}\sin\delta_{n_{act},j}) = 0
\end{aligned} \tag{2.42}$$

while $n_b - r - 1 = n_{react}$ reactive power equations concerning only the PQ load buses have the expressions

$$\begin{aligned}
\Delta Q_1 &= Q_1^{sp} - |V_1| \sum_{j=1}^{n_{react}} |V_j|(G_{1j}\sin\delta_{1j} - B_{1j}\cos\delta_{1j}) = 0 \\
\Delta Q_2 &= Q_2^{sp} - |V_2| \sum_{j=1}^{n_{react}} |V_j|(G_{2j}\sin\delta_{2j} - B_{2j}\cos\delta_{2j}) = 0 \\
&\vdots \\
\Delta Q_{n_{react}} &= Q_{n_{react}}^{sp} - |V_{n_{react}}| \sum_{j=1}^{n_{react}} |V_j|(G_{n_{react},j}\sin\delta_{n_{react},j} - B_{n_{react},j}\cos\delta_{n_{react},j}) = 0
\end{aligned} \tag{2.43}$$

From the above equations it is easily understandable that each PQ bus is described by two equations for both active and reactive power, while each PV bus is described by only one equation for the active power.

We will give a simple example, in order to understand the numbering of the equations involved in a typical load flow study. Let's assume a network with a total number of $n_b = 7$ buses. We assume that the specific $n_b = 7$ bus is the reference slack bus. If we have a number of $r = 1$ PV buses the number of PQ buses is $n_b - r - 1 = 7 - 1 - 1 = 5$. This leads to a load flow study with $n = n_b - 1 = 7 - 1 = 6$ active power mismatch equations for both PQ and PV buses, and $m = n - b - r - 1 = 7 - 1 - 1 = 5$ reactive power mismatch equations only for PQ buses. The total number of equations engaged is $2n_b - r - 2 = 2x7 - 1 - 2 = 11$.

From the above power mismatch equations it is evident that the power flow problem consists of a set of nonlinear algebraic equations. Since nonlinear systems are difficult to solve or even totally unsolvable, in order to find an acceptable solution a linearization is necessary and is achieved by utilizing the Taylor series neglecting the higher order

terms of the partial derivatives. Then, the power mismatch equations in matrix form, are expressed as follows:

$$\begin{bmatrix} \Delta P_1 \\ \Delta P_2 \\ \vdots \\ \Delta P_{n_{act}} \\ \cdots \\ \Delta Q_1 \\ \Delta Q_2 \\ \vdots \\ \Delta Q_{n_{react}} \end{bmatrix} = \begin{bmatrix} H_{1,1} & H_{1,2} & \cdots & H_{1,n_{act}} & \vdots & N_{1,1} & N_{1,2} & \cdots & N_{1,n_{react}} \\ H_{2,1} & H_{2,2} & \cdots & H_{2,n_{act}} & \vdots & N_{2,1} & N_{2,2} & \cdots & N_{2,n_{react}} \\ \vdots & \vdots & \vdots & \vdots & \vdots & \vdots & \vdots & & \\ H_{n_{act},1} & H_{n_{act},2} & \cdots & H_{n_{act},n_{act}} & \vdots & N_{n_{act},1} & N_{n_{act},2} & \cdots & N_{n_{act},n_{react}} \\ \cdots & \cdots & \cdots & \cdots & \cdots & \cdots & \cdots & & \\ K_{1,1} & K_{1,2} & \cdots & K_{1,n_{react}} & \vdots & L_{1,1} & L_{1,2} & \cdots & L_{1,n_{act}} \\ K_{2,1} & K_{2,2} & \cdots & K_{2,n_{react}} & \vdots & L_{2,1} & L_{2,2} & \cdots & L_{2,n_{act}} \\ \vdots & \vdots & \vdots & \vdots & \vdots & \vdots & \vdots & & \\ K_{n_{react},1} & K_{n_{react},2} & \cdots & K_{n_{react},n_{react}} & \vdots & L_{n_{act},1} & L_{n_{act},2} & \cdots & L_{n_{act},n_{act}} \end{bmatrix} \begin{bmatrix} \Delta\delta_1 \\ \Delta\delta_2 \\ \vdots \\ \Delta\delta_{n_{act}} \\ \cdots \\ \Delta V_1/|V_1| \\ \Delta V_2/|V_2| \\ \vdots \\ \Delta V_{n_{react}}/|V_{n_{react}}| \end{bmatrix} \tag{2.44}$$

The compact form of the above matrix is given as

$$\begin{bmatrix} \Delta P \\ \Delta Q \end{bmatrix} = \begin{bmatrix} H & N \\ K & L \end{bmatrix} \begin{bmatrix} \Delta\delta \\ \Delta V/|V| \end{bmatrix} \tag{2.45}$$

Another usual matrix formulation of the NR power flow model found in the literature is as follows

$$\begin{bmatrix} \Delta P \\ \Delta Q \end{bmatrix} = \begin{bmatrix} J_1 & J_2 \\ J_3 & J_4 \end{bmatrix} \begin{bmatrix} \Delta\delta \\ \Delta V/|V| \end{bmatrix} \tag{2.46}$$

Matrix equations 2.45 and 2.46 constitute the Newton-Raphson power flow model with the voltage vector $\Delta\delta$ and $\Delta V/V$ as the state variable and the power vector ΔP and ΔQ as the control variable, where each of the block submatrices H, N, K, L or J_1, J_2, J_3, J_4 consists of diagonal as well as off-diagonal elements being a block 2x2 submatrix.

Either form of two above formulations constitutes a linear system of the form

$$Ax = B \tag{2.47}$$

which for the power flow problem takes the form

$$-Jx = B \tag{2.48}$$

where

$$J = \begin{bmatrix} H & N \\ K & L \end{bmatrix} \tag{2.49}$$

or

$$J = \begin{bmatrix} J_1 & J_2 \\ J_3 & J_4 \end{bmatrix} \tag{2.50}$$

J is the Jacobian matrix of the Newton-Raphson power flow model,

$$x = \begin{bmatrix} \Delta\delta \\ \Delta V/|V| \end{bmatrix} \tag{2.51}$$

is the state variable (voltage vector or phasor), and

$$B = \begin{bmatrix} \Delta P \\ \Delta Q \end{bmatrix} \tag{2.52}$$

is the controlled variable (complex power vector. i.e., the active and reactive power).

The matrix expression of the NRPF model, incorporating the partial derivatives involved in the calculation of the block submatrices is

$$\begin{bmatrix} \Delta P \\ \Delta Q \end{bmatrix} = \begin{bmatrix} \frac{\partial \Delta P}{\partial \delta} & \frac{\partial \Delta P}{\partial V}|V| \\ \frac{\partial \Delta Q}{\partial \delta} & \frac{\partial \Delta Q}{\partial V}|V| \end{bmatrix} \begin{bmatrix} \Delta\delta \\ \Delta V/|V| \end{bmatrix} \tag{2.53}$$

In a more analytical formulation relative to matrix expression of eq. 2.44 is the following

$$\begin{bmatrix} \Delta P_1 \\ \vdots \\ \Delta P_{n_{act}} \end{bmatrix} = \begin{bmatrix} \frac{\partial \Delta P_1}{\partial \delta_1} & \cdots & \frac{\partial \Delta P_1}{\partial \delta_{n_{act}}} \\ \vdots & \vdots & \vdots \\ \frac{\partial \Delta P_{n_{act}}}{\partial \delta_1} & \cdots & \frac{\partial \Delta P_{n_{act}}}{\partial \delta_{n_{act}}} \end{bmatrix} \begin{bmatrix} \Delta\delta_1 \\ \vdots \\ \Delta\delta_{n_{act}} \end{bmatrix} \tag{2.54}$$

$$\begin{bmatrix} \Delta P_1 \\ \vdots \\ \Delta P_{n_{act}} \end{bmatrix} = \begin{bmatrix} \frac{\partial \Delta P_1}{\partial V_1} V_1 & \cdots & \frac{\partial \Delta P_1}{\partial V_{n_{react}}} V_{n_{react}} \\ \vdots & \vdots & \vdots \\ \frac{\partial \Delta P_{n_{act}}}{\partial V_1} V_1 & \cdots & \frac{\partial \Delta P_{n_{act}}}{\partial V_{n_{react}}} V_{n_{react}} \end{bmatrix} \begin{bmatrix} \Delta V_1/V_1 \\ \vdots \\ \Delta V_{n_{react}}/V_{n_{react}} \end{bmatrix} \tag{2.55}$$

$$\begin{bmatrix} \Delta Q_1 \\ \vdots \\ \Delta Q_{n_{react}} \end{bmatrix} = \begin{bmatrix} \frac{\partial \Delta Q_1}{\partial \delta_1} & \cdots & \frac{\partial \Delta Q_1}{\partial \delta_{n_{act}}} \\ \vdots & \vdots & \vdots \\ \frac{\partial \Delta Q_{n_{react}}}{\partial \delta_1} & \cdots & \frac{\partial \Delta Q_{n_{react}}}{\partial \delta_{n_{act}}} \end{bmatrix} \begin{bmatrix} \Delta \delta_1 \\ \vdots \\ \Delta \delta_{n_{act}} \end{bmatrix} \tag{2.56}$$

$$\begin{bmatrix} \Delta Q_1 \\ \vdots \\ \Delta Q_{n_{react}} \end{bmatrix} = \begin{bmatrix} \frac{\partial \Delta Q_1}{\partial V_1} V_1 & \cdots & \frac{\partial \Delta Q_1}{\partial V_{n_{react}}} V_{n_{react}} \\ \vdots & \vdots & \vdots \\ \frac{\partial \Delta Q_{n_{react}}}{\partial V_1} V_1 & \cdots & \frac{\partial \Delta Q_{n_{react}}}{\partial V_{n_{react}}} V_{n_{react}} \end{bmatrix} \begin{bmatrix} \Delta V_1 / V_1 \\ \vdots \\ \Delta V_{n_{react}} / V_{n_{react}} \end{bmatrix} \tag{2.57}$$

For the diagonal elements the next expressions are obtained by taking the first order partial derivatives:

$$H_{ii} = \frac{\partial \Delta P_i}{\partial \delta_i} = |V_i| \sum_{j \in ij \neq i} |V_j|(-G_{ij} \sin \delta_{ij} + B_{ij} \cos \delta_{ij}) \tag{2.58}$$

$$= -|V_i|^2 B_{ii} - Q_i \tag{2.59}$$

$$N_{ii} = \frac{\partial \Delta P_i}{\partial V_i} |V_i| = |V_i| \sum_{j \in ij \neq i} |V_j|(G_{ij} \cos \delta_{ij} + B_{ij} \sin \delta_{ij}) + 2|V_i|^2 G_{ii} \tag{2.60}$$

$$= |V_i|^2 G_{ii} + P_i \tag{2.61}$$

$$K_{ii} = \frac{\partial \Delta Q_i}{\partial \delta_i} = |V_i| \sum_{j \in ij \neq i} |V_j|(G_{ij} \cos \delta_{ij} + B_{ij} \sin \delta_{ij}) \tag{2.62}$$

$$= -|V_i|^2 G_{ii} + P_i \tag{2.63}$$

$$L_{ii} = \frac{\partial \Delta Q_i}{\partial V_i} |V_i| = |V_i| \sum_{j \in ij \neq i} |V_j|(G_{ij} \sin \delta_{ij} - B_{ij} \cos \delta_{ij}) - 2|V_i|^2 B_{ii} \tag{2.64}$$

$$= -|V_i|^2 B_{ii} + Q_i \tag{2.65}$$

For the off diagonal elements of the Jacobian matrix, i.e., $i \neq j$ the following expressions are obtained

$$H_{ij} = \frac{\partial \Delta P_i}{\partial \delta_j} = |V_i||V_j|(G_{ij}\sin\delta_{ij} - B_{ij}\cos\delta_{ij}) = Q_i \tag{2.66}$$

$$N_{ij} = \frac{\partial \Delta P_i}{\partial V_j}|V_j| = |V_i||V_j|(G_{ij}\cos\delta_{ij} + B_{ij}\sin\delta_{ij}) = P_i \tag{2.67}$$

$$K_{ij} = \frac{\partial \Delta Q_i}{\partial \delta_j} = -|V_i||V_j|(G_{ij}\cos\delta_{ij} + B_{ij}\sin\delta_{ij}) = -P_i = -N_{ij} \tag{2.68}$$

$$L_{ij} = \frac{\partial \Delta Q_i}{\partial V_j}|V_j| = -|V_i||V_j(G_{ij}\sin\delta_{ij} - B_{ij}\cos\delta_{ij}) = Q_i = H_{ij} \tag{2.69}$$

From the expression [8] of the off-diagonal elements of the Jacobian matrix it can be seen that they are related to only one element of the admittance matrix. Therefore if this element is zero the corresponding element of the Jacobian matrix is also zero. This means that the Jacobian matrix is a sparse matrix and has the same structure as the admittance matrix. Additionally the Jacobian matrix is not symmetrical in polar coordinated form.

Remark: Sometimes the above partial derivative terms of the Jacobian matrix are presented in the literature with the exact opposite signs. This happens if an opposite sign appears in front of the Jacobian matrix and is dependent on the matrix formulation of the power flow problem occasionally presented in some textbooks. Either way, the Jacobian matrix elements will take the proper sign during calculation.

The power mismatch equations can be rearranged in matrix form as follows for convenience

$$\begin{bmatrix} \Delta P_1 \\ \Delta Q_1 \\ \vdots \\ \Delta P_{n_{act}} \\ \Delta Q_{n_{react}} \end{bmatrix} = \begin{bmatrix} H_{1,1} & N_{1,1} & \cdots & H_{1,n_{act}} & N_{1,n_{react}} \\ K_{1,1} & L_{1,1} & \cdots & K_{1,n_{react}} & L_{1,n_{act}} \\ \vdots & \vdots & \vdots & \vdots & \vdots \\ H_{n_{act},1} & N_{n_{react},1} & \cdots & H_{n_{act},n_{act}} & N_{n_{react},n_{react}} \\ K_{n_{react},1} & L_{n_{act},1} & \cdots & K_{n_{react},n_{react}} & L_{n_{act},n_{act}} \end{bmatrix} \begin{bmatrix} \Delta\delta_1 \\ \Delta V_1/|V_1| \\ \vdots \\ \Delta\delta_{n_{act}} \\ \Delta V_{n_{react}}/|V_{n_{react}}| \end{bmatrix} \tag{2.70}$$

For the latter polar x_2 formulation the NRPF matrix equation includes block submatrices like the ones described by 2.54, 2.55, 2.56 and 2.57

The partial derivatives resulting to the diagonal elements of the Jacobian matrix are now calculated as follows

$$H_{ii} = \frac{\partial \Delta P_i}{\partial \delta_i} = \sum_{j \neq i} |V_i||V_j||Y_{ij}| \sin(\theta_{ij} - \delta_i + \delta_j) \tag{2.71}$$

$$= -\sum_{j \neq i} \frac{\partial \Delta P_i}{\partial \delta_j} \tag{2.72}$$

$$= -|V_i|^2 B_{ii} - Q_i \tag{2.73}$$

$$N_{ii} = \frac{\partial \Delta P_i}{\partial V_i}|V_i| = 2|V_i|^2|Y_{ii}| \cos\theta_{ii} + \sum_{j \neq i} |V_j||Y_{ij}| \cos(\theta_{ij} - \delta_i + \delta_j) \tag{2.74}$$

$$= 2|V_i|^2 G_{ii} + \sum_{j \neq i} |V_j||Y_{ij}| \cos(\theta_{ij} - \delta_i + \delta_j) \tag{2.75}$$

$$= \frac{\partial \Delta Q_i}{\partial \delta_i} + 2|V_i|^2 G_{ii} \tag{2.76}$$

$$= P_i + |V_i|^2 G_{ii} \tag{2.77}$$

$$K_{ii} = \frac{\partial \Delta Q_i}{\partial \delta_i} = \sum_{j \neq i} |V_i||V_j||Y_{ij}| \cos(\theta_{ij} - \delta_i + \delta_j) \tag{2.78}$$

$$= -\sum_{j \neq i} \frac{\partial \Delta Q_i}{\partial \delta_j} \tag{2.79}$$

$$= -|V_i|^2 G_{ii} + P_i \tag{2.80}$$

$$L_{ii} = \frac{\partial \Delta Q_i}{\partial V_i}|V_i| = -2|V_i|^2|Y_{ii}| \sin\theta_{ii} + \sum_{j \neq i} |V_j||Y_{ij}| \sin(\theta_{ij} - \delta_i + \delta_j) \tag{2.81}$$

$$= -2|V_i|^2 B_{ii} + \sum_{j \neq i} |V_j||Y_{ij}| \sin(\theta_{ij} - \delta_i + \delta_j) \tag{2.82}$$

$$= -\frac{\partial \Delta P_i}{\partial \delta_i} - 2|V_i|^2 B_{ii} \tag{2.83}$$

$$= Q_i - |V_i|^2 B_{ii} \tag{2.84}$$

The partial derivatives that lead to the Jacobian off-diagonal elements expressions are the following

$$H_{ij} = \frac{\partial \Delta P_i}{\partial \delta_j} = -|V_i||V_j||Y_{ij}| \sin(\theta_{ij} - \delta_i + \delta_j) \tag{2.85}$$

$$N_{ij} = \frac{\partial \Delta P_i}{\partial V_j}|V_j| = |V_i||V_j||Y_{ij}|\cos(\theta_{ij} - \delta_i + \delta_j) = -\frac{\partial \Delta Q_i}{\partial \delta_j} \tag{2.86}$$

$$K_{ij} = \frac{\partial \Delta Q_i}{\partial \delta_j} = -|V_i||V_j||Y_{ij}|\cos(\theta_{ij} - \delta_i + \delta_j) \tag{2.87}$$

$$L_{ij} = \frac{\partial \Delta Q_i}{\partial V_j}|V_j| = -|V_i||V_j||Y_{ij}|\sin(\theta_{ij} - \delta_i + \delta_j) = -\frac{\partial \Delta P_i}{\partial \delta_j} \tag{2.88}$$

2.4.3 AC Power Mismatch Flow in Rectangular Coordinates

Although the power flow is usually described in literature in its polar formulation, there is a rectangular form of the model which results by expressing the voltage vector in rectangular form as follows

$$V_i = e_i + jf_i \tag{2.89}$$

where

$$e_i = V_i \cos\delta_i \tag{2.90}$$

and

$$f_i = V_i \sin\delta_i. \tag{2.91}$$

The final form of the two power flow equations considering active and reactive power is the following

$$P_i = e_i \sum_{j=0}^{n}(G_{ij}e_j + B_{ij}f_j) + f_i \sum_{j=0}^{n}(G_{ij}f_j + B_{ij}e_j) \tag{2.92}$$

$$Q_i = f_i \sum_{j=0}^{n}(G_{ij}e_j + B_{ij}f_j) - e_i \sum_{j=0}^{n}(G_{ij}f_j + B_{ij}e_j) \tag{2.93}$$

Using this formulation the real and imaginary parts of the injected currents are described as

$$a_i = \sum_{j=0}^{n} (G_{ij} e_j + B_{ij} f_j) \tag{2.94}$$

$$b_i = \sum_{j=0}^{n} (G_{ij} f_j + B_{ij} e_j) \tag{2.95}$$

With the latter current expression the power mismatch equations take the final form

$$P_i = e_i a_i + b_i f_j \tag{2.96}$$

$$Q_i = f_i a_i - b_i e_j \tag{2.97}$$

for $i = 1, 2, \ldots n$

When the rectangular model is adopted the real and imaginary part of the voltage phasor are the state variables that must be solved in order for the controlled variables to calculated next. The controlled variables depend on the bus type, in that sense for PQ buses they are the active and reactive power, while for PV buses they are the active power as well as bus voltage. This means that in either case of a bus type (excluding swing bus) two equations are expressing the power flow problem. In that way regardless the bus type, the total number of equations is $2(n_b - 1)$ where n_b is the total number of buses. This gives the opportunity to express the equations without taking into account the different bus numbering as we did when studying the polar power flow expressions. In the following only the term $n_b - 1$ is used as a superscript to denote the last bus number for either PQ and PV buses, instead of using n_{act} and n_{react} as it was used in polar formulation.

When considering rectangular formulation of the NRPF model the final power mismatch equations for each PQ bus are taking the form

$$\Delta P_i = P_i^{sp} - e_i \sum_{j=0}^{n_b-1} (G_{ij} e_j - B_{ij} f_j) - f_i \sum_{j=0}^{n_b-1} (G_{ij} f_j + B_{ij} e_j) = 0 \tag{2.98}$$

$$\Delta Q_i = Q_i^{sp} - f_i \sum_{j=0}^{n_b-1} (G_{ij} e_j - B_{ij} f_j) + e_i \sum_{j=0}^{n_b-1} (G_{ij} f_j + B_{ij} e_j) = 0 \tag{2.99}$$

Based on the above two equations the load flow problem for PQ buses can be described as follows: for specified powers P_i^{sp}, Q_i^{sp} $(i = 1, 2, \ldots, n_b - 1)$ find voltage vector (real part e_i and imaginary part f_i) $(i = 1, 2, \ldots, n_b - 1)$ such that the power mismatch (errors) ΔP_i and ΔQ_i $(i = 1, 2, \ldots, n_b - 1)$ are less than an acceptable tolerance.

In the same way for each PV bus the equations are expressed as

$$\Delta P_i = P_i^{sp} - e_i \sum_{j=0}^{n_b-1} (G_{ij} e_j - B_{ij} f_j) - f_i \sum_{j=0}^{n_b-1} (G_{ij} f_j + B_{ij} e_j) = 0 \tag{2.100}$$

$$\Delta V_i^2 = (V_i^{sp})^2 + V_i^2 = (V_i^{sp})^2 + (e_i^2 + f_i^2) = 0 \tag{2.101}$$

where P_i^{sp}, Q_i^{sp} are the specified real and reactive powers at bus i and V_i is the PV bus voltage.

Based on the above PV equations the load flow problem can be described as follows: for specified powers P_i^{sp}, V_i^{sp} $(i = 1, 2, \ldots, n_b - 1)$ find voltage vector (real part e_i and imaginary part f_i) $(i = 1, 2, \ldots, n_b - 1)$ such that the power mismatch (errors) ΔP_i and ΔV_i $(i = 1, 2, \ldots, n_b - 1)$ are less than an acceptable tolerance.

The rectangular NRPF model has the following correction equation

$$-J\Delta V = \Delta F \tag{2.102}$$

which can written in matrix form as

$$\begin{bmatrix} \Delta F_1 \\ \Delta F_2 \\ \vdots \\ \Delta F_{n_b-1} \end{bmatrix} = \begin{bmatrix} J_{1,1} & J_{1,2} & \cdots & J_{1,n_b-1} \\ J_{2,1} & J_{2,2} & \cdots & J_{2,n_b-1} \\ \vdots & \vdots & \vdots & \vdots \\ J_{n-1,1} & J_{n-1,2} & \cdots & J_{n_b-1,n_b-1} \end{bmatrix} \begin{bmatrix} \Delta V_1 \\ \Delta V_2 \\ \vdots \\ \Delta V_{n_b-1} \end{bmatrix} \tag{2.103}$$

where

$$\begin{bmatrix} \Delta V_i \end{bmatrix} = \begin{bmatrix} \Delta e_i \\ \Delta f_i \end{bmatrix} \tag{2.104}$$

In a more analytical expression the matrix equation of the rectangular power flow model can be the following

$$\begin{bmatrix} \Delta P_1 \\ \Delta Q_1 \\ \Delta P_2 \\ \Delta Q_2 \\ \vdots \\ \Delta P_i \\ \Delta V_i^2 \\ \vdots \end{bmatrix} = \begin{bmatrix} \frac{\partial \Delta P_1}{\partial e_1} & \frac{\partial \Delta P_1}{\partial f_1} & \frac{\partial \Delta P_1}{\partial e_2} & \frac{\partial \Delta P_1}{\partial f_2} & \cdots & \frac{\partial \Delta P_1}{\partial e_i} & \frac{\partial \Delta P_1}{\partial f_i} & \cdots \\ \frac{\partial \Delta Q_1}{\partial e_1} & \frac{\partial \Delta Q_1}{\partial f_1} & \frac{\partial \Delta Q_1}{\partial e_2} & \frac{\partial \Delta Q_1}{\partial f_2} & \cdots & \frac{\partial \Delta Q_1}{\partial e_i} & \frac{\partial \Delta Q_1}{\partial f_i} & \cdots \\ \frac{\partial \Delta P_2}{\partial e_1} & \frac{\partial \Delta P_2}{\partial f_1} & \frac{\partial \Delta P_2}{\partial e_2} & \frac{\partial \Delta P_2}{\partial f_2} & \cdots & \frac{\partial \Delta P_2}{\partial e_i} & \frac{\partial \Delta P_2}{\partial f_i} & \cdots \\ \frac{\partial \Delta Q_2}{\partial e_1} & \frac{\partial \Delta Q_2}{\partial f_1} & \frac{\partial \Delta Q_2}{\partial e_2} & \frac{\partial \Delta Q_2}{\partial f_2} & \cdots & \frac{\partial \Delta Q_2}{\partial e_i} & \frac{\partial \Delta Q_2}{\partial f_i} & \cdots \\ \vdots & \vdots & \vdots & \vdots & \cdots & \vdots & \vdots & \cdots \\ \frac{\partial \Delta P_i}{\partial e_1} & \frac{\partial \Delta P_i}{\partial f_1} & \frac{\partial \Delta P_i}{\partial e_2} & \frac{\partial \Delta P_i}{\partial f_2} & \cdots & \frac{\partial \Delta P_i}{\partial e_i} & \frac{\partial \Delta P_i}{\partial f_i} & \cdots \\ 0 & 0 & 0 & 0 & \cdots & \frac{\partial \Delta V_i^2}{\partial e_i} & \frac{\partial \Delta V_i^2}{\partial f_i} & \cdots \\ \vdots & \vdots & \vdots & \vdots & \cdots & \vdots & \vdots & \cdots \end{bmatrix} \begin{bmatrix} \Delta e_1 \\ \Delta f_1 \\ \Delta e_2 \\ \Delta f_2 \\ \vdots \\ \Delta e_i \\ \Delta f_i \\ \vdots \end{bmatrix} \tag{2.105}$$

For a PQ bus

$$\Big[\Delta F_i\Big] = \begin{bmatrix} \Delta P_i \\ \Delta Q_i \end{bmatrix} \tag{2.106}$$

The diagonal block elements of the Jacobian matrix are

$$\Big[J_{ii}\Big] = \begin{bmatrix} \frac{\partial \Delta P_i}{\partial e_i} & \frac{\partial \Delta P_i}{\partial f_i} \\ \frac{\partial \Delta Q_i}{\partial e_i} & \frac{\partial \Delta Q_i}{\partial f_i} \end{bmatrix} \tag{2.107}$$

while the off-diagonal are given by

$$\Big[J_{ij}\Big] = \begin{bmatrix} \frac{\partial \Delta P_i}{\partial e_j} & \frac{\partial \Delta P_i}{\partial f_j} \\ \frac{\partial \Delta Q_i}{\partial e_j} & \frac{\partial \Delta Q_i}{\partial f_j} \end{bmatrix} \tag{2.108}$$

For a PV bus

$$\Big[\Delta F_i\Big] = \begin{bmatrix} \Delta P_i \\ \Delta V_i^2 \end{bmatrix} \tag{2.109}$$

The diagonal block elements of the Jacobian matrix are

$$\Big[J_{ii}\Big] = \begin{bmatrix} \frac{\partial \Delta P_i}{\partial e_i} & \frac{\partial \Delta P_i}{\partial f_i} \\ \frac{\partial \Delta V_i^2}{\partial e_i} & \frac{\partial \Delta V_i^2}{\partial f_i} \end{bmatrix} \tag{2.110}$$

while the off-diagonal are given by

$$\left[J_{ij}\right] = \begin{bmatrix} \frac{\partial \Delta P_i}{\partial e_j} & \frac{\partial \Delta P_i}{\partial f_j} \\ \frac{\partial \Delta V_i^2}{\partial e_j} & \frac{\partial \Delta V_i^2}{\partial f_j} \end{bmatrix} \tag{2.111}$$

The diagonal elements, by utilizing the partial derivatives, are computed as follows

$$\frac{\partial \Delta P_i}{\partial e_i} = -\sum_{j=0}^{n_b-1}(G_{ij}e_j - B_{ij}f_j) - G_{ii}e_i - B_{ii}f_i = -a_i - G_{ii}e_i - B_{ii}f_i \tag{2.112}$$

$$\frac{\partial \Delta P_i}{\partial f_i} = -\sum_{j=0}^{n_b-1}(G_{ij}f_j + B_{ij}e_j) - G_{ii}f_i + B_{ii}e_i = -b_i - G_{ii}f_i + B_{ii}e_i \tag{2.113}$$

$$\frac{\partial \Delta Q_i}{\partial e_i} = \sum_{j=0}^{n_b-1}(G_{ij}f_j + B_{ij}e_j) - G_{ii}f_i + B_{ii}e_i = b_i - G_{ii}f_i + B_{ii}e_i \tag{2.114}$$

$$\frac{\partial \Delta Q_i}{\partial f_i} = -\sum_{j=0}^{n_b-1}(G_{ij}e_j - B_{ij}f_j) + G_{ii}e_i + B_{ii}f_i = -a_i + G_{ii}e_i + B_{ii}f_i \tag{2.115}$$

$$\frac{\partial \Delta V_i^2}{\partial e_i} = -2e_i \tag{2.116}$$

$$\frac{\partial \Delta V_i^2}{\partial f_i} = -2f_i \tag{2.117}$$

The off-diagonal elements are also calculated as

$$\frac{\partial \Delta P_i}{\partial e_j} = \frac{\partial \Delta Q_i}{\partial f_j} = -(G_{ij}e_i + B_{ij}f_i) \tag{2.118}$$

$$\frac{\partial \Delta P_i}{\partial f_j} = \frac{\partial \Delta Q_i}{\partial e_j} = -(G_{ij}f_i - B_{ij}e_i) \tag{2.119}$$

$$\frac{\partial \Delta V_i^2}{\partial e_j} = -\frac{\partial \Delta V_i^2}{\partial f_j} = 0 \tag{2.120}$$

In the following tables 2.2 and 2.3 a brief review of the different power flow formulations and involved variables is illustrated.

method	admit. repres.	volt. repres.	PQ bus	PV bus
PM RP	rectangular, 2.27	polar, 2.28	2 eq. 2.32, 2.33	1 eq. 2.32
PM PP	polar, 2.36	polar, 2.28	2 eq. 2.38, 2.39	1 eq. 2.38
PM RR.	rectangular, 2.27	rectangular, 2.89, 2.90, 2.91	2 eq. 2.92, 2.93	1 eq.

TABLE 2.2: the power mismatch alternative forms of power flow equations

From the expressions of the elements of the Jacobian matrix in either coordinate form (polar or rectangular) it is obvious that the Jacobian matrix is non-symmetrical, although structurally, it shows some symmetry. The numerical non-symmetry can be found by checking

$$\frac{\partial \Delta P_i}{\partial \delta_j} \neq \frac{\partial \Delta P_j}{\partial \delta_i} \tag{2.121}$$

$$\frac{\partial \Delta Q_i}{\partial V_j} \neq \frac{\partial \Delta Q_j}{\partial V_i} \tag{2.122}$$

$$\frac{\partial \Delta P_i}{\partial e_j} \neq \frac{\partial \Delta P_j}{\partial e_i} \tag{2.123}$$

$$\frac{\partial \Delta Q_i}{\partial f_j} \neq \frac{\partial \Delta Q_j}{\partial f_i} \tag{2.124}$$

Considering rectangular coordinates an augmented load flow model is presented in [12]. This version of the rectangular formulation is based mostly on current rather than the power mismatch and it is shown to be competitive with the polar formulation especially for networks with a reduced number of PV buses. The key idea is to solve an augmented system in which both bus voltages and current injections appear as state variables and both power and current mismatches are zeroed. When rectangular coordinates are employed this yields a set of linearly-coupled quadratic equations rather than the usual set of fully-coupled nonlinear equations. The authors suggest a straightforward approach to dealing with PV buses. Simulation results confirm that depending on the number of PV buses the computational effort per iteration ranges about 50% and 80% of that required by polar formulations.

method	state var.	contr. var.
PM RP	$\|V\|, \delta$	$\Delta P, \Delta Q$, 2.34, 2.35
PM PP	$\|V\|, \delta$	$\Delta P, \Delta Q$, 2.40, 2.41
PM RR.	e_i, f_i	$\Delta P, \Delta Q$, 2.98, 2.99, 2.100, 2.101

TABLE 2.3: the power mismatch alternative forms of power flow equations control and state variables

2.4.4 Solution process for the power mismatch NRPF problem

Since power flow equations are, as already mentioned, nonlinear their solution involves a linearized iterative process for which proper initial conditions should be given to the state variables voltage magnitude and angle. The so-called flat start is generally the best choice for the load flow problem. According to this technique the angles of all buses are set to zero, while the voltage magnitudes for load buses are set to unity reflecting the fact that voltage magnitudes lie normally within a relatively narrow band around one p.u. while phase angle differences between adjacent buses are also quite small.

The iteration procedure of the full AC NRPF algorithm in polar formulation has the following steps:

1. Initialization of the state variable profile (voltage magnitude and phase angle) with a flat start that is described by setting $\delta_i = 0$ and $|V_i| = 1.0 p.u.$ As an alternative, the solution of a previous case study can also be utilized for the initial state.
2. Formulation of the bus admittance matrix Y.
3. Calculation of the power mismatch vectors ΔP_i and ΔQ_i according to equations 2.40 and 2.41.
4. Check if convergence conditions are satisfied, by

$$max|\Delta P_i^k| < \epsilon_1 \tag{2.125}$$

$$max|\Delta Q_i^k| < \epsilon_2 \tag{2.126}$$

5. If equations 2.125 and 2.126 are met, the iteration stops.If not the iteration continues with the next step.
6. The Jacobian matrix must be computed, by calculating all the block submatrices according to equations 2.58, 2.60, 2.62, 2.64 for the diagonal elements and equations 2.66, 2.67, 2.68 and 2.69 for the off-diagonal elements.

Calculation of the changes in the state variable (bus voltage magnitude and phase angle) by using equations 2.48, 2.49, 2.51 and 2.52.

Since the state variable changes are computed, calculation of the new bus voltage vector by the next equations

$$V_i^{k+1} = V_i^k + \Delta V_i^k \tag{2.127}$$

$$\delta_i^{k+1} = \delta_i^k + \Delta \delta_i^k \tag{2.128}$$

7. Return to step 3 and recomputation of the power mismatche vectors, utilizing the new values of bus voltages.

NRPF method has the following advantages over other iterative methods used for power flow analysis

1. Due to quadratic characteristics the convergence is very fast.
2. The results calculated are very accurate and reliable compared to other methods like GS.
3. The convergence is not dependent of the choice of the slack bus
4. The Newton method is able to be applied to large/extra large scale power systems.

If the buses powers are calculated then the power flows of all the interconnection elements like lines, transformers etc, are also calculated. Similarly, total network losses can be computed either by adding the power injections at all buses provided the complex power of the slack bus is available, or by adding the losses corresponding to each individual component. The second alternative is the only choice when losses corresponding to a specified area or subsystem are needed. The line flows can thus be defined as:

$$P_{ij} = |V_i||V_j|(G_{ij}\cos\delta_{ij} + B_{ij}\sin\delta_{ij}) - G_{ij}|V_i|^2 \tag{2.129}$$

$$Q_{ij} = |V_i||V_j|(G_{ij}\sin\delta_{ij} - B_{ij}\cos\delta_{ij}) + B_{ij}|V_i|^2 \tag{2.130}$$

In rectangular formulation the iterative process for the NR algorithm involves the following steps:

1. Initialization process for the voltage vector terms, real $e^{(0)}$ and $f^{(0)}$

2. Substitution of the above initial values into equations 2.98 and 2.99 for PQ buses and 2.100 and 2.101 for PV buses, in order for the initial values of power mismatches and voltage corrections $\Delta P^{(0)}$, $\Delta Q^{(0)}$ and $(\Delta V^2)^{(0)}$ be calculated;

3. Substitution of the initial values of voltage vector to equations that calculate the partial derivatives of diagonal and off-diagonal Jacobian matrix elements,in rectangular coordinates, 2.112, 2.113, 2.114, 2.115, 2.116, 2.117, 2.118, 2.119 and 2.120.

4. Solving eq. 2.103, with 2.107, 2.108, 2.110 and 2.111 in order to obtain the first correction values of $\Delta e^{(0)}$ and $\Delta f^{(0)}$.

5. Calculate the new voltage vector terms by equations

$$f^{(1)} = f^{(0)} + \Delta f^{(0)} \tag{2.131}$$

$$e^{(1)} = e^{(0)} + \Delta e^{(0)} \tag{2.132}$$

6. Substitution of the above values after the first iteration again in equations 2.98, 2.99, 2.100 and 2.101 in order to obtain $\Delta P^{(1)}$, $\Delta Q^{(1)}$ and $(\Delta V^2)^{(1)}$.

7. Check if the iteration leads to convergence. If not the calculated values $e^{(1)}$ and $f^{(1)}$ are used for the next iteration step by returning to step 3.

When applied to large-scale systems the NRPF method requires the use of very large matrices. As already mentioned each of the four block submatrix element of the Jacobian matrix is, in principle nxn (where n is the number of power nodes in the electric grid). Certain rows and columns within each Jacobian submatrix can be eliminated resulting in a smaller matrix. For instance the rows and columns corresponding to the reference (slack) bus or to reactive power mismatches/residues in PV nodes and columns corresponding to the respective voltage magnitudes are eliminated, thus decreasing the matrix dimension, which is very attractive and useful property when handling very large matrices.

Except elimination, reordering to group components that correspond to the same connections is another technique that improves the appearance and the computational efficiency of using the Jacobian matrix. Ordering of rows and columns to reduce the number of nonzero entries in the matrix after it is factored, is a very useful technique in large sparse matrix computations (like the Jacobian). Although these techniques will be analyzed in

a section during a future research review, the interested reader should refer to [10] for more information.

The conventional expression of the PFP can be modified in order to include regulating devices and associated limits. Such devices are utilized so as to keep a given electrical magnitude as close as possible to a target value for which they can act on a control variable within specified limits. Shunt compensators (regulating voltage magnitude by proper injection/withdrawn of reactive power), regulating transformers (voltage magnitude regulators and phase shifters) and series compensators (modifying the series impedance of transmission lines) are the most usually used control devices that can be incorporated in the power flow problem formulation by several techniques that can be found in [10].

The basic requirements of load flow calculation [8], from its beginning, until now, can be summed up as convergence properties, computing efficiency and memory requirements and convenience and flexibility of the implementation. Reliable convergence becomes a crucial issue in load flow analysis since the scale of power systems is continually expanding in the new era of deregulated electricity markets, leading to a high dimension of load flow equations (several thousands or even ten of thousands). Since the iterative methods like NR and GS have the difficulty of computational time consuming, many research efforts have been made during the last two decades in order to improve the power flow model solution by using methods reliable, efficient and faster. Such methods are based on the Krylov subspace iterative techniques and provide further improvement in load flow analysis in terms of computing efficiency and convergence especially for large to huge electric power systems. A review of these techniques is going to be presented in a future section of this study, but it is not in the scope, at this point of time.

2.4.5 AC Current Injection Power Flow Formulation

Several alternative models of the AC Power Flow problem have been presented in the literature. Such an alternative formulation of the PFP is presented in a journal paper form Bacher where a first attempt is being made so as to express the power flow problem, in a form different from the power mismatch flow equations, and a new modified model based on the so called "current mismatch" flow equations is introduced. The author continues the above project in [13]. In this paper the new formulation of current mismatch in terms of a linearized Jacobian NRPF is presented in more details. Using rectangular coordinates (as presented former in this report) it presents the following equations for the terms of real and imaginary part of current mismatch w.r.t the real and imaginary part of voltage

$$\Delta I_{r,i} = g_{i,1} = \frac{e_i P_i + f_i Q_i}{e_i^2 + f_i^2} - \sum_{j=1}^{n_b}(G_{ij}e_j + B_{ij}f_j) = 0 \tag{2.133}$$

$$\Delta I_{m,i} = g_{i,2} = \frac{-e_i Q_i + f_i P_i}{e_i^2 + f_i^2} - \sum_{j=1}^{n_b}(G_{ij}f_j + B_{ij}e_j) = 0 \tag{2.134}$$

$$g_{i,3} = -e_i^2 + f_i^2 + V_I^2 = 0 \tag{2.135}$$

where

$I_{r,i} = g_{i,1}$ is the real part of current mismatch
$I_{m,i} = g_{i,2}$ is the imaginary part of current mismatch
$g_{i,3}$ is the voltage equation
G_{ij} and B_{ij} are the conductance (real paert) and susceptance (imaginary part) of the bus admittance matrix
P_i and Q_i are the active and reactive power
e_i is the real part of voltage phasor f_i is the imaginary part of voltage phasor

The above equations 2.133 and 2.134 are used for PQ bus current mismatch representation. The third equation 2.135 is not needed. For PV buses, as is already known, reactive power Q_i is unknown and must be updated during all NR steps iterations. Therefore, PV buses are represented by equations 2.133 and 2.135.

The linearized NRPF can be formulated by computing the diagonal matrix terms, as follows,

$$\frac{\partial g_{i,1}}{\partial e_i} = \frac{\partial \Delta I_{r,i}}{\partial e_i} = -(\frac{P_i(e_i^2 - f_i^2) + 2e_i f_i Q_i}{(e_i^2 + f_i^2)^2}) - G_{ii} \tag{2.136}$$

$$\frac{\partial g_{i,1}}{\partial f_i} = \frac{\partial \Delta I_{r,i}}{\partial f_i} = -(\frac{Q_i(f_i^2 - e_i^2) + 2e_i f_i P_i}{(e_i^2 + f_i^2)^2}) + B_{ii} \tag{2.137}$$

$$\frac{\partial g_{i,2}}{\partial e_i} = \frac{\partial \Delta I_{m,i}}{\partial e_i} = -(\frac{Q_i(f_i^2 - e_i^2) + 2e_i f_i P_i}{(e_i^2 + f_i^2)^2}) - B_{ii} \tag{2.138}$$

$$\frac{\partial g_{i,2}}{\partial f_i} = \frac{\partial \Delta I_{m,i}}{\partial f_i} = (\frac{P_i(e_i^2 - f_i^2) + 2e_i f_i Q_i}{(e_i^2 + f_i^2)^2}) - G_{ii} \tag{2.139}$$

$$\frac{\partial g_{i,3}}{\partial e_i} = -2e_i \tag{2.140}$$

$$\frac{\partial g_{i,3}}{\partial f_i} = -2f_i \tag{2.141}$$

$$\frac{\partial g_{i,1}}{\partial Q_i} = \frac{\partial \Delta I_{r,i}}{\partial Q_i} = \frac{f_i}{e_i^2 + f_i^2} \tag{2.142}$$

$$\frac{\partial g_{i,2}}{\partial Q_i} = \frac{\partial \Delta I_{m,i}}{\partial Q_i} = -\frac{e_i}{e_i^2 + f_i^2} \tag{2.143}$$

$$\frac{\partial g_{i,3}}{\partial Q_i} = 0 \tag{2.144}$$

and the off-diagonal elements are

$$\frac{\partial g_{i,1}}{\partial e_j} = \frac{\partial \Delta I_{r,i}}{\partial e_j} = -G_{ij} \tag{2.145}$$

$$\frac{\partial g_{i,1}}{\partial f_j} = \frac{\partial \Delta I_{r,i}}{\partial f_j} = B_{ij} \tag{2.146}$$

$$\frac{\partial g_{i,2}}{\partial e_j} = \frac{\partial \Delta I_{m,i}}{\partial e_j} = -B_{ij} \tag{2.147}$$

$$\frac{\partial g_{i,2}}{\partial f_j} = \frac{\partial \Delta I_{m,i}}{\partial f_j} = -G_{ij} \tag{2.148}$$

$$\frac{\partial g_{i,1}}{\partial Q_j} = \frac{\partial \Delta I_{r,i}}{\partial Q_j} = 0 \tag{2.149}$$

$$\frac{\partial g_{i,2}}{\partial Q_j} = \frac{\partial \Delta I_{m,i}}{\partial Q_j} = 0 \tag{2.150}$$

$$\frac{\partial g_{i,3}}{\partial e_j} = 0 \tag{2.151}$$

$$\frac{\partial g_{i,3}}{\partial f_j} = 0 \tag{2.152}$$

$$\frac{\partial g_{i,3}}{\partial Q_j} = 0 \tag{2.153}$$

The basic characteristic of the Jacobian matrix obtained by the above process is that the off-diagonal block submatrices are dependent only on the bus admittance matrix elements which are constant. On the other hand, the diagonal elements have additional terms that have to be computed at every iteration step.

Following the idea of "current mismatch" some other researchers have attempted to extend the model in order to capture more features of the power flow problem, so as to improve its performance. One of the major contributions towards this extension has been done by the authors of [14], in which a modified proposition of a NR formulation based on current injections written in rectangular coordinates for both generator (PV) and load (PQ) buses is presented. The main differences are the polynomial representation of the active and reactive power, instead of the more simplified form already known in Bacher's formulation, as well as the new approach concerning the PV bus power flow equations.

The basic mathematical formulation for the current mismatch vectors begins with the complex current mismatch at a given PQ bus k given by

$$\Delta I_k = \frac{P_k^{sp} + Q_k^{sp}}{E_k^*} - \sum_{i=1}^{n} Y_k i E_i = 0 \tag{2.154}$$

where

$$\Delta P_k^{sp} = P_{G,k} - P_{L,k} \tag{2.155}$$

$$\Delta Q_k^{sp} = Q_{G,k} - Q_{L,k} \tag{2.156}$$

After manipulation the current mismatch vector is separated into real and imaginary part as follows

$$\Delta I_{rk} = \frac{P_k^{sp} V_{rk} + Q_k^{sp} V_{mk}}{V_{rk}^2 + V_{mk}^2} - \sum_{i=1}^{n} (G_{ki} V_{ri} - B_{ki} V_{mi}) = 0 \tag{2.157}$$

$$\Delta I_{mk} = \frac{P_k^{sp} V_{mk} - Q_k^{sp} V_{rk}}{V_{rk}^2 + V_{mk}^2} - \sum_{i=1}^{n} (G_{ki} V_{mi} + B_{ki} V_{ri}) = 0 \tag{2.158}$$

which can be written in a more compact form as

$$\Delta I_{rk} = I_{rk}^{sp} - I_{rk}^{calc} \tag{2.159}$$

$$\Delta I_{mk} = I_{mk}^{sp} - I_{mk}^{calc} \tag{2.160}$$

The above equations can take the alternative form

$$\Delta I_{rk} = \frac{(P_{Gk} - P_{Lk})V_{rk} + (Q_{Gk} - Q_{Lk})V_{mk}}{V_k^2} - I_{rk} = 0 \tag{2.161}$$

$$\Delta I_{mk} = \frac{(P_{Gk} - P_{Lk})V_{mk} - (Q_{Gk} - Q_{Lk})V_{rk}}{V_k^2} - I_{mk} = 0 \tag{2.162}$$

The power mismatches are as follows

$$\Delta P_k = P_k^{sp} - P_k^{calc} \tag{2.163}$$

$$\Delta Q_k = Q_k^{sp} - Q_k^{calc} \tag{2.164}$$

where

$$P_k^{calc} = V_{rk} I_{rk}^{calc} + V_{mk} I_{mk}^{calc} \tag{2.165}$$

$$Q_k^{calc} = V_{mk} I_{rk}^{calc} - V_{rk} I_{mk}^{calc} \tag{2.166}$$

By manipulating equations 2.163, 2.164, 2.165 and 2.166 and substituting to equations 2.159 and 2.160 the current mismatch equations can be rearranged as follows

$$\Delta I_{rk} = \frac{V_{rk}\Delta P_k + V_{mk}\Delta Q_k}{V_k^2} \tag{2.167}$$

$$\Delta I_{mk} = \frac{V_{mk}\Delta P_k + V_{rk}\Delta Q_k}{V_k^2} \tag{2.168}$$

where

$$V_k^2 = V_{rk}^2 + V_{mk}^2 \tag{2.169}$$

where the following notation has been used for the above equations

$V_{rk} + jV_{mk}$ is the voltage at bus k
$\Delta V_{rk} + j\Delta V_{mk}$ is the complex voltage mismatch at bus k
$\Delta I_{rk} + j\Delta I_{mk}$ is the complex current mismatch at bus k
$I_{rk}^{sp} + jI_{mk}^{sp}$ is the net scheduled current at bus k
$I_{rk}^{calc} + jI_{mk}^{calc}$ is the calculated current at bus k
$P_{Gk} + jQ_{Gk}$ is the complex power generated at bus k
$P_{Lk} + jQ_{Lk}$ is the complex power consumed at bus k
$P_k^{sp} + jQ_k^{sp}$ is the net scheduled complex power at bus k
$P_k^{calc} + jQ_k^{calc}$ is the calculated complex power at bus k
$\Delta P_k + j\Delta Q_k$ is the complex power mismatch at bus k
$G_{km} + JB_{km}$ is the (k,m)th element of the bus admittance matrix
δ_k, V_k is the voltage magnitude and phase angle at bus k
$\Delta\delta, \Delta V$ are the voltage magnitude and angle mismatches
$Ek^* = V_k e^- j\delta_k$ complex conjugate voltage phasor at bus k
n is the number of buses
h is the number of iterations

The two equations 2.159 and 2.160 are the PQ bus current mismatches which constitute the control variables for the current mismatch NRPF and are used in the left hand side of the power flow algorithm as it will be shown later on. They will be used for the calculation of the voltage rectangular vector, which is the state variable.

The Jacobian matrix has the form of current mismatches instead of power mismatches related to the state variables being the bus voltage real and imaginary part (rectangular coordinates). The calculation of real and imaginary current mismatches is straightforward for PQ buses because the associated real and reactive power mismatches are known. These calculations are needed so as the voltage mismatches can then be calculated by solving the equations of the NR Jacobian formulation, relating current to voltage mismatches.

For PV buses a quite different approach is introduced by an additional linearized equality constraint imposing that the voltage mismatch is zero for a PV bus. The new power

equations contain the reactive power mismatch as a control variable replacing the voltage real part mismatch. This seems to follow the same concept introduced in the power mismatch rectangular form NRPF. The interested reader is referred to the specific paper to get a clear understanding of matrix manipulations needed in order to describe the PV bus power flow formulation.

The final linear matrix equation involving the Jacobian matrix is now the following

$$\begin{bmatrix} \Delta I_{m1} \\ \Delta I_{r1} \\ \Delta I_{m2} \\ \Delta I_{r2} \\ \cdots \\ \vdots \\ \cdots \\ \Delta I_{mk} \\ \Delta I_{rk} \end{bmatrix} = \begin{bmatrix} J_{11} & J_{12} & \cdots & J_{1k} \\ J_{21} & J_{22} & \cdots & J_{2k} \\ \cdots & \cdots & \cdots & \cdots \\ \vdots & \vdots & \vdots & \vdots \\ \cdots & \cdots & \cdots & \cdots \\ J_{k1} & J_{k2} & \cdots & J_{kk} \end{bmatrix} \begin{bmatrix} \Delta V_{r1} \\ \Delta V_{m1} \\ \Delta V_{r2} \\ \Delta V_{m2} \\ \cdots \\ \vdots \\ \cdots \\ \Delta V_{rk} \\ \Delta V_{mk} \end{bmatrix} \tag{2.170}$$

which in a more analytical formulation is expressed as follows,

$$\begin{bmatrix} \Delta I_{m1} \\ \Delta I_{r1} \\ \cdots \\ \vdots \\ \cdots \\ \Delta I_{mk} \\ \Delta I_{rk} \\ \cdots \\ \vdots \\ \cdots \\ \Delta I_{mp} \\ \Delta I_{rp} \\ \cdots \\ \vdots \\ \cdots \\ \Delta V_p^2 \end{bmatrix} = \begin{bmatrix} \frac{\partial \Delta I'_{m1}}{\partial V_{r1}} & \frac{\partial \Delta I'_{m1}}{\partial V_{m1}} & \cdots & B_{1k} & G_{1k} & \cdots & B_{1p} & G_{1p} & \cdots & 0 \\ \frac{\partial \Delta I'_{r1}}{\partial V_{r1}} & \frac{\partial \Delta I'_{r1}}{\partial V_{m1}} & \cdots & G_{1k} & -B_{1k} & \cdots & G_{1p} & -B_{1p} & \cdots & 0 \\ \vdots & \vdots & \vdots & \vdots & \vdots & \vdots & \vdots & \vdots & \vdots & \vdots \\ B_{k1} & G_{k1} & \cdots & \frac{\partial \Delta I'_{mk}}{\partial V_{rk}} & \frac{\partial \Delta I'_{mk}}{\partial V_{mk}} & \cdots & G_{kp} & -B_{kp} & \cdots & 0 \\ G_{k1} & -B_{k1} & \cdots & \frac{\partial \Delta I'_{rk}}{\partial V_{rk}} & \frac{\partial \Delta I'_{rk}}{\partial V_{mk}} & \cdots & B_{kp} & G_{kp} & \cdots & 0 \\ \vdots & \vdots & \vdots & \vdots & \vdots & \vdots & \vdots & \vdots & \vdots & \vdots \\ B_{p1} & G_{p1} & \cdots & B_{pk} & G_{pk} & \cdots & \frac{\partial \Delta I'_{mp}}{\partial V_{rp}} & \frac{\partial \Delta I'_{mp}}{\partial V_{mp}} & \cdots & \frac{V_{rp}}{V_p^2} \\ G_{p1} & -B_{p1} & \cdots & G_{pk} & -B_{pk} & \cdots & \frac{\partial \Delta I'_{rp}}{\partial V_{rp}} & \frac{\partial \Delta I'_{rp}}{\partial V_{mp}} & \cdots & \frac{-V_{mp}}{V_p^2} \\ \vdots & \vdots & \vdots & \vdots & \vdots & \vdots & \vdots & \vdots & \vdots & \vdots \\ 0 & 0 & \cdots & 0 & 0 & \cdots & 2V_{rp} & 2V_{mp} & 0 & 0 \end{bmatrix} \begin{bmatrix} \Delta V_{r1} \\ \Delta V_{m1} \\ \cdots \\ \vdots \\ \cdots \\ \Delta V_{rk} \\ \Delta V_{mk} \\ \cdots \\ \vdots \\ \cdots \\ \Delta V_{rp} \\ \Delta V_{mp} \\ \cdots \\ \vdots \\ \cdots \\ \Delta Q_{Gp} \end{bmatrix} \tag{2.171}$$

By using a polynomial representation for the load power in the form

$$P_{D,k} = P_{0,k}(a_p + b_p V_k + c_p V_k^2) \tag{2.172}$$

$$Q_{D,k} = Q_{0,k}(a_q + b_q V_k + c_q V_k^2) \tag{2.173}$$

where

$$a_p + b_p + c_p = 1 \tag{2.174}$$

$$a_q + b_q + c_q = 1 \tag{2.175}$$

the diagonal elements of the Jacobian matrix 2.171 take the form

$$\left[Y_{kk}^*\right] = \begin{bmatrix} B_{kk} - a_k & G_{kk} - b_k \\ G_{kk} - c_k & -B_{kk} - d_k \end{bmatrix} = \begin{bmatrix} \frac{\partial \Delta I'_{m,i}}{\partial V_{r,i}} & \frac{\partial \Delta I'_{m,i}}{\partial V_{m,i}} \\ \frac{\partial \Delta I'_{r,i}}{\partial V_{r,i}} & \frac{\partial \Delta I'_{r,i}}{\partial V_{m,i}} \end{bmatrix} \tag{2.176}$$

where the terms a_k,b_k, c_k, d_k are given by,

$$a_k = \frac{Q'_k(V_{r,k}^2 - V_{m,k}^2) - 2V_{r,k}V_{m,k}P'_k}{V_k^4} + \frac{V_{r,k}V_{m,k}P_{0,k}b_p + Q_{0,k}b_q V_{m,k}^2}{V_k^3} + Q_{0,k}c_q \tag{2.177}$$

$$b_k = \frac{P'_k(V_{r,k}^2 - V_{m,k}^2) + 2V_{r,k}V_{m,k}Q'_k}{V_k^4} - \frac{V_{r,k}V_{m,k}Q_{0,k}b_q + P_{0,k}b_p V_{r,k}^2}{V_k^3} - P_{0,k}c_p \tag{2.178}$$

$$c_k = \frac{P'_k(V_{m,k}^2 - V_{r,k}^2) - 2V_{r,k}V_{m,k}Q'_k}{V_k^4} + \frac{V_{r,k}V_{m,k}Q_{0,k}b_q - P_{0,k}b_p V_{m,k}^2}{V_k^3} - P_{0,k}c_p \tag{2.179}$$

$$d_k = \frac{Q'_k(V_{r,k}^2 - V_{m,k}^2) - 2V_{r,k}V_{m,k}P'_k}{V_k^4} + \frac{V_{r,k}V_{m,k}P_{0,k}b_p - Q_{0,k}b_q V_{r,k}^2}{V_k^3} - Q_{0,k}c_q \tag{2.180}$$

where

$$P'_k = P_{G,k} - P_{0,k}a_p \tag{2.181}$$

$$Q'_k = Q_{G,k} - Q_{0,k}a_q \tag{2.182}$$

while the same terms, for only constant power load are expressed as

$$a_k = d_k = \frac{Q'_k(V_{r,k}^2 - V_{m,k}^2) - 2V_{r,k}V_{m,k}P'_k}{V_k^4} \tag{2.183}$$

$$b_k = -c_k = \frac{P'_k(V_{r,k}^2 - V_{m,k}^2) + 2V_{r,k}V_{m,k}Q'_k}{V_k^4} \tag{2.184}$$

The off-diagonal elements of the current mismatch Jacobian matrix are given as

$$\left[Y_{km}^*\right] = \begin{bmatrix} B_{km} & G_{km} \\ G_{km} & -B_{km} \end{bmatrix} \tag{2.185}$$

An important feature of the particular formulation is that most of the 2×2 blocks of the Jacobian matrix remain unchanged during the solution process. In other words, the off-diagonal elements are constant and equal to the terms of nodal admittance matrix except for PV buses whose elements are obtained with a little more effort. The representation does not include non linear terms like sine and cosine calculated at each iteration.

Considering PV buses the current mismatches are given by

$$\Delta I_{m,k}^* = \frac{V_{m,k}\Delta P_k}{V_k^2} \tag{2.186}$$

$$\Delta I_{r,k}^* = \frac{V_{r,k}\Delta P_k}{V_k^2} \tag{2.187}$$

thus the $2x2$ diagonal block submatrices have the form

$$\begin{bmatrix} \Delta I_{m,k}^* \\ \Delta I_{r,k}^* \end{bmatrix} = \begin{bmatrix} \frac{V_{m,k}\Delta P_k}{V_k^2} \\ \frac{V_{r,k}\Delta P_k}{V_k^2} \end{bmatrix} = \begin{bmatrix} (G_{kk} - b_k) - \frac{(B_{kk} - a_k)V_{m,k}}{V_{r,k}} & \frac{V_{r,k}}{V_k^2} \\ (-B_{kk} - d_k) - \frac{(G_{kk} - c_k)V_{m,k}}{V_{r,k}} & \frac{V_{m,k}}{V_k^2} \end{bmatrix} \begin{bmatrix} \Delta V_{m,k} \\ \Delta Q_k \end{bmatrix} \tag{2.188}$$

When dealing with PV buses the diagonal elements have the form

$$\left[Y_{kk}^{**}\right] = \begin{bmatrix} (G_{kk} - b_k) - \frac{(B_{kk} - a_k)V_{m,k}}{V_{r,k}} & \frac{V_{r,k}}{V_k^2} \\ (-B_{kk} - d_k) - \frac{(G_{kk} - c_k)V_{m,k}}{V_{r,k}} & -\frac{V_{m,k}}{V_k^2} \end{bmatrix} \tag{2.189}$$

The off-diagonal elements of a PV bus connected to a branch $k - l$ are given by

$$\left[Y_{lk}^{**}\right] = \begin{bmatrix} G_{lk} - \frac{B_{lk}V_{m,k}}{V_{r,k}} & 0 \\ -B_{lk} - \frac{G_{lk}V_{m,k}}{V_{r,k}} & 0 \end{bmatrix} \tag{2.190}$$

and

$$\left[Y_{kl}^{**}\right] = \begin{bmatrix} B_{kl} & G_{kl} \\ G_{kl} & -B_{kl} \end{bmatrix} \tag{2.191}$$

Finally when a PV bus is connected to a PQ bus the $2x2$ diagonal block submatrices are computed by

$$\left[Y_{kl}^{**}\right] = \begin{bmatrix} B_{kl} & G_{kl} \\ G_{kl} & -B_{ii} \end{bmatrix} \tag{2.192}$$

The proposed NR algorithm for for a case where a PV bus k is connected to PQ buses i, l can take the form

$$\begin{bmatrix} \vdots \\ \Delta I_{m,i}^* \\ \Delta I_{r,i}^* \\ \Delta I_{m,k}^* \\ \Delta I_{r,k}^* \\ \Delta I_{m,l}^* \\ \Delta I_{r,l}^* \\ \vdots \end{bmatrix} = \begin{bmatrix} \vdots & \vdots & \vdots & \vdots & \vdots \\ \cdots & Y_{i,i}^* & Y_{i,k}^* & Y_{i,l}^* & \cdots \\ \cdots & Y_{k,i}^* & Y_{k,k}^{**} & Y_{k,l}^* & \cdots \\ \cdots & Y_{l,i}^* & Y_{l,k}^{**} & Y_{l,l}^* & \cdots \\ \vdots & \vdots & \vdots & \vdots & \vdots \end{bmatrix} \begin{bmatrix} \vdots \\ \Delta V_{r,i} \\ \Delta V_{m,i} \\ \Delta V_{m,k} \\ \Delta Q_k \\ \Delta V_{r,l} \\ \Delta V_{m,l} \\ \vdots \end{bmatrix} \tag{2.193}$$

where

$Y_{i,i}^*$ and $Y_{l,l}^*$ are calculated by use of 2.176
$Y_{i,l}^*$ and $Y_{l,i}^*$ are calculated by use of 2.185

$Y^{*}{*}_{k,k}$ is calculated by use of 2.189
$Y^{*}_{i,k}$ is calculated by use of 2.190
$Y^{*}_{k,i}$ and $Y^{*}_{k,l}$ iare calculated by use of 2.192 or 2.185
$Y^{**}_{l,k}$ is calculated by use of 2.191

The iterative process consists, after the initialization process, of calculating current mismatches from equations 2.167 and 2.168 to be used for calculating the bus voltage corrections using the matrix equation 2.171. After that an update of the state variable is expressed by equations

$$V_r^{h+1} = V_r^h + \Delta V_r^h \tag{2.194}$$

$$V_m^{h+1} = V_m^h + \Delta V_m^h \tag{2.195}$$

which can also be written in polar form as

$$V_k^{h+1} = V_k^h + \Delta V_k^h \tag{2.196}$$

$$\delta_k^{h+1} = \delta_k^h + \Delta \delta_k^h \tag{2.197}$$

where

$$\Delta V_k = \frac{V_{rk}}{V_k}\Delta V_{rk} + \frac{V_{mk}}{V_k}\Delta V_{rk} \tag{2.198}$$

$$\Delta \delta_k = \frac{V_{rk}}{V_k^2}\Delta V_{mk} - \frac{V_{mk}}{V_k^2}\Delta V_{rk} \tag{2.199}$$

In addition the reactive power generation at each PV bus which can be initialized as zero, can be updated by

$$Q_G^{h+1} = Q_G^h + \Delta Q_G^h \tag{2.200}$$

The iterative process stops when it reaches the maximum number of iterations.

Simulation results show the speed of convergence being superior compared to the polar form conventional AC NR method.

2.4.5.1 Current Injections Alternative Formulations

Case I The same authors in [15], extend the applicability of the above current mismatch method to handle three phase unbalanced power networks, creating an algorithm that can be utilized for solving power flow problems in distribution systems (which are handled as unbalanced) and is thus already used by software packages like GridlaD.

Case II A further development of the current mismatch power flow method is proposed by the same authors in [16] in which, easier incorporation of control device models and power flow controls of any kind is allowed. The formulation also directly incorporates more realistic modelling of power system components such as static VAR compensators, TCSC and voltage control through multiple reactive sources. The current injection equations are used for both PQ and PV buses. For each PV bus a new variable (Q) is introduced and an equation that imposes the bus voltage constraint is also formulated. This leads to a Jacobian matrix in which the 2×2 off-diagonal blocks equal to those of the bus admittance matrix, independent of the bus type to be considered. The elements of the 2×2 diagonal blocks are modified at each iteration according to the load model being considered. The proposed method is an augmented formulation of the conventional CIM that starts by first expressing voltage phase angle as

$$\delta_k = \tan^{-1} \frac{V_{m_k}}{V_{r_k}} \tag{2.201}$$

whose linearised form is

$$\Delta\delta_k = \frac{V_{r_k}}{V_k^2}\Delta V_{m_k} - \frac{V_{m_k}}{V_k^2}\Delta V_{r_k} \tag{2.202}$$

The well-established CIM is described by the analytical matrix formulation 2.170 in which the Jacobian matrix with J_{ij} submatrices can be writen in the form

$$\Big[Y\Big] = \begin{bmatrix} Y_{11} & Y_{12} & \cdots & Y_{1k} \\ Y_{21} & Y_{22} & \cdots & Y_{2k} \\ \cdots & \cdots & \cdots & \cdots \\ \vdots & \vdots & \vdots & \vdots \\ \cdots & \cdots & \cdots & \cdots \\ Y_{k1} & Y_{k2} & \cdots & Y_{kk} \end{bmatrix} \tag{2.203}$$

For describing that the reactive power is an unknown so in that sense a dependent variable an additional equation is introduced for voltage

$$V_k^2 = V_{r_k}^2 + V_{m_k}^2 \tag{2.204}$$

whose linearised form is

$$\Delta V_k = \frac{V_{r_k}}{V_k}\Delta V_{r_k} + \frac{V_{m_k}}{V_k}\Delta V_{m_k} \tag{2.205}$$

where V_{r_k}, V_{m_k} are the real and imaginary part of the voltage phasor.

Equations 2.205, 2.202 and 2.203 can be written in matrix form as follows:

$$\begin{bmatrix} 0 \\ 0 \\ \Delta\delta \\ \Delta V \end{bmatrix} = \begin{bmatrix} Y^* & B \\ C & 0 \end{bmatrix} \begin{bmatrix} \Delta V_m \\ \Delta V_r \\ \Delta P \\ \Delta Q \end{bmatrix} \tag{2.206}$$

which can also be written as

$$\begin{bmatrix} 0 \\ \Delta_{\delta V} \end{bmatrix} = \begin{bmatrix} Y^* & B \\ C & 0 \end{bmatrix} \begin{bmatrix} \Delta V_{rm} \\ \Delta_{PQ} \end{bmatrix} \tag{2.207}$$

where Y^* is the matrix given by 2.203,

and the matrices B and C are given as

$$\Big[B\Big] = \begin{bmatrix} B_1 & & & \\ & B_2 & & \\ & & \ddots & \\ & & & B_n \end{bmatrix} \tag{2.208}$$

$$\Big[C\Big] = \begin{bmatrix} C_1 & & & \\ & C_2 & & \\ & & \ddots & \\ & & & C_n \end{bmatrix} \tag{2.209}$$

where each of the above elements is a block $2x2$ submatrix of the form

$$\Big[B_i\Big] = \begin{bmatrix} -\frac{V_{m_i}}{V_i^2} & \frac{V_{r_i}}{V_i^2} \\ -\frac{V_{r_i}}{V_i^2} & -\frac{V_{m_i}}{V_i^2} \end{bmatrix} \tag{2.210}$$

$$\Big[C_i\Big] = \begin{bmatrix} -\frac{V_{m_i}}{V_i^2} & \frac{V_{r_i}}{V_i^2} \\ -\frac{V_{r_i}}{V_i} & -\frac{V_{m_i}}{V_i} \end{bmatrix} \tag{2.211}$$

$$\left[\Delta_{\delta V}\right] = \left[\Delta\delta_1 \quad \Delta V_1 \quad \Delta\delta_2 \quad \Delta V_2 \ldots \Delta\delta_n \quad \Delta V_n\right] \tag{2.212}$$

$$\left[\Delta_{PQ}\right] = \left[\Delta P_1 \quad \Delta Q_1 \quad \Delta P_2 \quad \Delta Q_2 \ldots \Delta P_n \quad \Delta Q_n\right] \tag{2.213}$$

$$\left[\Delta V_{rm}\right] = \left[\Delta V_{r_1} \quad \Delta V_{m_1} \quad \Delta V_{r_2} \quad \Delta V_{m_2} \ldots \Delta V_{r_n} \quad \Delta V_{m_n}\right] \tag{2.214}$$

The term ΔV_{rm} is eliminated by equation 2.207, so the remaining term is

$$\Delta_{\delta V} = J_{red}^{-1}\Delta_{PQ} \tag{2.215}$$

where

$$J_{red}^{-1} = -CY *^{-1} B \tag{2.216}$$

Equation 2.207, shows that the system to be solved is augmented since unlike the conventional CIM definition it engages not only the voltage mismatches ΔV_r and ΔV_m, as state variables bus the mismatches ΔP and ΔQ for PQ buses or ΔQ for PV buses. This leads to a two step solution procedure with the following algorithm:

1. step 1: first the following matrix equation is solved for the state variables ΔV_r as well as ΔV_m

$$\begin{bmatrix} 0 \\ \Delta_{PQ} \end{bmatrix} = \begin{bmatrix} Y^* & B \\ 0 & I \end{bmatrix} \begin{bmatrix} \Delta V_{rm} \\ \Delta_{PQ} \end{bmatrix} \tag{2.217}$$

   where I is the identity matrix

2. step 2: Since ΔV_r as well as ΔV_m have been computed the remaining state variables, that is $\Delta_{\delta V}$ are determined by the following expression

$$\Delta_{\delta V} = C\Delta V_{rm} \tag{2.218}$$

   Updating the solution by

$$V^{h+1} = V^h + \Delta V^h \tag{2.219}$$

$$\delta^{h+1} = \delta^h + \Delta\delta^h \tag{2.220}$$

terminates when the predefined tolerances criteria are satisfied.

The above procedure is also applied on a on-load tap changing transformer as well as a phase shifting transformer, giving the opportunity to involve flow regulating devices in the power flow formulation problem. So a more realistic modelling of power system components through multiple reactive sources can be incorporated in power flow solutions. The method maintains all the advantages of the conventional CIM having non-diagonal constant value elements, thus accelerating the whole iterative procedure and keeping the convergence rate characteristics.

Case III A comparative analysis of the three most popular NRPF methods, namely the polar form of NR, the rectangular form of NR and the current mismatch NR is presented in [17]. The paper presents the mathematical formulation of each method around the differences in the Jacobian matrix expression as well as the representation of PV buses. It presents a general algorithm which can be used for each method and compares the methods by simulations of well-conditioned systems, ill-conditioned systems and systems with high loading. For well-conditioned systems all methodologies present a very similar performance, meaning that they converge for the same solution with basically the same number of iterations. The three techniques present a good convergence pattern and therefore they are all good candidates for solving the well-conditioned power flow problem. Test results concerning the convergence performance of the three compared methods are presented in the following figures 2.17, 2.18, 2.19 for three test cases. However, their performance is different for ill-conditioned systems. In that case simulations show that the polar NR formulation fails to converge, while the rectangular NR form and the current injection converge in all situations. Moreover, even when the methodologies converge, they do not often achieve a single solution. When higher loading power flow systems are of concern, the polar and the current injection forms present a similar performance while the rectangular form may or may not be a successful tool for solving this kind of problem. Test results are presented in figures 2.20 and 2.21 The paper concludes that each methodology must be considered as a promising candidate to satisfactorily solve the power flow problem.

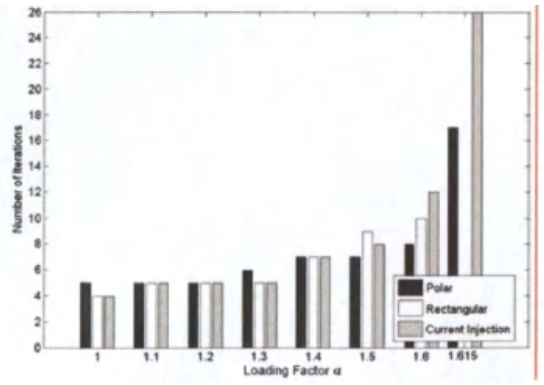

FIGURE 2.17: Convergence characteristics as a function of loading factor - IEEE118

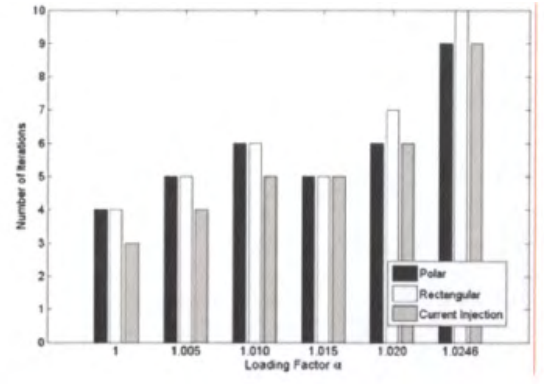

FIGURE 2.18: Convergence characteristics as a function of loading factor - IEEE300

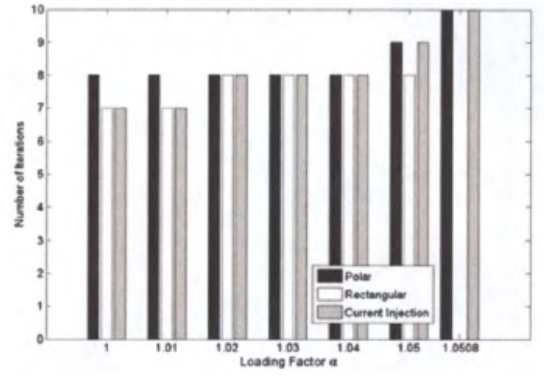

FIGURE 2.19: Convergence characteristics as a function of loading factor - IEEE730

Case IV In [18] the authors propose a novel method for representing PV buses in current mismatch injections. The Jacobian matrix expression uses a combination between two NR techniques. This combination involves PQ buses represented as revised NR current injection load flow buses, based on real and imaginary parts of current injection, while PV buses are represented using power injection mismatches formulation. The combined power and current injection mismatches

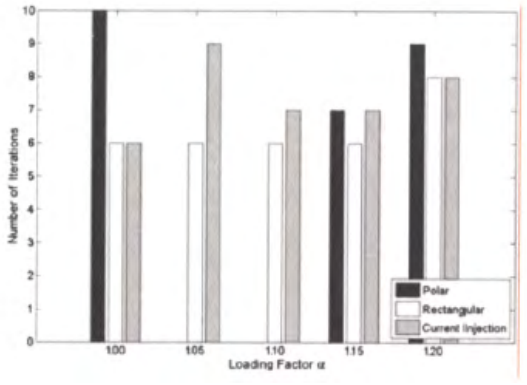

FIGURE 2.20: Convergence characteristics as a function of loading factor - 11-bus with $Q_g = 120MVar$

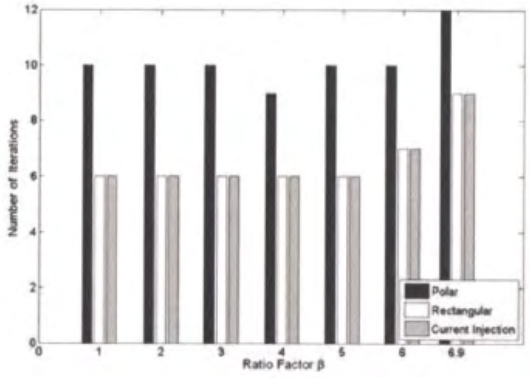

FIGURE 2.21: Convergence characteristics as a function of R/X ratio - 11-bus with $Q_g = 120MVar$

load flow formulation can be calculated by the matrix equation

$$\begin{bmatrix} \Delta I_{m1} \\ \Delta I_{r1} \\ \vdots \\ \vdots \\ \Delta P_k \\ \vdots \\ \vdots \\ \Delta I_{mn} \\ \Delta I_{rn} \end{bmatrix} = \begin{bmatrix} \frac{\partial I_{m1}}{\partial V_{r1}} & \frac{\partial I_{m1}}{\partial V_{m1}} & \cdots & \cdots & \frac{\partial I_{m1}}{\partial \delta_k} & \cdots & \cdots & \frac{\partial I_{m1}}{\partial V_{rn}} & \frac{\partial I_{m1}}{\partial V_{mn}} \\ \frac{\partial I_{r1}}{\partial V_{r1}} & \frac{\partial I_{r1}}{\partial V_{m1}} & \cdots & \cdots & \frac{\partial I_{r1}}{\partial \delta_k} & \cdots & \cdots & \frac{\partial I_{r1}}{\partial V_{rn}} & \frac{\partial I_{r1}}{\partial V_{mn}} \\ \vdots & \vdots & \vdots & \vdots & \vdots & \vdots & \vdots & \vdots & \vdots \\ \vdots & \vdots & \vdots & \vdots & \vdots & \vdots & \vdots & \vdots & \vdots \\ \frac{\partial P_k}{\partial V_{r1}} & \frac{\partial P_k}{\partial V_{m1}} & \cdots & \cdots & \frac{\partial P_k}{\partial \delta_k} & \cdots & \cdots & \frac{\partial P_k}{\partial V_{rn}} & \frac{\partial P_k}{\partial V_{mn}} \\ \vdots & \vdots & \vdots & \vdots & \vdots & \vdots & \vdots & \vdots & \vdots \\ \vdots & \vdots & \vdots & \vdots & \vdots & \vdots & \vdots & \vdots & \vdots \\ \frac{\partial I_{mn}}{\partial V_{r1}} & \frac{\partial I_{mn}}{\partial V_{m1}} & \cdots & \cdots & \frac{\partial I_{mn}}{\partial \delta_k} & \cdots & \cdots & \frac{\partial I_{mn}}{\partial V_{rn}} & \frac{\partial I_{mn}}{\partial V_{mn}} \\ \frac{\partial I_{rn}}{\partial V_{r1}} & \frac{\partial I_{rn}}{\partial V_{m1}} & \cdots & \cdots & \frac{\partial I_{rn}}{\partial \delta_k} & \cdots & \cdots & \frac{\partial I_{rn}}{\partial V_{rn}} & \frac{\partial I_{rn}}{\partial V_{mn}} \end{bmatrix} \begin{bmatrix} \Delta V_{r1} \\ \Delta V_{m1} \\ \vdots \\ \vdots \\ \Delta \delta_k \\ \vdots \\ \vdots \\ \Delta V_{rn} \\ \Delta V_{mn} \end{bmatrix} \tag{2.221}$$

where the real and imaginary components of injected currents for PQ buses at a bus i are expressed as:

$$I_{ri}^{cal} = I_{ri}^{sp} - (\frac{P_i^{sp}V_{ri} + Q_i^{sp}V_{mi}}{V_{ri}^2 + V_{mi}^2}) + \sum_{j=1}^{n}(G_{ij}Vri - B_{ij}V_{mi}) \tag{2.222}$$

$$I_{mi}^{cal} = I_{mi}^{sp} - (\frac{P_i^{sp}V_{mi} - Q_i^{sp}V_{ri}}{V_{ri}^2 + V_{mi}^2}) + \sum_{j=1}^{n}(G_{ij}Vmi - B_{ij}V_{ri}) \tag{2.223}$$

At the same time the active power at a bus i is calculated by:

$$P_i^{cal} = \sum_{j=1}^{n}|V_i||V_j|(G_{ij}\cos\delta_{ij} + B_{ij}\sin\delta_{ij}) \tag{2.224}$$

The Jacobian elements in the modified combined matrix formulation, concerning PQ buses are identical to the form of the original CIM (calculated above). The relative elements for PV buses under the new formulation are given by

1. Diagonal elements

$$\frac{\partial P_i}{\partial \delta_i} = -V_i\sum_{j=1}^{n}V_i(G_{ij}\sin\delta_{ij} - B_{ij}\cos\delta_{ij}) \tag{2.225}$$

2. Off-diagonal elements

$$\frac{\partial I_{mi}}{\partial \delta_j} = V_j(G_{ij}\cos\delta_j - B_{ij}\sin\delta_j) \tag{2.226}$$

$$\frac{\partial I_{ri}}{\partial \delta_j} = V_j(G_{ij}\sin\delta_j + B_{ij}\cos\delta_j) \tag{2.227}$$

$$\frac{\partial P_j}{\partial V_{mi}} = V_j(G_{ji}\sin\delta_j - B_{ji}\cos\delta_j) \tag{2.228}$$

$$\frac{\partial P_j}{\partial V_{ri}} = V_j(G_{ji}\cos\delta_j + B_{ji}\sin\delta_j) \tag{2.229}$$

The above partial derivatives have been obtained by equations 2.222 and 2.223, if in these equations the variables V_r and V_m take the forms $V_r = V\cos\delta$ and $V_m = V\sin\delta$.

According to the authors it is evident that the Jacobian elements related to PQ buses are not changed in this combined formulation, where the off-diagonal elements and a few diagonal elements are constant and equal to the terms of the admittance matrix (see above formulations of CIM method). Only the PV buses elements are modified and also only one equation is required for PV bus representation. In the following figures 2.22, 2.23, 2.24, and 2.25 a comparison analysis

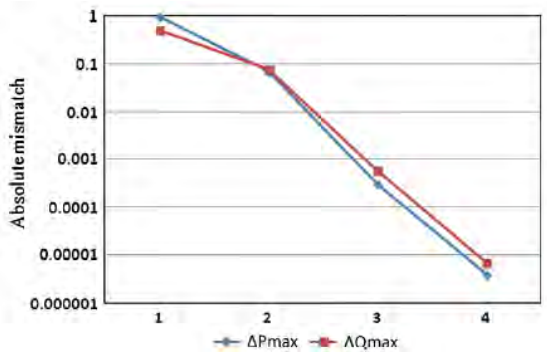

FIGURE 2.22: Convergence characteristics of IEEE 30-bus system with conventional NR

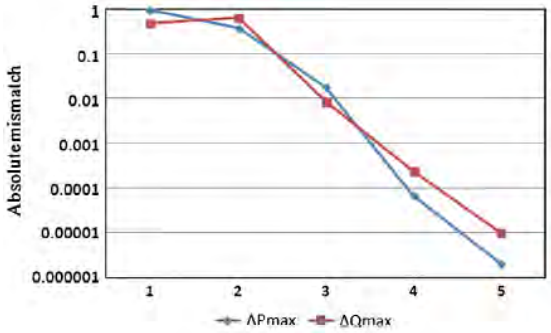

FIGURE 2.23: Convergence characteristics of IEEE 30-bus system with the proposed CIM NR

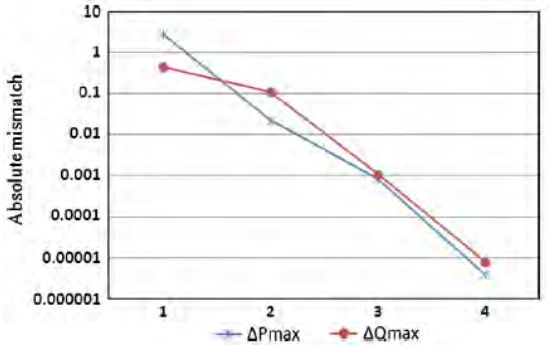

FIGURE 2.24: Convergence characteristics of IEEE 57-bus system with conventional NR

concerning convergence characteristics is presented for two test-cases a 30-bus system and a 57-bus system

The contribution of the proposed method, as the final conclusion, is that an improved and simpler PV bus representation is capable of reducing the required number of equations, while improving convergence characteristics in case of high loading and high R/X ratios, especially for PV buses.

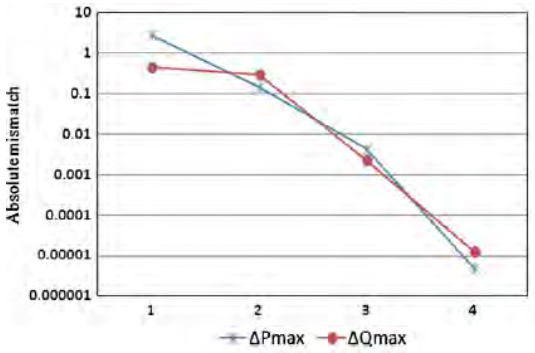

FIGURE 2.25: Convergence characteristics of IEEE 57-bus system with the proposed CIM NR

Case V In [19] the authors provide a hybrid power flow method consisting of the current balance equations in rectangular coordinates for PQ buses, which have the form

$$\frac{P_i^{inj} e_i + Q_i^{inj} f_i}{|V_i|^2} = \sum_{j=1}^{n} (G_{ij} e_j - B_{ij} f_j) \tag{2.230}$$

$$\frac{-Q_i^{inj} e_i + P_i^{inj} f_i}{|V_i|^2} = \sum_{j=1}^{n} (B_{ij} e_j + G_{ij} f_j) \tag{2.231}$$

as a consequence of

$$(\frac{S_i^{inj}}{V_i})^* = \sum_{j=1}^{n} (G_{ij} + jB_{ij}) V_j \tag{2.232}$$

and of the rectangular voltage expression

$$V_i = e_i + jf_i \tag{2.233}$$

while PV buses are represented by the rectangular coordinates of the power balance equation and an additional voltage magnitude constraint equation, which are expressed as,

$$P_i^{inj} = e_i \sum_{j=1}^{n} (G_{ij} e_j - B_{ij} f_j) + f_i \sum_{j=1}^{n} (B_{ij} e_j + G_{ij} f_j) \tag{2.234}$$

and

$$e_i^2 + f_i^2 = |V_i^{sp}|^2 \tag{2.235}$$

The proposed formulation leads to a Jacobian matrix formulation, where the Jacobian rows corresponding to PQ bus equations have constant off-diagonal terms, resulting in a significant decrease in computational time making the method more attractive for large scale power systems. The solution of the NRPF model is achieved by using LU factorization and proper variables grouping and equations ordering. Simulation tests show promising results for several test case systems. The most promising feature is the speedup of almost 2X as compared with the conventional power balance formulation.

Case VI A novel scheme of the current mismatch power flow algorithm is presented in [20]. In this paper the iterative NR method is still employed as the main solution framework. The essential difference is that the proposed algorithm is to find roots of the current mismatch equations, instead of those of the power mismatch equations. The basic idea is to reformulate the classic NRPF algorithm in terms of current mismatches dependent on the same state variables, namely the voltage magnitude and angle, which is performed by a slight modification of the Jacobian matrix. This is done by formulating the mismatch power balance equations as the current mismatch balance equations.

The proposed algorithm can be formally expressed as follows. recall that the current mismatch is expressed as

$$I_{gen,k} - I_{dem,k} - \sum_{j=1}^{n} Y_{ki} V_i = 0 \tag{2.236}$$

where

$I_{gen,k}$ is the complex vector of the bus k generation power current
$I_{dem,k}$ is the complex vector of the bus k demand load power current
Y_{ki} is the bus admittance of the line connecting buses k and i
V_i is the complex vector of bus i (denoting all the buses interconnected to bus k)

If we denote by I_k the complex net current of bus k then

$$I_k = I_{r,k} + jI_{m,k} = \frac{S^*_{gen,k} - S^*_{dem,k}}{V_k{}^*} - \sum_{j=1}^{n} Y_{ki} V_i = 0 \tag{2.237}$$

in which the complex vectors are described in polar form as,

$$V_k = |V_k| \angle \delta_k \tag{2.238}$$

$$Y_{ki} = |Y_{ki}| \angle \theta_{ki} \tag{2.239}$$

$$S_{gen,k} - S_{dem,k} = S_{sch,k} = |S_{sch,k}|\angle\phi_k \tag{2.240}$$

where

$S_{gen,k}$ is the complex power vector of generation power at bus k $S_{dem,k}$ is the complex power vector of demand power at bus k V_k is the complex vector of bus k $I_{r,k}$ is the real part of the current at bus k $I_{m,k}$ is the imaginary part of the current at bus k

Substituting expressions 2.238, 2.239 and 2.240 into equation 2.237 the following current expressions are formulated

$$I_k = \frac{|S_{sch,k}|}{|V_k|}\angle(-\phi_k + \delta_k) - \sum_{i=1}^{n}|Y_{ki}||V_i|\angle(\theta_{ki} + \delta_i) = 0 \tag{2.241}$$

$$I_{r,k} = \frac{|S_{sch,k}|}{|V_k|}\cos(-\phi_k + \delta_k) - \sum_{i=1}^{n}|Y_{ki}||V_i|\cos(\theta_{ki} + \delta_i) = 0 \tag{2.242}$$

$$I_{m,k} = \frac{|S_{sch,k}|}{|V_k|}\sin(-\phi_k + \delta_k) - \sum_{i=1}^{n}|Y_{ki}||V_i|\sin(\theta_{ki} + \delta_i) = 0 \tag{2.243}$$

By expanding the above equations 2.242 and 2.243 in a Taylor series (familiar to NR technique) and taking into consideration only the first order partial derivatives the next equations are obtained

$$I_{r,k} = \sum_{i=1^n i\neq s}\frac{\partial I_{r,k}}{\partial\delta_i}\Delta\delta_i + \sum_{i=1^n i\neq s}\frac{\partial I_{r,k}}{\partial|V_i|}\Delta|V_i| \tag{2.244}$$

$$I_{m,k} = \sum_{i=1^n i\neq s}\frac{\partial I_{m,k}}{\partial\delta_i}\Delta\delta_i + \sum_{i=1^n i\neq s}\frac{\partial I_{m,k}}{\partial|V_i|}\Delta|V_i| \tag{2.245}$$

The power flow matrix equation in the form of the NRPF with a modified Jacobian matrix is given by

$$\begin{bmatrix}\Delta I_{r,k}\\ \Delta I_{m,k}\end{bmatrix} = \begin{bmatrix}J_1 & J_2\\ J_3 & J_4\end{bmatrix}\begin{bmatrix}\Delta\delta\\ \Delta|V|\end{bmatrix} = \begin{bmatrix}\frac{\partial I_{r,k}}{\partial\delta_i} & \frac{\partial I_{r,k}}{\partial|V_i|}\\ \frac{\partial I_{m,k}}{\partial\delta_i} & \frac{\partial I_{m,k}}{\partial|V_i|}\end{bmatrix}\begin{bmatrix}\Delta\delta\\ \Delta|V|\end{bmatrix} \tag{2.246}$$

The partial derivatives of the Jacobian matrix elements diagonal and off-diagonal are obtained by the expressions

For submatrix J1 - partial derivatives of real current w.r.t. voltage phase angle

$$\frac{\partial I_{r,k}}{\partial \delta_k} = -|V_k||Y_{kk}|\sin(\theta_{kk}+\delta_k) + \frac{|S_{sch,k}|}{|V_k|}\sin(-\phi_k+\delta_k) \tag{2.247}$$

$$\frac{\partial I_{r,k}}{\partial \delta_i} = -|V_k||Y_{ki}|\sin(\theta_{ki}+\delta_i) \tag{2.248}$$

For submatrix J2 - partial derivatives of real current w.r.t. voltage magnitude

$$\frac{\partial I_{r,k}}{\partial |V_k|} = |Y_{kk}|\cos(\theta_{kk}+\delta_k) + \frac{|S_{sch,k}|}{|V_k|^2}\cos(-\phi_k+\delta_k) \tag{2.249}$$

$$\frac{\partial I_{r,k}}{\partial |V_i|} = |Y_{ki}|\cos(\theta_{ki}+\delta_i) \tag{2.250}$$

For submatrix J3 - partial derivatives of imaginary current w.r.t. voltage phase angle

$$\frac{\partial I_{m,k}}{\partial \delta_k} = |Y_{kk}||V_k|\cos(\theta_{kk}+\delta_k) - \frac{|S_{sch,k}|}{|V_k|}\cos(-\phi_k+\delta_k) \tag{2.251}$$

$$\frac{\partial I_{m,k}}{\partial \delta_i} = |Y_{ki}||V_i|\cos(\theta_{ki}+\delta_i) \tag{2.252}$$

For submatrix $J4$ - partial derivatives of imaginary current w.r.t. voltage magnitude

$$\frac{\partial I_{m,k}}{\partial |V_k|} = |Y_{kk}|\sin(\theta_{kk}+\delta_k) + \frac{|S_{sch,k}|}{|V_k|^2}\sin(-\phi_k+\delta_k) \tag{2.253}$$

$$\frac{\partial I_{m,k}}{\partial |V_k|} = |Y_{ki}|\sin(\theta_{ki}+\delta_i) \tag{2.254}$$

The iterative process is exactly the same as for the conventional NRPF with the difference that instead power mismatches, current mismatches have to be computed. The modified Jacobian matrix has the same block setting but the partial derivatives of the currents with respect to voltage magnitude and angle lead to simplified terms that contain a smaller amount of floating operations (FLOPs), i.e., lesser multiplications and divisions which means that the computational time is reduced. Numerical examples and simulation results show that the performance of the proposed algorithm is almost the same with the conventional NRPF, but the total number of operations required by the proposed NRPF is linearly proportional to the size of the Jacobian matrix, while that of the standard NRPF method is quadratic. The effectiveness of the proposed method was tested for 5

test cases, that is, a 5-bus, a 6-bus, a 24-bus a 30-bus and finally a 57-bus system. Three different processors were used for simulation purposes and are presented in the following figure 2.26

Specification of three processors used to perform the tests.

Machine ID	Machine specification
MC1	Intel pentium IV 1.5 GHz, 256 DDR-RAM
MC2	AMD Athlon (TM) XP 2000plus 1.67 GHz, 256 DDR-RAM
MC3	Duron 1.2 GHz, 384 DDR-RAM

FIGURE 2.26: Specification of three processors used to perform the tests

The following figure 2.27 shows the results for the 5 tests cases mentioned above

Simulation results of all test cases.

Case		Required iteration			Calculation time (s)			Calculation time ratio		
		MC1	MC2	MC3	MC1	MC2	MC3	MC1	MC2	MC3
TC1	SNR	5	5	5	0.025	0.016	0.016	1.563	1.600	1.455
	PNR	4	4	4	0.016	0.010	0.011	Average = 1.539		
TC2	SNR	5	5	5	0.047	0.038	0.042	1.516	1.462	1.400
	PNR	5	5	5	0.031	0.026	0.030	Average = 1.459		
TC3	SNR	7	7	7	0.616	0.305	0.359	1.124	1.151	1.122
	PNR	8	8	8	0.548	0.265	0.320	Average = 1.132		
TC4	SNR	5	5	5	0.711	0.338	0.410	1.344	1.325	1.318
	PNR	5	5	5	0.529	0.255	0.311	Average = 1.329		
TC5	SNR	4	4	4	2.438	1.856	1.991	1.794	1.681	1.709
	PNR	3	3	3	1.359	1.104	1.165	Average = 1.728		

FIGURE 2.27: Simulation results of all 5 test cases

In the following figures the solution convergence for the first two of the test cases are presented.

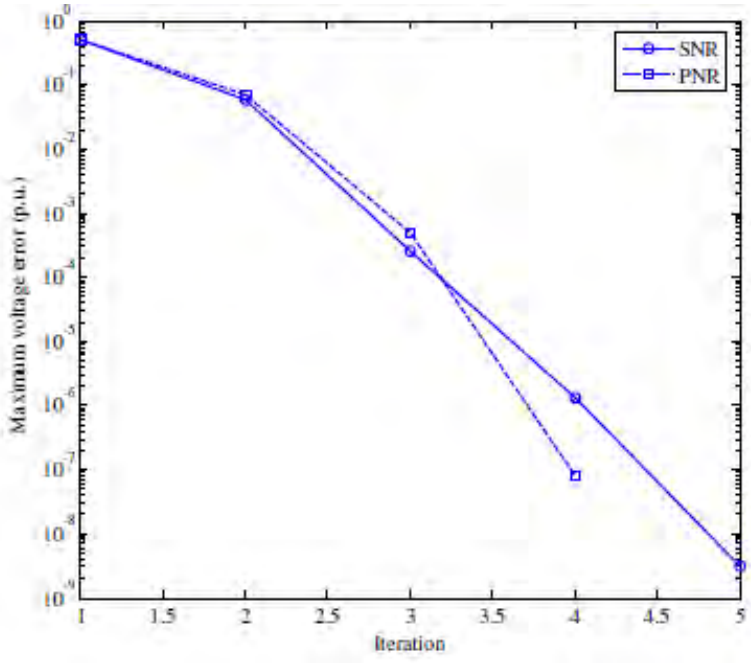

FIGURE 2.28: Solution convergence for TC1

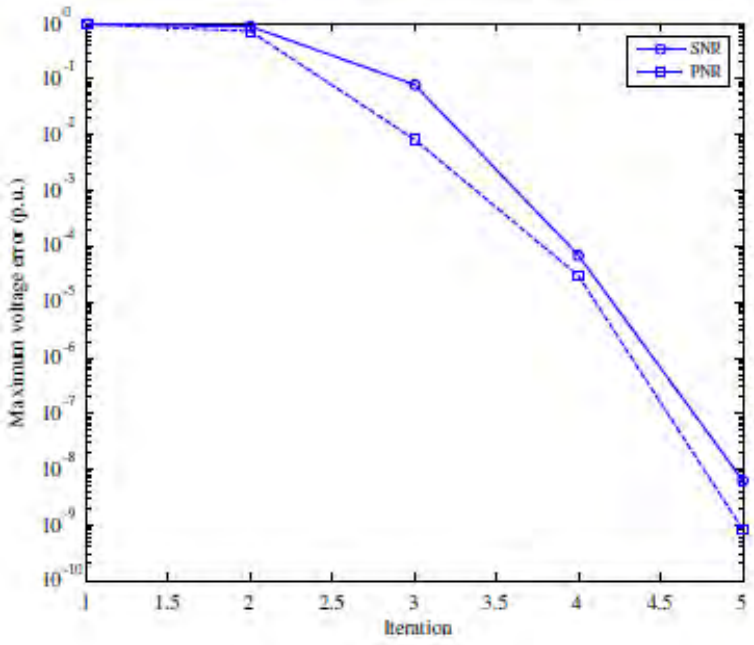

FIGURE 2.29: Solution convergence for TC2

From the above figures it is clear that the proposed method leads to improved maximum voltage error (reduced in the proposed NR method). Similar results are also apparent for the rest three test cases TC3, TC4, TC5. The proposed method could be seen as an alternative to both full polar form NRPF and current mismatch in rectangular coordinates in which current mismatch are related to the real and imaginary part of bus voltage.

2.4.6 AC Power Flow Alternatives and Extensions

Case I A new modified compared to the conventional, NR algorithm is presented is [21]. The method is called an incremental power flow algorithm (IPF) since it proposes an incremental form relating the voltage increment to the current increment through the use of the bus impedance matrix. The current mismatch consisting of the difference between the initially specified current and the calculated current is updated, at each iteration, leading to an equivalent voltage mismatch calculation. The voltage correction updates the voltage itself until a pre-specified tolerance is satisfied. The method has the advantage that it does not involve any Jacobian matrix formulation so it needs not matrix inversion. Tested in small to medium scale bus type systems the method gives good results concerning convergence characteristics compared to conventional NR and GS power flow methods.

The basic idea behind the proposed method starts with the well-known Kirchhoff's law in the form

$$I_i = \frac{S_i{}^*}{V_i{}^*} = \sum_{j=1}^{n} Y_{ij} V_j \tag{2.255}$$

Expanding the right hand side of the above equation in Taylor series the following equation is obtained

$$I_i = \frac{S_i{}^*}{V_i{}^*} = [\sum_{j=1}^{n} Y_{ij} V_j]^0 + \sum_{j=1}^{n} Y_{ij} V_j \tag{2.256}$$

which can be written in the form

$$I_i^{sp} - I_i^{calc} = \sum_{j=1}^{n} Y_{ij} V_j \tag{2.257}$$

and in vector form can be written

$$\Big[\Delta I\Big] = \Big[Y\Big] \Big[\Delta V\Big] \tag{2.258}$$

By rearranging the above equation and solving for voltage instead of current the incremental power flow algorithm is introduced by

$$\Big[\Delta V\Big] = \Big[Z\Big] \Big[\Delta I\Big] \tag{2.259}$$

where there exist the following relations

$$I_i^{sp} = \frac{S_i{}^*}{V_i{}^*} = \frac{P_i{}^{sp} - jQ_i}{V_i{}^*} \tag{2.260}$$

and

$$I_i^{cal} = \frac{S_i{}^*}{V_i{}^*} = \sum_{j=1}^{n} Y_{ij} V_j \tag{2.261}$$

where $Q_i = Q_i^{sp}$ for a PQ bus and $Q_i = Q_i^{cal}$ for a PV bus.

The iterative process involves equations 2.260, 2.261, for the current calculation, their difference calculation by

$$\Delta I_i = I_i^{sp} - I_i^{cal} \tag{2.262}$$

the corresponding voltage difference by eq. 2.259 and finally the voltage profile update by equation

$$V^{k+1} = V^k + \Delta V^k \tag{2.263}$$

where all the above are matrix notations. The iterative process stops when the maximum voltage correction value ΔV satisfies a given tolerance criterion, otherwise the iteration returns to each first step and keeps going.

The mentioned procedure stands as it os for the PQ buses. For PV buses one more equation for the reactive power calculation is

$$Q_i^{cal} = -Im(V_i^* I_i^{cal}) \tag{2.264}$$

After convergence has been succeeded the line flows, line losses, and the rest of variables are computed. The flow chart of the proposed method is shown in figure 2.30

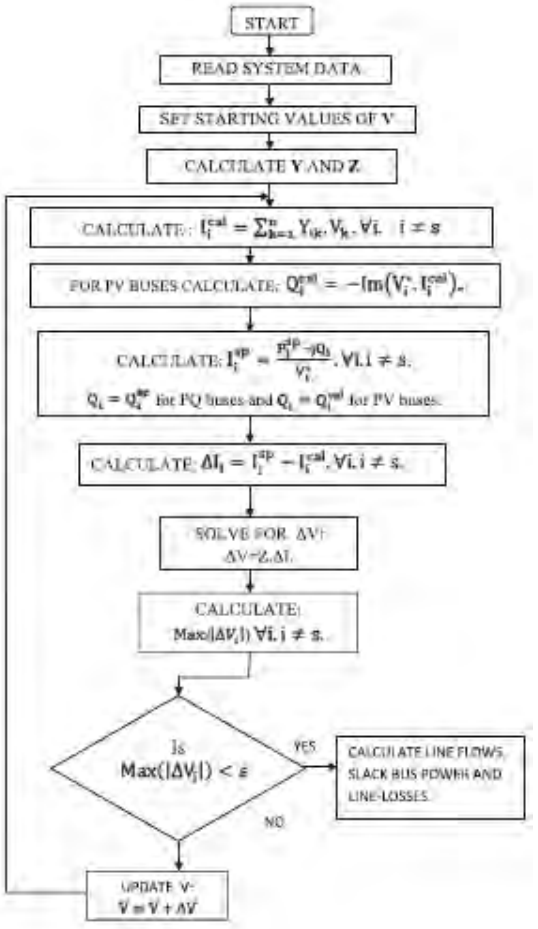

FIGURE 2.30: Flow chart of the incremental power flow method

The performance of the proposed IPF, according to the authors, was evaluated in 6 test cases, that is an IEEE 5-bus, 14-bus, 30-bus, 57-bus, 118-bus and finally 300-bus well-conditioned test systems. The load was varied from 70% to 120% in steps of 10%. The comparison concerning convergence characteristics is performed between the IPF with the conventional NRPF, the G-S method and the FDLF method that will be analyzed later on. The figures 2.31, 2.32, 2.33 below illustrate the comparison of the methods

Comparison of convergence characteristics of different methods at 70% loading ($\varepsilon = 0.0000001$).

IEEE test system	G–S method		N–R method		FDLF method		IPF method	
	No. of iterations	Convergence time (in s)	No. of iterations	Convergence time (in s)	No. of iterations	Convergence time (in s)	No. of iterations	Convergence time (in s)
5 Bus	17	0.0018	4	0.0500	3	0.0270	7	0.0154
14 Bus	56	0.0207	4	0.0538	3	0.0379	9	0.0218
30 Bus	147	0.1245	3	0.0588	2	0.0358	9	0.0279
57 Bus	224	0.4592	4	0.0888	5	0.0501	10	0.0364
118 Bus	649	3.8275	4	0.1919	9	0.0917	18	0.0540

FIGURE 2.31: Comparison of convergence characteristics of different methods at 70% loading ($\epsilon = 0.0000001$)

Comparison of convergence characteristics of different methods at 100% loading ($\varepsilon = 0.0000001$).

IEEE test system	G–S method		N–R method		FDLF method		IPF method	
	No. of iterations	Convergence time (in s)	No. of iterations	Convergence time (in s)	No. of iterations	Convergence time (in s)	No. of iterations	Convergence time (in s)
5 Bus	20	0.0020	4	0.0499	3	0.0354	8	0.0158
14 Bus	62	0.0202	3	0.0531	3	0.0377	11	0.0224
30 Bus	165	0.1396	3	0.0588	2	0.0356	13	0.0293
57 Bus	233	0.4780	4	0.0872	6	0.0528	16	0.0479
118 Bus	565	3.3314	4	0.1779	10	0.0981	20	0.0808

FIGURE 2.32: Comparison of convergence characteristics of different methods at 100% loading ($\epsilon = 0.0000001$)

Comparison of convergence characteristics of different methods at 120% loading ($\varepsilon = 0.0000001$).

IEEE test system	G–S method		N–R method		FDLF method		IPF method	
	No. of iterations	Convergence time (in s)	No. of iterations	Convergence time (in s)	No. of iterations	Convergence time (in s)	No. of iterations	Convergence time (in s)
5 Bus	22	0.0022	4	0.0499	3	0.0357	9	0.0156
14 Bus	69	0.0224	5	0.0547	3	0.0379	14	0.0234
30 Bus	186	0.1549	5	0.0655	2	0.0356	16	0.0317
57 Bus	223	0.4560	5	0.0969	7	0.0563	21	0.0597
118 Bus	741	4.3433	5	0.2014	10	0.1640	22	0.0898

FIGURE 2.33: Comparison of convergence characteristics of different methods at 120% loading ($\epsilon = 0.0000001$)

The following figure 2.34 shows the comparison of the methods, for a test case of 300-bus system for three different loading conditions

Comparison of convergence characteristics of different methods for IEEE 300-bus test system ($\varepsilon = 0.0000001$).

Bus loading (%)	G–S method		N–R method		FDLF method		IPF method	
	No. of iterations	Convergence time (in s)	No. of iterations	Convergence time (in s)	No. of iterations	Convergence time (in s)	No. of iterations	Convergence time (in s)
98.5	4698	142.38	5	1.7602	13	1.0216	22	0.5561
100	4796	147.28	5	1.8442	13	1.0426	24	0.6690
101.5	6790	177.48	5	1.8744	14	1.0918	27	0.7852

FIGURE 2.34: Comparison of convergence characteristics of different methods for a test system of 300-bus ($\epsilon = 0.0000001$)

Figures 2.35, 2.36, 2.37 and 2.38 illustrate the comparison of the mentioned methods concerning convergence time versus accuracy for different test case systems. Simulation results show that the proposed IPF method requires smaller time to converge, especially at higher accuracy.

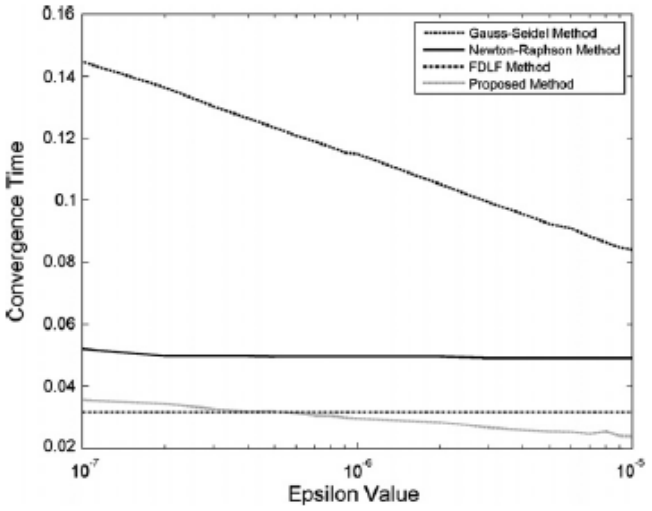

FIGURE 2.35: Comparison of convergence characteristics for bus loading of 110% on IEEE 30-bus system

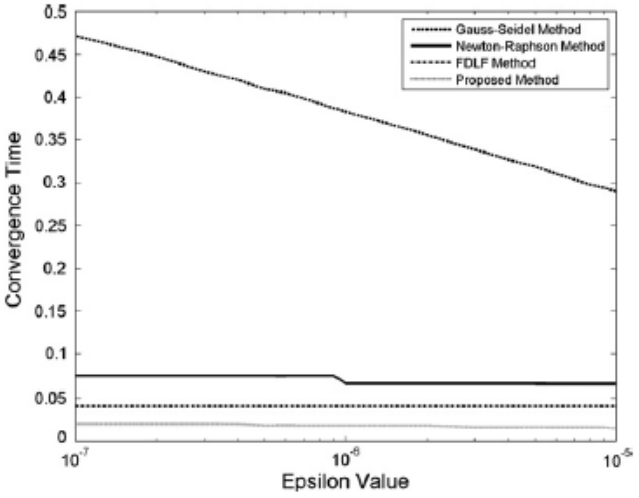

FIGURE 2.36: Comparison of convergence characteristics for bus loading of 80% on IEEE 57-bus system

Figures 2.39, 2.40, 2.41, 2.42, 2.43, 2.44 and 2.45 show the comparison of the above mentioned methods concerning voltage magnitude and phase angle as well as active and reactive power and finally MVA power flows for specific buses of the test case systems.

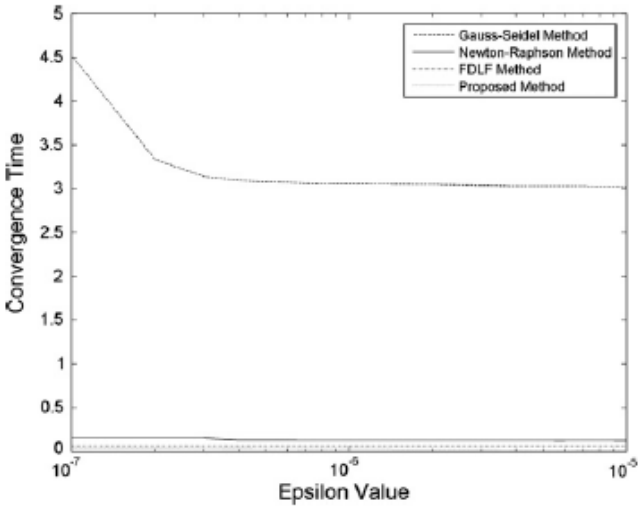

FIGURE 2.37: Comparison of convergence characteristics for bus loading of 70% on IEEE 118-bus system

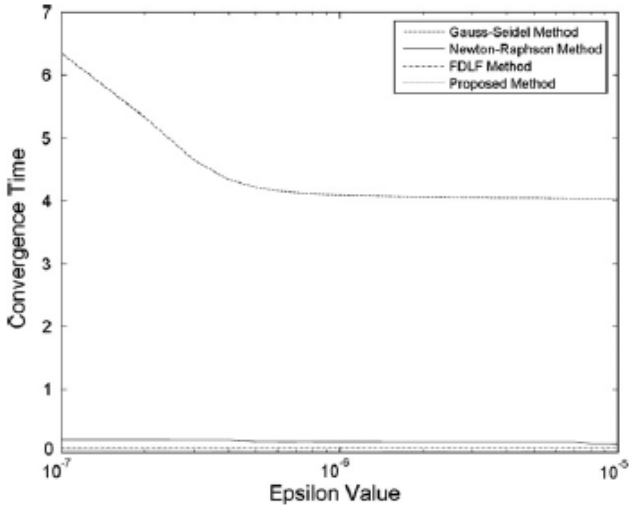

FIGURE 2.38: Comparison of convergence characteristics for bus loading of 100% on IEEE 300-bus system

Finally figures 2.46, 2.47, 2.48 illustrate in table form the comparison of the methods for voltage magnitude and angle, active and reactive power and line MVA power flows a test case IEEE 300-bus system with 100% bus loading.

According to the authors of the paper simulation results have shown that the method converges with the least time and the memory requirement is comparatively much less than other popular power flow methods, as the proposed method does not require complex and computationally expensive matrix manipulations like matrix inversion during iterations.

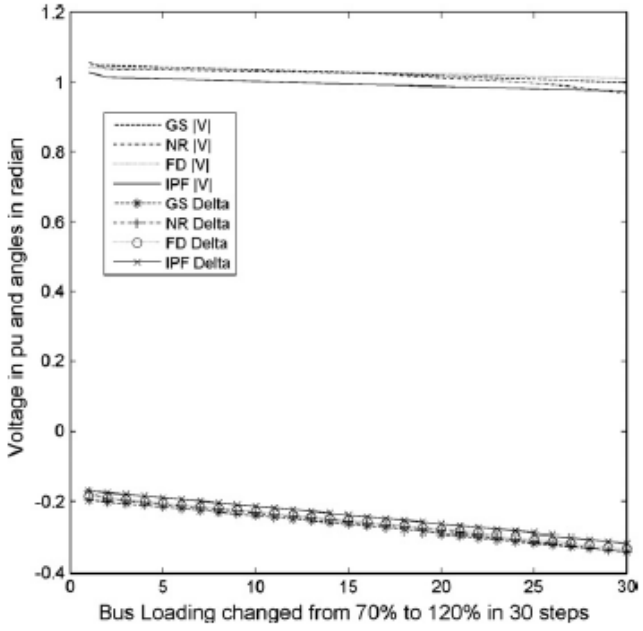

FIGURE 2.39: Comparison of voltage magnitude and phase angle of bus number 5 on IEEE 30-bus system

FIGURE 2.40: Comparison of voltage magnitude and phase angle of bus number 16 on IEEE 57-bus system

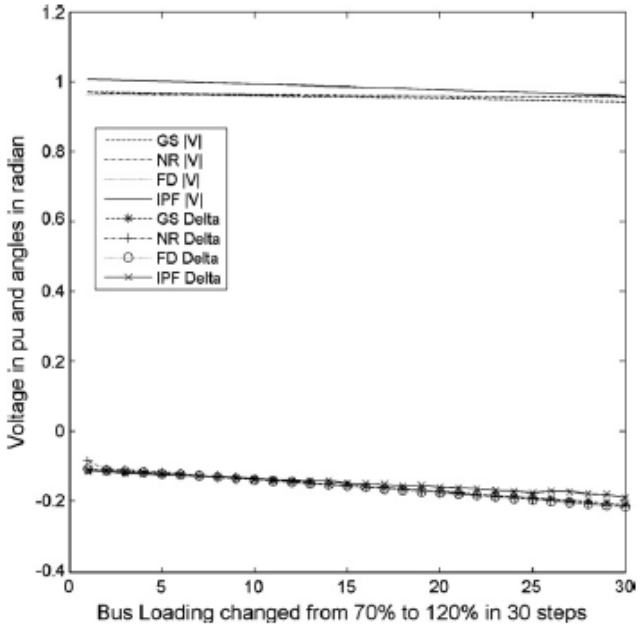

FIGURE 2.41: Comparison of voltage magnitude and phase angle of bus number 106 on IEEE 118-bus system

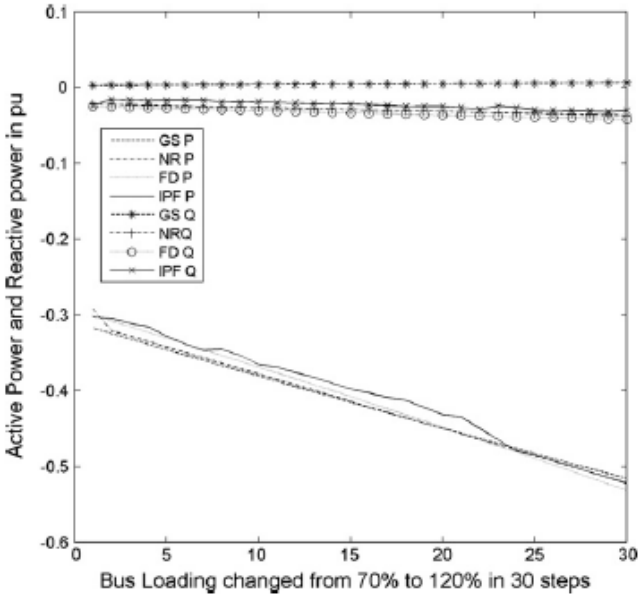

FIGURE 2.42: Comparison of active and reactive power of bus number 16 on IEEE 57-bus system

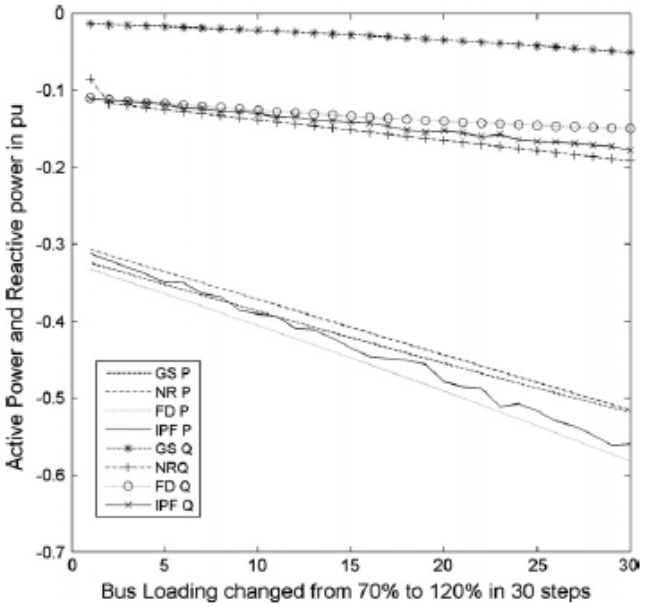

FIGURE 2.43: Comparison of active and reactive power of bus number 106 on IEEE 118-bus system

Case II An extension of NRPF problem is presented in [22], where the power flow problem is reformulated in order to include a variety of flow limits (thermal, small signal stability, voltage difference), generation redispatch and phase shifters. Both generation redispatch and phase shifting have been recognized as useful means to handle line flow limits. These considerations can be thought as being a part of an optimization problem called the optimal power flow (it will be mentioned

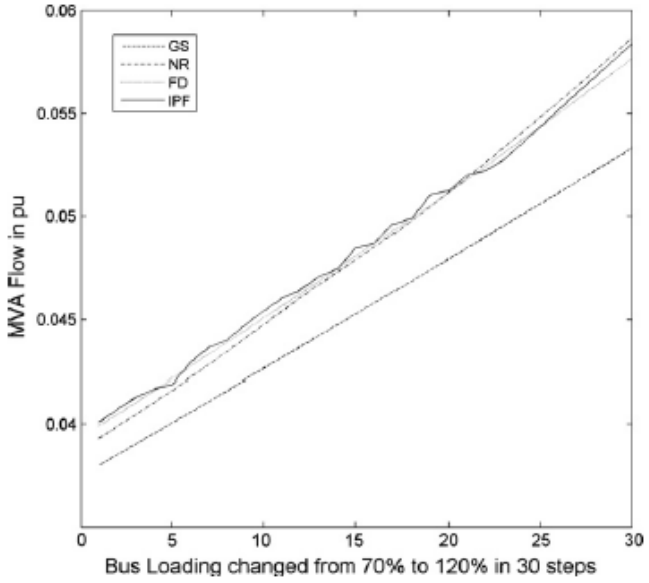

FIGURE 2.44: Comparison of active and reactive power of bus number 51 on IEEE 57-bus system

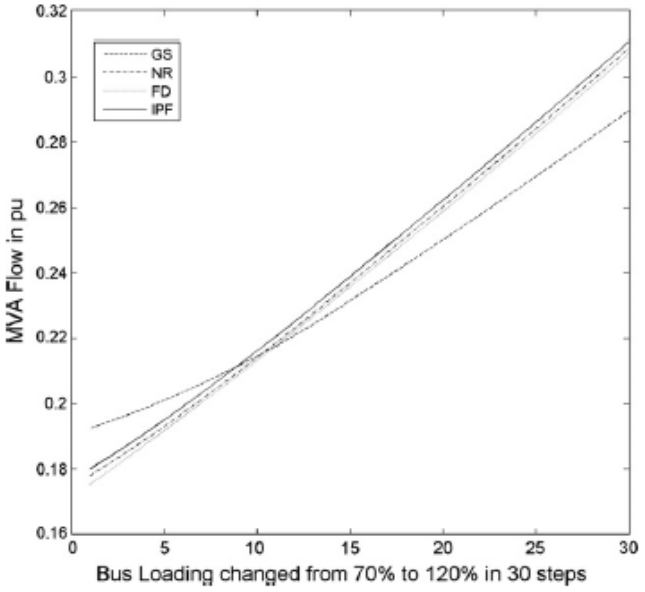

FIGURE 2.45: Comparison of active and reactive power of bus number 181 on IEEE 118-bus system

later on). Although Optimal power flow leads to the best and more accurate solution of the problem that has to solve, it is generally not so effective as the direct solution of the conventional power flow problem. This fact challenged the authors of the paper to try handling generation redispatch and line flow limits as a part of the conventional power flow algorithm, thus achieving a fast as well as reliable solution, so that power system operators can make quick yet efficient

Comparison of voltage magnitudes and phase angles between G–S, N–R, FDLF and the proposed IPF for IEEE 300-bus test system at 100% bus loading ($\varepsilon = 0.0000001$).

Bus no	Area no	G–S method		N–R method		FDLF method		IPF method	
		Voltage magnitude	Phase angle	Voltage magnitude	phase angle	Voltage magnitude	Phase angle	Voltage magnitude	Phase angle
8	1	1.0274	0.0853	1.0153	0.0448	1.0153	0.0322	1.0142	0.0483
138	2	1.0535	−0.0567	1.055	−0.1079	1.055	−0.1193	1.0502	−0.1103
250	3	1.023	−0.3522	1.0232	−0.4055	1.026	−0.3893	1.0228	−0.4002
9021	4	0.9763	−0.2933	0.9888	−0.3288	0.9888	−0.3245	0.9858	−0.3191

FIGURE 2.46: Comparison of voltage magnitudes and phase angles between the four methods for a test system of 300-bus at 100% loading ($\epsilon = 0.0000001$)

Comparison of active power (Pbus) and reactive powers (Qbus) between G–S, N–R, FDLF and the proposed IPF for IEEE 300-bus test system at 100% bus loading ($\varepsilon = 0.0000001$).

Bus no	Area no	G–S method		N–R method		FDLF method		IPF method	
		Pbus	Qbus	Pbus	Qbus	Pbus	Qbus	Pbus	Qbus
1	1	−0.659	−0.352	−0.801	−0.809	−0.811	−0.79	−0.889	−0.78
119	2	19.922	10.668	19.46	10.119	19.466	9.177	19.034	10.692
205	3	0.020	0.03	0.024	0.046	0.023	0.047	0.017	0.038
9002	4	−0.045	0.029	−0.046	0.03	−0.047	0.031	−0.041	0.026

FIGURE 2.47: Comparison of active and reactive bus power between the four methods for a test system of 300-bus at 100% loading ($\epsilon = 0.0000001$)

Comparison of line MVA power flows between G–S, N–R, FDLF and the proposed IPF for IEEE 300-bus test system at 100% bus loading ($\varepsilon = 0.0000001$).

Line no	Area no	From bus	To bus	G–S method	n–r method	FDLF method	IPF method
40	1	2	6	1.566	1.581	1.579	1.615
247	2	173	174	0.247	0.255	0.242	0.248
327	3	243	245	0.257	0.278	0.277	0.264
7	4	9005	9053	0.307	0.288	0.303	0.295

FIGURE 2.48: Comparison of line MVA power flows between the four methods for a test system of 300-bus at 100% loading ($\epsilon = 0.0000001$)

decisions under stressed conditions of the power system. The power flow problem becomes complicated when one or more additional variables are to be engaged in the algorithm, of the basic problem. In the proposed method such an attempt is made by adding one or more variables when the flow on a particular line or corridor exceeds its designated capability. In other words the problem is stated as extend the formulation and solutions method of the power flow so that when the flow on a given line (or on any line or set of lines) exceeds some specified limit, generation is redispatched just until the point where the limit is no longer violated. The problem is stated as to find the generator pair that has the greatest impact on a particular line flow. This impact can be considered as the impact of an injection at one bus (the bus that will increase its generation) and the impact of a decrease of power injection at another bus (the bus that will decrease its generation).

The authors utilize AC sensitivity analysis in the form of partial derivatives of generation active power with respect to voltage magnitudes and angles that is

executed in order to serve formulating the new line flow limit equations in the system model.

The equation of the line flow of a branch that interconnects buses k and i and denoted on behalf of the "from end" bus is given by

$$P_k^{from} = \sum_{i \in i|Y \neq 0} (V_i V_j (G_{ki} \cos \delta_{ki} + V_i V_j B_{ki} \sin \delta_{ki}) \tag{2.265}$$

Sensitivity analysis is performed in two steps. First the sensitivity of a branch flow with respect to changes in voltages and angles for all the buses of the system is being done. The power flow analysis is meaningful for only the branch lines that are of interest since they are near the limiting values. Two types of derivatives of the under violation branch flow with respect to voltage and angle are derived having the form of vector matrices. The derivative expressions are given by equations

$$\begin{aligned} H_f^{ki} = \frac{\partial \Delta P_{ki}}{\partial \delta_i} &= 0 \qquad if \quad Y_f^{ki} = 0 && (2.266)\\ &= -V_k V_i G_{ki} \sin \delta_{ki} + V_k V_i B_{ki} \cos \delta_{ki} \quad if \quad k \neq i && (2.267)\\ &= 2 V_k G_{ki} \quad if \quad k = i && (2.268) \end{aligned}$$

$$\begin{aligned} N_f^{ki} = \frac{\partial \Delta P_{ki}}{\partial V_i} &= 0 \qquad if \quad Y_f^{ki} = 0 && (2.269)\\ &= V_k G_{ki} \cos \delta_{ki} + V_k B_{ki} \sin \delta_{ki} \qquad if \quad k \neq i && (2.270)\\ &= 2 V_k G_{ki} \qquad if \quad k = i && (2.271) \end{aligned}$$

The dimension of this matrix is initially the number of line flows of interest (near the violation limits) m by the number of state variables in the power flow. This matrix is expanded by introducing zero values for all other matrix elements that typically describe sensitivities of line flows of branches not under consideration. The matrix that is produced by the above procedure has the form of a "flow" Jacobian matrix, where "flow" possibly identifies that it involves line flows under violation conditions.

The second step in sensitivity analysis performs a calculation of the sensitivity of the line flow on the limited line with respect to active and reactive power injections by using a modified Jacobian matrix in equation

$$\begin{bmatrix}\Delta P_f\end{bmatrix} = \begin{bmatrix}J_f\end{bmatrix}\begin{bmatrix}\Delta\delta \\ \Delta V\end{bmatrix} \tag{2.272}$$

where

$$\begin{bmatrix}\Delta P \\ \Delta Q\end{bmatrix} = \begin{bmatrix}J\end{bmatrix}\begin{bmatrix}\Delta\delta \\ \Delta V\end{bmatrix} \tag{2.273}$$

By utilizing matrix equation 2.273 a vector matrix is obtained with the sensitivities of the limited line i.e., its impact on all the other bus power injections. From the values of this vector a sorting procedure results in the maximum to minimum value ordering of the sensitivities for only active power injections (denoting our interest on generation redispatch where reactive power is not involved). The active power maximum and minimum sensitivity values indicate the pair of generator units that is the most effective providing the greatest impact on line flows so denoting the pair candidate to redispatch.

By solving matrix equation 2.272, a vector is produced with all other values zeroed and only two values with a +1 and -1 denoting the two generators with the largest sensitivity value and smallest sensitivity values respectively.

Every limit adds a new column and a new row in the conventional Jacobian matrix, modifying it by the power flow restriction. By this addition the information that was derived previously is now engaged in the power flow problem.

The matrix formulation of this modified NRPF is described by the matrix equations

$$\begin{bmatrix}\Delta P \\ \Delta Q \\ \cdots \\ rhs - rdspP^r\end{bmatrix} = \begin{bmatrix}H & N & \vdots & k1 \\ M & L & \vdots & 0 \\ \cdots & \cdots & \vdots & \cdots \\ FF1 & 0 & \vdots & 0\end{bmatrix}\begin{bmatrix}\Delta\delta \\ \Delta V \\ P_1^r\end{bmatrix} \tag{2.274}$$

which is solved for one line flow limit under consideration, while for two limits the equation becomes

$$\begin{bmatrix}\Delta P \\ \Delta Q \\ \cdots \\ rhs1 - rdspP_1^r \\ rhs2 - rdspP_2^r\end{bmatrix} = \begin{bmatrix}H & N & \vdots & k1 & \vdots & 0 \\ M & L & \vdots & 0 & \vdots & k2 \\ \cdots & \cdots & \vdots & \cdots & \vdots & 0 \\ FF1 & 0 & \vdots & 0 & \vdots & 0 \\ 0 & FF2 & \vdots & 0 & \vdots & 0\end{bmatrix}\begin{bmatrix}\Delta\delta \\ \Delta V \\ P_1^r \\ P_2^r\end{bmatrix} \tag{2.275}$$

where $k1$ and $k2$ describe the vector matrices incorporating the sensitivities of the line flow of limited line w.r.t. voltage magnitude and angle and FF1, FF2 describe the vector matrices of the sensitivities of the line flow of limited line w.r.t. all other buses power flow injections.

By following approximately the same procedure adjustments setting of transformers can also be handled in a way to resolve the power flow problem with line flow limit constraints.

This new feature provides a powerful tool and accurate helper for operating a power system within its security constraints. As for the line flow limits problem the ISO is allowed to identify effective generator pair according to four different options based on topology analysis, sensitivity studies, generator margins or cost consideration as well as most effective phase-shifting transformers.

The novelty of the approach is the three step procedure: run ordinary power flow (and identify flow limits violated), solve a set of linear equations using extended power flow Jacobian by adding a new column and a new row that characterize the particular limit and resolve ordinary power flow with initial solution obtained after the correction made by solution of linear equations.

Case III A modified Jacobian matrix formulation of the NRPF problem is presented in [23]. The elements of the Jacobian matrix are obtained considering the power flows in the network elements. Recognizing that the elements of the Jacobian matrix are contributed by the partial derivatives of the line power flows in the network elements a simple algorithm to construct the Jacobian matrix is proposed. The network elements are considered one-by- one. Required partial derivatives of the line flows are computed and the Jacobian matrix is updated suitably. When all the elements are added the final Jacobian is obtained. For example when a bus under study is connected to three other buses, its power flows (active and reactive) are dependent on the corresponding line power flows for the three interconnected lines between bus under study and the three interconnected buses. In the same way, the partial derivatives of the bus power flows can be expressed in terms of partial derivatives of the line power flows in the network elements. Simulation results show that the proposed method converges after the same number of iterations compared to the conventional NRPF but is computationally more efficient for solving large scale power flow problems.

2.4.7 Fast Decoupled Load Flow

To overcome the nonlinearity difficulties several approximate models using physical properties of power systems have been proposed in the literature. The most frequently adopted are the fast decoupled power flow problem (FDPFP) and its consequence the so-called DC load flow analysis. The reader is referred to [11].

FDPFP is based on the observation that there is a weak interaction between real power and voltage magnitude and between reactive power and voltage angle. This is due to the fact that the reactance of a branch line is generally quite greater than the resistance in practical electric power systems. The physical meaning of this fact is that there exists a strong coupling between real power and voltage angle and quite weaker coupling with voltage magnitude. This means the real power is little influenced by changes in voltage magnitude,which means that

$$\frac{\partial \Delta P_i}{\partial V_j} = 0 \tag{2.276}$$

while reactive power is little influenced by changes in voltage angle which is described as

$$\frac{\partial \Delta Q_i}{\partial \delta_j} = 0 \tag{2.277}$$

This weakness allows related elements of the NR Jacobian matrix, namely the off-diagonal elements which consist of the partial derivatives that reflect the weak coupling to be ignored so in that way the computation time can be significantly reduced. The bus real power mismatch is only used to revise the voltage angle, and the bus reactive power mismatch is only used to revise the voltage magnitude. The ratio of the resistance to reactance value plays an important role in the formulation of the FDPFP. Recalling eq. 2.49 it is obvious that the off-diagonal elements of the Jacobian matrix,

$$N_{ij} = \frac{\partial \Delta P_i}{\partial V_j}|V_j| = 0 \tag{2.278}$$

and

$$K_{ij} = \frac{\partial \Delta Q_i}{\partial \delta_j} = 0 \tag{2.279}$$

Thus eq. 2.45 now becomes

$$\begin{bmatrix} \Delta P \\ \Delta Q \end{bmatrix} = \begin{bmatrix} H & 0 \\ 0 & L \end{bmatrix} \begin{bmatrix} \Delta \delta \\ \Delta V/|V| \end{bmatrix} \tag{2.280}$$

which results in the following set of equations

$$\Delta P = -H\Delta\delta \tag{2.281}$$

$$\Delta Q = -L\frac{\Delta V}{V} \tag{2.282}$$

Since only two of the four Jacobian block submatrices have left for the calculation procedure it is obvious that the computational time can be significantly reduced.

Equations 2.281 and 2.282 can be further simplified if the phase angle differences (as they are calculated through simulations) are observed. These differences result in small values which means that $\sin(\delta_i - \delta_j)$ is also relatively small and can even be considered as zero. Thus the following relations are evident

$$\cos\delta_{ij} = \cos(\delta_i - \delta_j) \equiv 1 \tag{2.283}$$

$$G_{ij}\sin\delta_{ij} \ll B_{ij} \tag{2.284}$$

With the assumption

$$Q_i \ll V_i^2 B_{ii} \tag{2.285}$$

equations 2.58, 2.60, 2.62 and 2.64 are changed to

$$H_{ii} = \frac{\partial \Delta P_i}{\partial \delta_i} = |V_i| \sum_{j\in ij\neq i} |V_j|(-G_{ij}\sin\delta_{ij} + B_{ij}\cos\delta_{ij}) \tag{2.286}$$

$$= -|V_i|^2 B_{ii} - Q_i = -|V_i|^2 B_{ii} = -|V_i|B_{ii}|V_i| \tag{2.287}$$

$$H_{ij} = \frac{\partial \Delta P_i}{\partial \delta_j} = |V_i||V_j|(G_{ij}\sin\delta_{ij} - B_{ij}\cos\delta_{ij}) = |V_i|B_{ij}|V_j| \tag{2.288}$$

$$L_{ii} = \frac{\partial \Delta Q_i}{\partial V_i}|V_i| = |V_i| \sum_{j \in ij \neq i} |V_j|(G_{ij}\sin\delta_{ij} - B_{ij}\cos\delta_{ij}) - 2|V_i|^2 B_{ii} \quad (2.289)$$

$$= -|V_i|^2 B_{ii} + Q_i = -|V_i|^2 B_{ii} = -|V_i|B_{ii}|V_i| \quad (2.290)$$

$$L_{ij} = \frac{\partial \Delta Q_i}{\partial V_j}|V_j| = -|V_i||V_j(G_{ij}\sin\delta_{ij} - B_{ij}\cos\delta_{ij}) = Q_i = H_{ij} = |V_i|B_{ij}|V_j| \quad (2.291)$$

Therefore block submatrices H and L can now be written as follows (note that we again use n_{act} for bus numbering

$$\left[H\right] = \begin{bmatrix} H_{1,1} & H_{1,2} & \cdots & H_{1,n_{act}} \\ H_{2,1} & H_{2,2} & \cdots & H_{2,n_{act}} \\ \vdots & \vdots & \vdots & \vdots \\ H_{n_{act},1} & H_{n_{act},2} & \cdots & H_{n_{act},n_{act}} \end{bmatrix} = \begin{bmatrix} V_1 B_{1,1} V_1 & V_1 B_{1,2} V_2 & \cdots & V_1 B_{1,n_{act}} V_{n_{act}} \\ V_2 B_{2,1} V_1 & V_2 B_{2,2} V_2 & \cdots & V_2 B_{2,n_{act}} V_{n_{act}} \\ \vdots & \vdots & \vdots & \vdots \\ V_{n_{act}} B_{n_{act},1} V_1 & V_{n_{act}} B_{n_{act},2} V_2 & \cdots & V_{n_{act}} B_{n_{act},n_{act}} V_{n_{act}} \end{bmatrix}$$

$$= \begin{bmatrix} V_1 & & & \\ & V_2 & & \\ & & \ddots & \\ & & & V_{n_{act}} \end{bmatrix} \begin{bmatrix} B_{1,1} & B_{1,2} & \cdots & B_{1,n_{act}} \\ B_{2,1} & B_{2,2} & \cdots & B_{2,n_{act}} \\ \vdots & \vdots & \vdots & \vdots \\ B_{n_{act},1} & B_{n_{act},2} & \cdots & B_{n_{act},n_{act}} \end{bmatrix} \begin{bmatrix} V_1 & & & \\ & V_2 & & \\ & & \ddots & \\ & & & V_{n_{act}} \end{bmatrix} = \left[V\right]\left[B'\right]\left[V\right] \quad (2.292)$$

$$\left[L\right] = \begin{bmatrix} L_{1,1} & L_{1,2} & \cdots & L_{1,n_{react}} \\ L_{2,1} & L_{2,2} & \cdots & L_{2,n_{react}} \\ \vdots & \vdots & \vdots & \vdots \\ L_{n_{react},1} & L_{n_{react},2} & \cdots & L_{n_{react},n_{react}} \end{bmatrix} = \begin{bmatrix} V_1 B_{1,1} V_1 & V_1 B_{1,2} V_2 & \cdots & V_1 B_{1,n_{react}} V_{n_{react}} \\ V_2 B_{2,1} V_1 & V_2 B_{2,2} V_2 & \cdots & V_2 B_{2,n_{react}} V_{n_{react}} \\ \vdots & \vdots & \vdots & \vdots \\ V_{n_{react}} B_{n_{react},1} V_1 & V_{n_{react}} B_{n_{react},2} V_2 & \cdots & V_{n_{react}} B_{n_{react},n_{react}} V_{n_{react}} \end{bmatrix}$$

$$= \begin{bmatrix} V_1 & & & \\ & V_2 & & \\ & & \ddots & \\ & & & V_{n_{react}} \end{bmatrix} \begin{bmatrix} B_{1,1} & B_{1,2} & \cdots & B_{1,n_{react}} \\ B_{2,1} & B_{2,2} & \cdots & B_{2,n_{react}} \\ \vdots & \vdots & \vdots & \vdots \\ B_{n_{react},1} & B_{n_{react},2} & \cdots & B_{n_{react},n_{react}} \end{bmatrix} \begin{bmatrix} V_1 & & & \\ & V_2 & & \\ & & \ddots & \\ & & & V_{n_{react}} \end{bmatrix} = \left[V\right]\left[B''\right]\left[V\right.$$

Substituting eq.2.292 to eq. 2.281 the active power mismatch equation can be rewritten in the form

$$\begin{bmatrix} \Delta P_1 \\ \Delta P_2 \\ \vdots \\ \Delta P_{n_{act}} \end{bmatrix} = \begin{bmatrix} V_1 & & & \\ & V_2 & & \\ & & \ddots & \\ & & & V_{n_{act}} \end{bmatrix} \begin{bmatrix} B_{1,1} & B_{1,2} & \cdots & B_{1,n_{act}} \\ B_{2,1} & B_{2,2} & \cdots & B_{2,n_{act}} \\ \vdots & \vdots & \vdots & \vdots \\ B_{n_{act},1} & B_{n_{act},2} & \cdots & B_{n_{act},n_{act}} \end{bmatrix} \begin{bmatrix} \Delta\delta_1 V_1 \\ \Delta\delta_2 V_2 \\ \vdots \\ \Delta\delta_{n_{act}} V_{n_{act}} \end{bmatrix} \quad (2.294)$$

In the same way substituting eq.2.293 to eq.2.282 the reactive power mismatch equation can be rewritten in the form

$$\begin{bmatrix} \Delta Q_1 \\ \Delta Q_2 \\ \vdots \\ \Delta Q_{n_{react}} \end{bmatrix} = \begin{bmatrix} V_1 & & & \\ & V_2 & & \\ & & \ddots & \\ & & & V_{n_{react}} \end{bmatrix} \begin{bmatrix} B_{1,1} & B_{1,2} & \cdots & B_{1,n_{react}} \\ B_{2,1} & B_{2,2} & \cdots & B_{2,n_{react}} \\ \vdots & \vdots & \vdots & \vdots \\ B_{n_{react},1} & B_{n_{react},2} & \cdots & B_{n_{react},n_{react}} \end{bmatrix} \begin{bmatrix} \Delta V_1 \\ \Delta V_2 \\ \vdots \\ \Delta V_{n_{react}} \end{bmatrix} \tag{2.295}$$

The above matrix equations 2.294 and 2.295 can be written in a compact form as

$$\Big[\Delta P\Big] = \Big[-V\Big] \Big[B'\Big] \Big[V\Delta\delta\Big] \tag{2.296}$$

$$\Big[\Delta Q\Big] = \Big[-V\Big] \Big[B''\Big] \Big[\Delta V\Big] \tag{2.297}$$

This constitutes the general form of the Fast Decoupled Load Flow problem. The above equations can be rewritten in another form, usually found in the literature if both sides of eq. 2.294 and 2.295 are multiplied with the matrix

$$\begin{bmatrix} V_1 & & & \\ & V_2 & & \\ & & \ddots & \\ & & & V_{n_{act}} \end{bmatrix}^{-1} = \begin{bmatrix} 1/V & & & \\ & 1/V_2 & & \\ & & \ddots & \\ & & & 1/V_{n_{act}} \end{bmatrix} \tag{2.298}$$

and

$$\begin{bmatrix} V_1 & & & \\ & V_2 & & \\ & & \ddots & \\ & & & V_{n_{react}} \end{bmatrix}^{-1} = \begin{bmatrix} 1/V & & & \\ & 1/V_2 & & \\ & & \ddots & \\ & & & 1/V_{n_{react}} \end{bmatrix} \tag{2.299}$$

respectively. The following active and reactive power mismatches are then obtained

$$\begin{bmatrix} \Delta P_1/V_1 \\ \Delta P_2/V_2 \\ \vdots \\ \Delta P_{n_{act}}/V_{n_{act}} \end{bmatrix} = \begin{bmatrix} B_{1,1} & B_{1,2} & \cdots & B_{1,n_{act}} \\ B_{2,1} & B_{2,2} & \cdots & B_{2,n_{act}} \\ \vdots & \vdots & \vdots & \vdots \\ B_{n_{act},1} & B_{n_{act},2} & \cdots & B_{n_{act},n_{act}} \end{bmatrix} \begin{bmatrix} V_1\Delta\delta_1 \\ V_2\Delta\delta_2 \\ \vdots \\ V_{n_{act}}\Delta\delta_{n_{act}} \end{bmatrix} \tag{2.300}$$

$$\begin{bmatrix} \Delta Q_1/V_1 \\ \Delta Q_2/V_2 \\ \vdots \\ \Delta Q_{n_{react}}/V_{n_{react}} \end{bmatrix} = \begin{bmatrix} B_{1,1} & B_{1,2} & \cdots & B_{1,n_{react}} \\ B_{2,1} & B_{2,2} & \cdots & B_{2,n_{react}} \\ \vdots & \vdots & \vdots & \vdots \\ B_{n_{react},1} & B_{n_{react},2} & \cdots & B_{n_{react},n_{react}} \end{bmatrix} \begin{bmatrix} \Delta V_1 \\ \Delta V_2 \\ \vdots \\ \Delta V_{n_{react}} \end{bmatrix} \tag{2.301}$$

The above matrix equations 2.300 and 2.301 can now be written in their compact form as follows

$$\Big[\Delta P/V\Big] = \Big[-B'\Big]\Big[V\Delta\delta\Big] \tag{2.302}$$

$$\Big[\Delta Q/V\Big] = \Big[-B''\Big]\Big[\Delta V\Big] \tag{2.303}$$

As it can be seen the H and L formulations are similar. However there is a clear distinction based on the different dimensions of matrices B' and B'' denoting the imaginary part of the bus admittance, i.e., the susceptance matrices. The dimension of matrix B' is $n_b - 1$ while the dimension of B'' is lower than $n_b - 1$ because it does not include the equations related to PV buses, so it is denoted as n_{react}. Hence if the systems has r PV buses then $n_{react} = n - r - 1$. With V the voltage magnitude diagonal matrix is denoted. Practically in real systems applications the voltage magnitude of the right hand side of the equations 2.300 and 2.303 is assumed to be 1.0 p.u. (per unit).

Thus the above equations can be finally expressed as follows

$$\begin{bmatrix} \Delta P_1/V_1 \\ \Delta P_2/V_2 \\ \vdots \\ \Delta P_{n_{act}}/V_{n_{act}} \end{bmatrix} = \begin{bmatrix} B_{1,1} & B_{1,2} & \cdots & B_{1,n_{act}} \\ B_{2,1} & B_{2,2} & \cdots & B_{2,n_{act}} \\ \vdots & \vdots & \vdots & \vdots \\ B_{n_{act},1} & B_{n_{act},2} & \cdots & B_{n_{act},n_{act}} \end{bmatrix} \begin{bmatrix} \Delta\delta_1 \\ \Delta\delta_2 \\ \vdots \\ \Delta\delta_{n_{act}} \end{bmatrix} \tag{2.304}$$

which in compact form is

$$\Big[\Delta P/V\Big] = \Big[-B'\Big]\Big[\Delta\delta\Big] \tag{2.305}$$

In literature there exist two additional versions of the FDLF algorithm according to the different manipulation of the constant susceptance matrices B' and B''. They are called the BX version and the XB version.

For the XB version the resistance is ignored during the calculation of matrix B'. This means that the elements of the two susceptance matrices are

$$B'_{ij} = B_{ij} \tag{2.306}$$

$$B'_{ii} = -\sum_{j \neq i} B'_{ij} \tag{2.307}$$

$$B''_{ij} = \frac{B_{ij}^2 + G_{ij}^2}{B_{ij}} \tag{2.308}$$

$$B''_{ii} = -2B_{i0} - \sum_{j \neq i} B''_{ij} \tag{2.309}$$

where B_{i0} is the shunt reactance to the ground.

Practically in real application the following assumptions are adopted in the XB version of the FDLF algorithm

1. Assume $r_{ij} \ll x_{ij}$ which leads to $B_{ij} = -\frac{1}{x_{ij}}$.
2. The shunt reactances to ground are eliminated.
3. All the efects of the phase shift transformers are omitted.

With these assumptions in mind the XB version of the FDLF algorithm can be simplified in the following expressions

$$B'_{ij} = -\frac{1}{x_{ij}} \tag{2.310}$$

$$B'_{ii} = -\sum_{j \neq i} \frac{1}{x_{ij}} \tag{2.311}$$

$$B''_{ij} = -\frac{x_{ij}}{r_{ij}^2 + x_{ij}^2} \tag{2.312}$$

$$B''_{ii} = -\sum_{j \neq i} B''_{ij} \tag{2.313}$$

where r_{ij} and x_{ij} are the resistance and reactance of branch line interconnecting buses i and j respectively.

For the BX version of the FDLF algorithm, the resistance is ignored during the calculation of B''. Then the elements of the susceptance matrices B' and B'' are given by

$$B'_{ij} = \frac{B_{ij}^2 + G_{ij}^2}{B_{ij}} \tag{2.314}$$

$$B'_{ii} = -\sum_{j \neq i} B'_{ij} \tag{2.315}$$

$$B''_{ij} = B_{ij} \tag{2.316}$$

$$B''_{ii} = -2B_{i0} - \sum_{j \neq i} B''_{ij} \tag{2.317}$$

while the simplified BX version now becomes

$$B'_{ij} = -\frac{1}{x_{ij}} \tag{2.318}$$

$$B'_{ii} = -\sum_{j \neq i} \frac{x_{ij}}{r_{ij}^2 + x_{ij}^2} \tag{2.319}$$

$$B''_{ij} = -\frac{1}{x_{ij}} \tag{2.320}$$

$$B''_{ii} = -\sum_{j \neq i} B''_{ij} \tag{2.321}$$

Since the FDLF algorithm is a NRPF model simplification, based on specific assumptions, it is obvious that it may fail to converge if these assumptions, like $r_{ij} \ll x_{ij}$ do

not hold. In this situation the full AC NRPF algorithm is recommended for efficiency in convergence.

2.4.7.1 Fast Decoupled Load Flow alternative formulations

Since its first appearance, FDPFP has been examined in quite a lot real power systems and several modified methods have been proposed dealing with its efficiency improvement concerning the computational effort. Such a technique is proposed in [24] in order to handle the problem of a high resistance to reactance ratio and low voltage values. The $Q-V$ partial derivative (strong coupling) iteration is multiplied with a new parameter which may be chosen as the minimum of the average resistance to reactance ratio and unity. The low bus voltages values are coped with by use of the Voltage Normalization Method (VNM). The result of their combination is a robust fast decoupled power flow method (RFDPFM) which has the ability to improve the convergence of FDPFM and overcome the above mentioned difficulties. Simulation results prove that fact.

Flexible alternatives to decoupled load flow are presented in [25]. These methods can be used in case the P-Q coupling becomes significant, case in which fast decoupled method faces severe convergence problems. The two methods are called the enhanced decoupled load flow (ECDL) and the simplified Newton-Raphson load flow (SNRL), and they are based on the gradual approximation of the state update vector expression in the full NRPF method by lessening the effects of the off-diagonal submatrices in the Jacobian. It is a simplification method based on the Neumann series expansion. Proper mathematical manipulation of the off-diagonal elements of the Jacobian matrix leads to terms easily computed, while offering convergence properties to the methods.

A further study of the $P-V$ and $Q-\delta$ decoupling is presented in [26]. Using basic principles the authors demonstrate that decoupling can be strengthened by combining real and reactive power flows, multiplied by proper parameter factors. These factors depend on ratio of the total branch reactance to the number of branches, as well as the ratio of total branch resistance to the number of branches. Two algorithms have been proposed and have been tested for normal and abnormal operating conditions. The algorithms are named as (G,B) and (1/X, 1/X), the latter being superior since it has very simple and symmetric coefficient matrix. Simulation results show that both methods can solve normal and difficult systems with high R/X ratios.

Following the above idea, another novel decoupled power flow method (DNRCM) is presented in [27]. The idea is a matrix manipulation of the diagonal elements of the Jacobian matrix in order to be formed exclusively with elements of the matrices of conductance

and susceptance which are constant. The algorithm is based on the conventional NRPF as has been presented analytically in a previous chapter. The basic matrix equation is

$$\begin{bmatrix} \Delta P \\ \Delta Q \end{bmatrix} = \begin{bmatrix} H & N \\ M & L \end{bmatrix} \begin{bmatrix} \Delta \delta \\ \Delta V/|V| \end{bmatrix} \tag{2.322}$$

Initially premultiplying the ΔP equations in 2.322 by MH^{-1} and adding the resulting equations to the ΔQ equations, the following equation is obtained

$$\Delta Q - MH^{-1}\Delta P = (L - MH^{-1}N)(\frac{\Delta V}{V}) \tag{2.323}$$

From the above equation the voltage magnitude can be calculated. Through a similar procedure, premultiplying the ΔQ equations by NL^{-1} and adding the resulting equation to the ΔP equations, the following equation is obtained

$$\Delta P - NL^{-1}\Delta Q = (H - NL^{-1}M)(\Delta \delta) \tag{2.324}$$

Taking into account that $\cos_{\delta_{km}} = 1$ and $\sin_{\delta_{km}} = 0$ and also that $V_k = V_m = 1.0p.u$ and after matrix manipulation the Jacobian elements H, M, L, N are formed in terms of conductances and susceptances where new matrices $B1$ with dimension of matrix H, $B2$ with dimension of matrix L, $G1$ with dimension of N and $G2$ with dimension of M are now involved instead of the original H, N, M, L matrices. Thus new equations for the proposed decoupled Newton-Raphson with constant matrices (DNRCM) are obtained as follows

$$\Delta \delta = (\Delta P - G1B2^{-1}\Delta Q)^{-1}(B1 - G1B2^{-1}G2) \tag{2.325}$$

$$\Delta V = (\Delta Q - G2B1^{-1}\Delta P)^{-1}(B2 - G2B1^{-1}G1) \tag{2.326}$$

$$\delta = \delta + \Delta \delta \tag{2.327}$$

$$V = V + \Delta V \tag{2.328}$$

The proposed algorithm is shown in the following figure 2.49

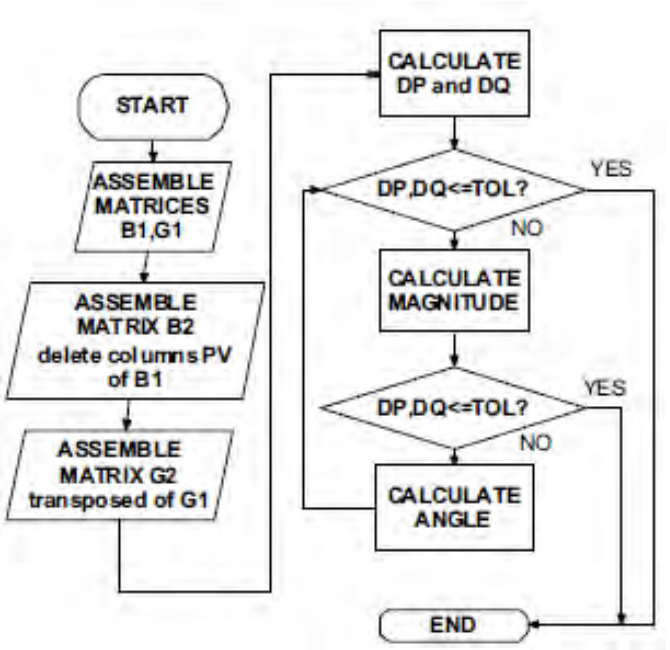

FIGURE 2.49: Basic flowchart of the DNRCM method

The simulation results of the proposed method show a good convergence even in the case of high resistance to reactance (r/x) ratio. Also the method has better convergence compared to the decoupled forms of BX, XB and Primal of transmission systems. However it is less efficient than the XB, BX method on memory requirements and total execution time/iteration.

2.4.8 DC load flow

Although AC power flow algorithms have high calculation precision and great accuracy they do not have fast computational speed due to the need for the Jacobian matrix computation in each iteration step. Following the basic concept of fast decoupled method and making some more reasonable assumptions power flow analysis takes the form of the DC load flow [11] model which seems to be the best simplification of the full AC power flow model and leads to relatively accurate results. The DC load flow model assumes that voltage magnitudes at all buses are flat meaning their values are around one p.u., the angle differences on the two ends of each branch are very small and reactive power flows are neglected.

The main disadvantage of the DC load flow algorithm is that it cannot be used for voltage limit violation checking. On the other hand, since it is a linear model it is suitable in treating the problem of line outages efficiently, and also to form linear optimization problems as it will shown next, when the basic theory of optimal power flow is presented.

Because of its advantages DC load flow has been a valuable tool for power systems planning and operation.

The first step in formulating the DC load flow model is to consider that the $Q-V$ equation of the FDLF model is completely omitted. Only the $P-\delta$ equation is used to correct the phase angle of the bus voltage vector and has the form

$$\begin{bmatrix} \Delta P_1/V_1 \\ \Delta P_2/V_2 \\ \vdots \\ \Delta P_{n_{act}}/V_{n_{act}} \end{bmatrix} = \begin{bmatrix} B_{1,1} & B_{1,2} & \cdots & B_{1,n_{act}} \\ B_{2,1} & B_{2,2} & \cdots & B_{2,n_{act}} \\ \vdots & \vdots & \vdots & \vdots \\ B_{n_{act},1} & B_{n_{act},2} & \cdots & B_{n_{act},n_{act}} \end{bmatrix} \begin{bmatrix} \Delta\delta_1 \\ \Delta\delta_2 \\ \vdots \\ \Delta\delta_{n_{act}} \end{bmatrix} \tag{2.329}$$

This equation constitutes an algorithm called the "MW only" in which the voltage magnitude can be assumed as constant or as 1.0 p.u. during each $P-\delta$ iteration. The basic assumptions further introduced that lead to the DC load flow model are the following:

1. All the voltage magnitudes are taken equal to 1.0 p.u..
2. The branch line resistance is ignored so the susceptance of the branch is

$$B_{ij} = -\frac{1}{x_{ij}} \tag{2.330}$$

3. The phase angle difference of the two interconnected buses, in other words of the two branch ends is very small so it is assumed that

$$\sin\delta_{ij} = \delta_i - \delta_j \tag{2.331}$$

$$\cos\delta_{ij} = 1 \tag{2.332}$$

4. All ground branches are ignored, that is,

$$B_{i0} = B_{j0} = 0 \tag{2.333}$$

Under these assumptions the $P-\delta$ equation consisting the DC load flow model takes the following form

$$\begin{bmatrix} \Delta P_1 \\ \Delta P_2 \\ \vdots \\ \Delta P_{n_{act}} \end{bmatrix} = \Big[B'\Big] \begin{bmatrix} \Delta\delta_1 \\ \Delta\delta_2 \\ \vdots \\ \Delta\delta_{n_{act}} \end{bmatrix} \tag{2.334}$$

or in more compact form

$$\Big[\Delta P\Big] = \Big[B'\Big]\Big[\Delta\delta\Big] \tag{2.335}$$

which in a simple form is as follows

$$P_i = \sum B_{ij}\delta_j \tag{2.336}$$

where the elements of the B' matrix are given by the same equations as in the FDLF XB version ignoring the matrix B". So the B' elements are computed as follows

$$B'_{ij} = -\frac{1}{x_{ij}} \tag{2.337}$$

$$B'_{ii} = -\sum_{j\neq i}\frac{1}{x_{ij}} = -\sum_{j\neq i} B'_{ij} \tag{2.338}$$

Since the DC load flow algorithm is a purely linear model it needs only one iteration to obtain the power flow solution, that is the main advantage over the pure AC load flow model. The power flowing on each line in the DC power flow model is calculated as

$$P_{ij} = -B_{ij}(\delta_i - \delta_j) = -\frac{\delta_i - \delta_j}{x_{ij}} \tag{2.339}$$

In [28] a useful insight into DC power flow analysis is presented. The authors of this paper (being among great experts in the field of power flow analysis since the early years), feel the need to give a quite analytical presentation of this linear power flow algorithm since it is - as already mentioned - based on assumptions that do not always match real power systems. The main features of the presentation are, the basic concept behind the use of DC load flow models, the advantages over AC load flow model and

possible objections about its use, the modeling procedure and challenges, the different types of DC models with their inherent characteristics, the application of DC model in security-constrained optimization, and an analytic presentation about its accuracy. To reduce error to be within 5% on average the authors of the paper suggest that the ratio X/R (reactance to resistance ratio) should be greater than 4 and the standard voltage deviation to be less than 0.01. The results from time-domain simulations show that the DC modeling accuracy should never be taken for granted in any power system application. However, as long as certain power system applications continue to rely on linear network models DC-type modeling will remain of high interest.

A recently new improved DC load flow method is presented in [29] [Lu, Zhou, Kumar, Samaan, Chakrabarti]. DC load flow, it is known, suffers from relatively poor accuracy compared to the full AC power flow. Since its superiority has to do with the computation cost (it is non-linear and non-iterative method) attempts to improve its accuracy without sacrificing its advantages are at least very welcoming. Such an approach is proposed in the specific paper where historical knowledge data are utilized for the purpose. In other words, empirical knowledge of the system including voltage magnitude and angle from historical data are used to formulate correction terms that lead to improved DC load flow performance. The basic idea of the proposed method is better understandable if first, one considers the following multi-bus system presented in figure 2.50

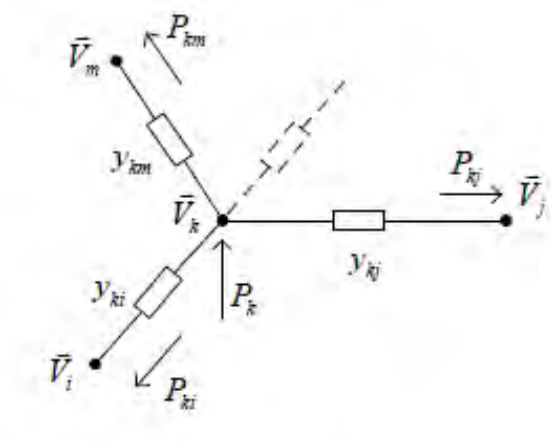

FIGURE 2.50: Power flow in a multi-bus system

From the above figure the active power injection in an AC formulation, according to Kirchhoff's law is

$$P_k = \sum_{m=1}^{n} V_k V_m (G_{km} \cos \delta_{km} + B_{km} \sin \delta_{km}) \tag{2.340}$$

On the other hand the equivalent DC formulation of the same active power injection, based on the well-known reasonable assumptions, as previously mentioned, is

$$P_k = \sum_{m=1}^{n} B_{km}\delta_{km} \tag{2.341}$$

Rearranging equation 2.340 one can take

$$P_k - \sum_{m=1}^{n} V_k V_m G_{km} \cos\delta_{km} = \sum_{m=1}^{n} V_k V_m B_{km} \sin\delta_{km}) \tag{2.342}$$

By comparing equations 2.341 and 2.342 it is clear that the right hand side of 2.342 can take, by assumptions, the same form of the r.h.s. of 2.341, but on the contrary this is not the case concerning the l.h.s of the equations, since the term involving the conductance G_{km}, that is, the term $V_k V_m G_{km} \cos\delta_{km}$ is missing from the DC power flow expression, and this is a serious candidate for the errors of the DC load flow. This is a reason for an attempt to correct this situation. The basic concept comes from the fact that in real-world power systems have a rather certain pattern concerning voltage magnitude and line flows. It is well-known that voltage magnitude always is in the region of values 1.0 p.u. to 1.05 p.u. almost for every bus in the system, that is proved by many power flow simulations and measurements. At the same time in a typical transmission system line flows are always in the same direction and above some certain values. These patterns offer useful empirical knowledge of the system operating point and can thus be utilized for DC load flow improvement. Two new terms are introduced, carrying the idea of "correction" terms given by the equations

$$P_{k_{corr}} = -\sum_{m=1}^{n} V_k V_m G_{km} \cos\delta_{km} \tag{2.343}$$

$$B_{km_{corr}} = \frac{V_k V_m \sin\delta_{km}}{\delta_{km}} \tag{2.344}$$

where $P_{k_{corr}}$ is the correction term for active power injection and $B_{km_{corr}}$ is the correction term for the susceptance of the branch km.

By using the notations given in the following equations

$$P_k^* = P_k + P_{k_{corr}} \tag{2.345}$$

$$B^*_{km} = B_{km} B_{km_{corr}} \tag{2.346}$$

and substituting them in equation 2.342 the following equation is obtained

$$P^*_k = \sum_{m=1}^{n} B^*_{km} \delta_{km} \tag{2.347}$$

It is clear that equation 2.347 has the same formulation as equation 2.341, with the difference that the modified DC load flow incorporates the correction terms, that leads to more accurate calculation. An algorithm for the modified DC load flow method is presented in figure

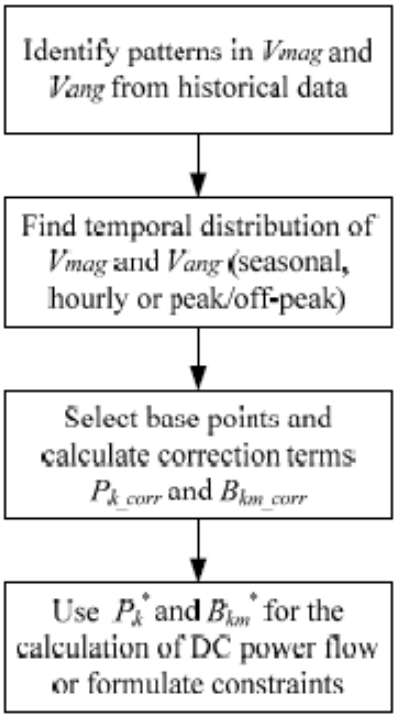

FIGURE 2.51: Implementation procedure for the improved DC power flow method

The proposed method has been validated during simulation tests on the IEEE 30-bus case system, compared with the traditional DC load flow algorithm. Simulation results are presented in the following figures 2.52, 2.53, 2.54, 2.55.

Results are very encouraging in terms of errors reduction in line power flows and voltage angles, so this is a rather promising method for future DC load flow applications.

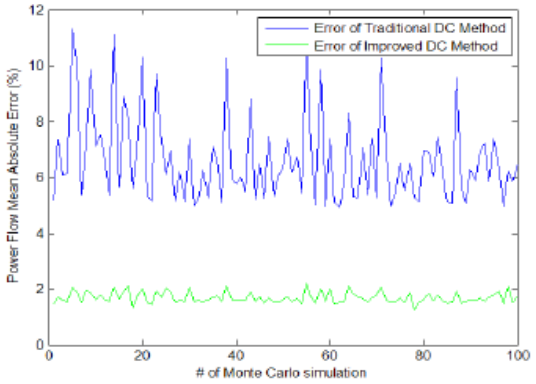

FIGURE 2.52: Comparison of power flow errors between traditional DC method and the improved DC method: 130% loading of base case

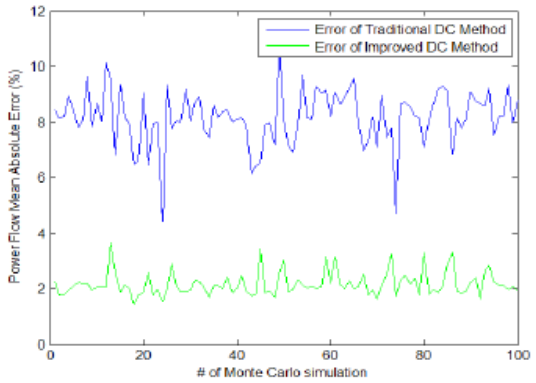

FIGURE 2.53: Comparison of power flow errors between traditional DC method and the improved DC method: 70% loading of base case

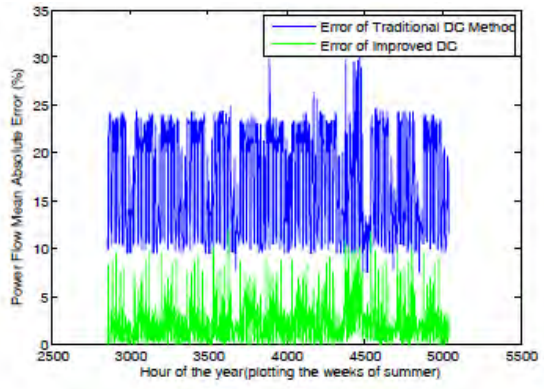

FIGURE 2.54: Comparison of power flow errors between traditional DC method and the improved DC method: IEEE 118 bus system

2.4.9 AC versus DC power flow

Case I Computationally the DC power flow has at least three advantages over the standard NRPF, as the authors of [30] claim. First, by just solving the real power

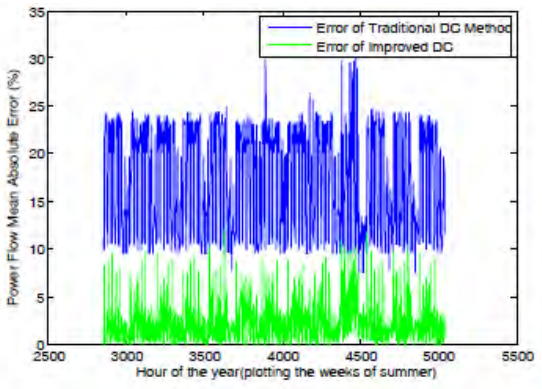

FIGURE 2.55: Comparison of bus voltage angle errors between traditional DC method and the improved DC method: IEEE 118 bus system

balance equations, its equation set is about half the size of the full problem. Second, the DC power flow is an non-iterative process requiring just a single solution of a linear expression relating the active power with the angle difference between buses. Third, because the admittance matrix in the form of susceptance elements is state-independent provided the system topology does not change, it need only be factored once. Therefore, one would expect the DC power flow to be about ten times faster than the regular power flow for the initial solution, and even faster for the subsequent solutions since solving for the angle with a modified power would only require a forward/backward substitution. DC power flow is a faster method for contingency analysis too. When line outage is considered as a contingency condition, its effects can be measured by the use of the line outage distribution factor (LODF) which are state independent and can be calculated once and used many times for contingency analysis. Once the factored susceptance matrix is available the computation requirements to calculate each LODF vector are proportional to a fast forward/full backward substitution. This allows the contingencies to be linearly approximated many times faster than the approach of actually solving the power flow for the contingent system. In the same paper a comparative analysis between AC and DC load flow methods is investigated. Although concerned with the locational marginal price calculation it concludes with the remarks that the comparison of the AC and DC approaches, through simulation results, has shown that the methods are almost identical in revealing the congestion patterns, but the DC approach does the work quit faster.

Summarizing, the DC load flow model approximation creates a totally linear problem which has a very fast solution. Since simulations have proved DC load flow advantages, it has become a commonly used analysis technique in power systems and market applications. References present the DC load flow analysis applied

for contingency analysis, calculation of power transfer distribution factors, line outage distribution factors, transmission interchange limit analysis, market clearing procedures and financial transmission rights calculations. However, because of inherent approximations the DC model may cause errors in these applications.

Case II Several references with comparative studies of AC and DC load flow can be found in the literature. For example in [31] where a comparison between AC and DC power flow methodologies on the optimal power flow based locational marginal price calculation for real power systems is considered, where the authors apply three methods, namely the full AC, the simplified DC without losses and the extended DC with losses in a local national real power system trying to configure the possible differences between them in the computation of power prices. The simulation tests show that although, in many cases, the three algorithms show relatively similar results, in certain cases it may turn out that the discrepancy of the results obtained (even in the case between AC power flow and the extended DC power flow with losses incorporated) is large enough to make it reasonable to implement the AC model for the sake of correctness. The authors propose a mixed power flow algorithm in which the AC model is used for preliminary calculations concerning the day-ahead market while the DC model is used for calculations in the intra-day market and real-time market.

Case III A combination of AC plus DC model is presented in [32]. The basic concept behind this approach is that power flow problems can be solved with the use of AC model for certain buses where accuracy plays an important role, and with the use of DC model for the others. In other words, the power flow equations which require accurate solution are formulated with the AC model and the rest are done with the DC model for a faster but less accurate solution. After that the NR method can be used to solve the reduced set of nonlinear equations. The area can be divided depending on the importance of a certain section with a viewpoint of power system operation and control. The proposed algorithm is presented in the following figure 2.56 while in figure 2.57 the bus selection is illustrated

The important buses belong to the AC region while all other not so important buses belong to the DC region. Some buses of the DC region that have a connection with buses in the AC region are called the boundary buses. The given condition for BD buses is only real power injection therefore a proper guess for reactive power injection or voltage magnitude is required to improve accuracy in AC region. The proposed method creates nonlinear real power flow balance equations for the BD buses. In other words the approach assumes that the BD bus is considered to be a generator PV bus in the AC region with flat unity voltage magnitude. Simulation results are obtained on a IEEE 14-bus system as presented in figure 2.58. In

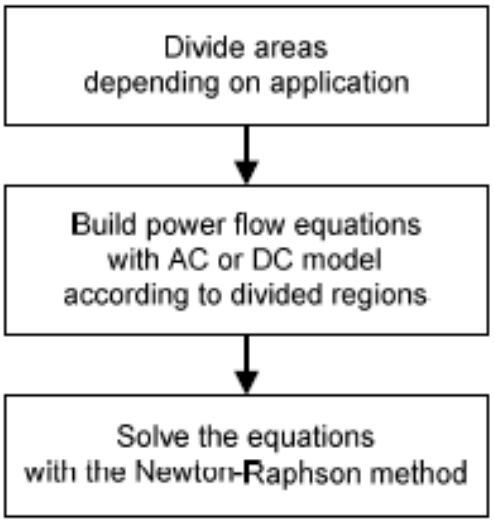

FIGURE 2.56: Procedure of the hybrid AC+DC power flow approach

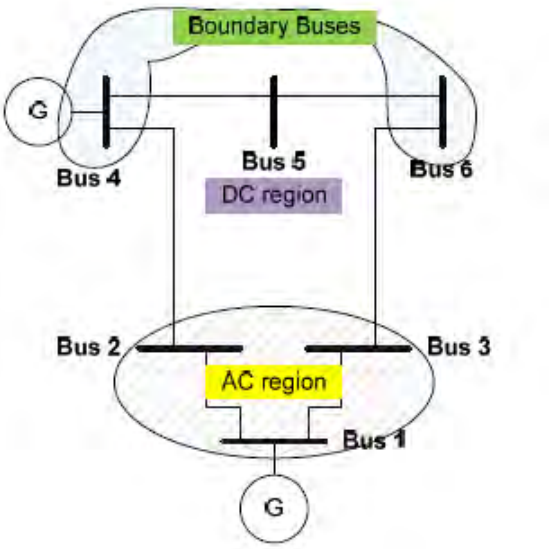

FIGURE 2.57: AC, BD and DC area selection

this system buses 1,4,5,14 are selected for the AC region (great accuracy), buses 2,3,6,7,9,13 are boundary buses (BD) and the remaining are DC region buses.

The results are based on the mean absolute percentage error (MAPE) of active line power flows by taking AC results as a reference

$$MAPE = |\frac{P_{AC} - P_{test}}{P_{AC}}|x100\% \tag{2.348}$$

and show that there is a 70% of reduction in error compared to the results from the DC model as illustrated in figure 2.59

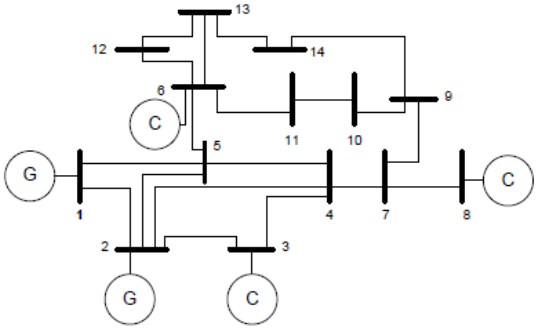

FIGURE 2.58: IEEE 14-bus system

From	To	Real power flow (MW)			MAPE (%)	
		AC	DC	Hybrid	DC	Hybrid
1	2	159.6	147.9	157.9	7.4	1.1
1	5	75.3	71.1	74.5	5.6	1.1
2	3	75.9	70.1	75.5	7.7	0.6
2	4	55.7	55.2	55.2	0.8	0.9
2	5	41.1	40.9	40.4	0.4	1.6
3	4	-21.1	-24.1	-21.5	14.5	1.9
4	5	-60.0	-62.3	-60.6	3.9	1.0
4	7	28.0	29.6	27.9	5.8	0.6
4	9	16.2	17.2	16.1	6.2	0.5
5	6	44.1	45.2	42.2	2.3	4.5
6	11	7.4	6.3	6.0	14.3	18.3
6	12	7.8	7.5	7.3	3.3	6.1
6	13	17.8	17.0	17.6	4.2	0.8
7	9	28.0	29.0	27.9	3.4	0.6
9	10	5.2	6.2	4.5	18.3	13.9
9	14	9.4	9.9	9.9	5.0	5.1
10	11	-3.8	-2.8	-3.3	25.8	13.8
13	14	5.6	5.0	5.2	11.9	8.6
Average					7.8	4.5

FIGURE 2.59: IEEE 14-bus system

The authors of the paper find this improved power flow algorithm as a basis for further investigation on power flow analysis The authors of this review report share the same challenging perspective for this AC+DC power flow algorithm, since they feel that based on technical as well as economical criteria, concerning the buses and model separation, the proposed algorithm could become very valuable introducing new frontiers in power flow analysis.

Case IV A recent paper with a novel efficient model for the power flow analysis is presented in [33]. The purpose of the new method is to present a novel power flow scheme in which neither voltage nor reactive power quantities are sacrificed as it is done in the DC load flow model. The proposed method is based on a slightly different power flow model, in which the transmission line load flow equations

instead of the bus load flow equations are formulating the power flow model. This line flow-based power flow model adopts active line flows, reactive line flows and the square of the voltage magnitudes as the state variables. The authors extend the model by using simple and not threatening assumptions relative to the assumptions of the DC load flow model. In that way a set of linearized equations of active and reactive power are obtained which are expressed in terms of the bus voltage magnitudes, phase angles and line losses. The final matrix arrangement gives the vectors of the controlled active and reactive power variables dependent on conductance and susceptance block matrices with the additional line losses term. This formulation constitutes nonlinearity which imposes an iterative approach for solving the system. Active and reactive line losses are initially set to zero and are updated after each iteration. Hence they are treated as known parameters in each iteration. This assumption linearizes the model and makes it solvable by means of matrix inversion techniques. The iterative procedure is terminated only when the losses are not changed in successive iterations. The proposed method is compared to the conventional NRPF model, the DC load flow model and the original line load flow based model in IEEE small to medium scale bus test cases and the results show that it provides an appropriate compromise between accuracy of the AC model and speed of the DC model. The authors suggest the method for power system reliability assessment in which many possible outage scenarios must be analyzed in a reasonable time span.

2.4.10 Sensitivity analysis

Real power systems, in the deregulated environment [34], contain producers and consumers sharing a common transmission system, in which power and energy are delivered from the former to the latter participants. A large number of power transactions occur in daily operation of the electric grid through transmission networks, since its major task is to satisfy consumer demands by equal power supply. Since transmission network operates under certain limitations, concerning its ability to transfer the demanded power, as well as overloading conditions, it is crucial, to know the available transfer capability of each transmission line, at each time step that a transaction between producers and consumers occurs. Power transactions between sellers and buyers can be committed only if available transfer capability is available for each particular transaction. Automatic transfer capability is one of the daily calculated operations in electric transmission networks. ATC is closely related to power flow studies.

By extending the load flow calculation concept, additional interesting terms for the transmission transaction evaluation, like the several sensitivities factors can be computed. Load flow analysis can be considered as the means for evaluating ATC by utilizing sensitivity analysis. Both AC and DC load flow can be used for calculating proper sensitivity factors capable for evaluating ATC. Power transfer distribution factor, generation shift factor, line outage distribution factor, line losses distribution factors are the most usual and are used to evaluate the transmission transactions either bilateral or multilateral, for the interested reader see [11].

Network system sensitivities play an important role in transmission calculations. They are system coefficients relating the amount of one change to another change. The most usually employed for transmission calculations are

1. Power Transfer Distribution Factor (PTDF)

   (PTDF) relates the amount of transaction to line power flow. More specifically is the fraction of the amount of a transaction from one zone to another that flows over a given transmission line. In other words a PTDF specifies the incremental flow induced on each transmission line by injecting one MW at one node and withdrawing it at some designated reference node. Simply, PTDF measures the sensitivity of line MW flows to a MW transfer.

   In general, if q_{line} is the transmission line quantity, i.e. power in line l connecting buses i and j, and t_p is a transaction between a generator bus k and a load bus m, then PTDF is given as

$$PTDF_{q_{line}} = \frac{\Delta q_{line}}{\Delta t_p} \tag{2.349}$$

   If the power quantity is active power P_{ij} then the above equation is

$$PTDF_{P_{ij}} = \frac{\Delta P_{ij}}{\Delta t_p} \tag{2.350}$$

   From the above definition it is clear that PTDF depends on the power line flow (the flow created in transmission lines connecting buses), which is a function of the voltages and angles at its terminal buses.

   The sensitivity relationship coming out by the Newton-Raphson load flow analysis in polar coordinates for a base case load flow is given by

$$\begin{bmatrix} \Delta\delta \\ \Delta V \end{bmatrix} = \begin{bmatrix} S_T \end{bmatrix} \begin{bmatrix} \Delta P \\ \Delta Q \end{bmatrix} \tag{2.351}$$

where $S_T = [J]^{-1}$ is the inverse of the well-known Jacobian matrix J, standing as a sensitivity matrix.

Transaction transfers are modeled as a change in injection power flows, which would otherwise be zero after a base case load flow calculation where supply equals demand. This means that the only non-zero terms, concerning power mismatches ΔP and ΔQ are the ones that have to do with the specified transactions. Let the buyer (consumer) transaction denoted as T_b while T_s stands for the seller transaction, both of them following the general expression of t_p. Then equation 2.351 takes the form

$$\begin{bmatrix} \Delta\delta_b \\ \Delta V_b \end{bmatrix} = \Big[J\Big]^{-1} \begin{bmatrix} \Delta T_b \\ 0 \end{bmatrix} \tag{2.352}$$

for the buyer, while for the seller is as follows

$$\begin{bmatrix} \Delta\delta_s \\ \Delta V_s \end{bmatrix} = \Big[J\Big]^{-1} \begin{bmatrix} \Delta T_s \\ 0 \end{bmatrix} \tag{2.353}$$

These two matrix equations, are the power flow algorithm that now needs to be solved, where $\Delta\delta_s$, $\Delta\delta_b$, ΔV_s and ΔV_b are the sensitivities of the buyer and seller sending power to the slack bus. By solving equations 2.352 and 2.353 a new voltage phasor profile can be calculated. It is noted that the above formulation is based on the full AC NRPF.

For DC power flow, the linear equation that describes the power flow algorithm is

$$\Big[\Delta\delta\Big] = \Big[B'^{-1}\Big]\Big[\Delta P\Big] \tag{2.354}$$

The sensitivities now, concern only the phase angle, so for power transactions for seller T_s and for buyer T_B, the sensitivities take the form

$$\Big[\Delta\delta_b\Big] = \Big[B'^{-1}\Big]\Big[\Delta T_B\Big] \tag{2.355}$$

$$\Big[\Delta\delta_S\Big] = \Big[B'^{-1}\Big]\Big[\Delta T_S\Big] \tag{2.356}$$

Since DC load flow always ignores losses, the final phase angle is

$$\Delta\delta = \Delta\delta_b - \Delta\delta_s \tag{2.357}$$

Using the chain rule the PTDF is simply a function of these voltage magnitudes and angles sensitivities. If P_{ij} is the power line flow between buses i and j, then PTDF can be calculated by

$$PTDF = \Delta P_{ij} = \frac{\partial P_{ij}}{\partial V_i}\Delta V_i + \frac{\partial P_{ij}}{\partial V_j}\Delta V_j + \frac{\partial P_{ij}}{\partial \delta_i}\Delta \delta_i + \frac{\partial P_{ij}}{\partial \delta_j}\Delta \delta_j \tag{2.358}$$

where $\Delta\delta_i$, $\Delta\delta_j$, ΔV_i and ΔV_j are the voltage magnitude and angle sensitivities of the buses participating in power transaction. The partial derivatives are computed by

$$\frac{\partial P_{ij}}{\partial \delta_i} = V_i V_j(-G_{ij}\sin\delta_{ij} + B_{ij}\cos\delta_{ij}) \tag{2.359}$$

$$\frac{\partial P_{ij}}{\partial \delta_i} = V_i V_j(G_{ij}\sin\delta_{ij} - B_{ij}\cos\delta_{ij}) \tag{2.360}$$

$$\frac{\partial P_{ij}}{\partial V_i} = 2V_i G_{ii}(G_{ij}\cos\delta_{ij} + B_{ij}\sin\delta_{ij}) \tag{2.361}$$

$$\frac{\partial P_{ij}}{\partial V_j} = V_i(G_{ij}\cos\delta_{ij} + B_{ij}\sin\delta_{ij}) \tag{2.362}$$

if the AC NRPF is adopted, while for DC load flow the corresponding partial derivatives take the form

$$\frac{\partial P_{ij}}{\partial \delta_i} = B_{ij} \tag{2.363}$$

$$\frac{\partial P_{ij}}{\partial \delta_j} = -B_{ij} \tag{2.364}$$

$$\frac{\partial P_{ij}}{\partial V_i} = 0 \tag{2.365}$$

$$\frac{\partial P_{ij}}{\partial V_j} = 0 \tag{2.366}$$

The PTDF matrix which characterizes the flow pattern in a network can be easily computed through simulation or directly from the electrical properties (susceptances) of each transmission line. The PTDF matrix can be used to determine the impact of injections and withdrawals at any pair of nodes on any transmission line by using superposition.

Based on the DC load flow model a simpler PTDF is presented, defined as

$$PTDF_{ij,mn} = \frac{X_{im} - X_{jm} - X_{in} + X_{jn}}{x_{ij}} \tag{2.367}$$

where

x_{ij} is the reactance of the transmission line connecting bus/zone i and bus/zone j; X_{im} is the entry in the i-th row and m-th column of the bus reactance matrix X

It is worth noting that reactance matrix contains constant element values.

The change in the line flow for a new transaction is now given by

$$\Delta P_{ij}^{new} = PTDF_{ij,mn} P_{mn}^{new} \tag{2.368}$$

where,

i and j terminal buses for the line under consideration m and n "from" and "to" buses/zones numbers for the new transaction P_{mn}^{new} is the new transaction MW amount.

2. Line Outage Distribution Factor (LODF) Another useful coefficient is the line outage distribution factor which is a measure of the redistribution of power flow from an outaged line onto the remaining lines in the system. It is the fraction of the power flowing on the line between two buses/zones before outage and now is distributed over another line between two other buses/nodes.

   If a line l_o between buses r and s is outaged having pre-outaged power flow P_{rs}^o from bus-r to bus-s and P_{sr}^o from bus-s to bus-r and P_{ij,l_o} is the post outaged power flow in another line between buses i and j, then the change in its power flow is given by:

$$\Delta P_{ij,l_o} = P_{ij,l_o} - P_{ij}^o \tag{2.369}$$

   Then LODF is defined as the ratio of $\Delta P_{ij,l_o}$ to the real power flow transmitted in the line taken for outage and connected between bus-r and bus-s, given by

$$LODF_{ij,l_o} = \frac{\Delta_{ij,l_o}}{P_{rs}^o} \tag{2.370}$$

   LODF is obtained by simulating power flow studies, modeling line outages as some kind of transfer transactions. Power mismatches of the matrix equation 2.351, now have the form:

$$\Delta P_r = P^o_{rs}, \Delta P_s = P^o_{sr} \tag{2.371}$$

$$\Delta Q_r = Q^o_{rs}, \Delta Q_s = Q^o_{sr} \tag{2.372}$$

By using these power mismatches a new load flow analysis is being executed, resulting in a new voltage profile. The only no-zero elements are the above four elements corresponding to bus-r and bus-s. The solution of the power flow model gives the voltage magnitude and angle from the pre-outage to the post-outage condition for the outaged line-l. By calculating the changes in voltage magnitude and angle, post-outage calculations of the bus as well as line flows can also be calculated. By using the above calculated values, the LODF's can finally be computed. If the PTDF is known, then LODF can also be calculated by the relation

$$LODF_{ij,l_o} = \frac{PTDF}{1 - PTDF} \tag{2.373}$$

Using the DC load flow in [][christie] a similar to PTDF, calculation of LODF is presented as follows

$$LODF_{ij,rs} = \frac{N_{rs}x_{rs}}{N_{ij}x_{ij}} \frac{(X_{ir} - X_{is} - X_{jr} + X_{js})}{N_{rs}x_{rs} - (X_{rr} + X_{ss} - 2X_{rs})]} \tag{2.374}$$

where,

x_{ij} is the reactance of the transmission line connecting bus/zone i and bus/zone j; X_{ir} is the entry in the i-th row and r-th column of the bus reactance matrix X, N_{ij} denotes the number of circuits connecting bus/zone i and bus/zone j.

3. Generator Shift Factor (GSF) The generator shift factor is defined as the ratio of the change in megawatt power flow on a network branch when one megawatt change in generation occurs at a bus compensated by a withdrawal of one megawatt at the reference bus. In other words it is the sensitivity of the contribution to a line flow from a bus. The generator shift factor is used for the computation of loss factor. Simply, GSF shows how the flow in a branch (connecting line) will change if the injection at a bus changes by one MW.

4. Loss Factor (LF) It can be viewed as the change of total system loss with respect to one megawatt increase in injection at a specified bus. In other words, a loss factor at the bus shows how system losses will change if the injection at the bus is changed by one MW. Since the slack (reference) bus has the task to cover system

losses, it is evident that the values of the loss factors are dependent of the reference bus. The LF can be defined by the equation [36][Li,Bo,Zhang]

$$LF_i = \frac{\partial P_{loss}}{\partial P_i} \tag{2.375}$$

where,

∂P_i is the change in the injected power at bus i ∂P_{loss} is the relative change in power system losses.

5. Delivery Factor (DF) Finally the delivery factor at a bus represents the effective megawatt delivered to the customers to serve the load at that bus. DF can be defined as

$$DF_i = 1 - LF_i = 1 - \frac{\partial P_{loss}}{\partial P_i} \tag{2.376}$$

DF shows how much power is going to reach the reference bus is additional one MW is injected at a bus denoted i. This means that if one injects additional MW of power at the bus i only $1 - LF_i$ MW will reach the reference bus, the rest is only system losses.

6. Voltage Distribution Factor (VDF) VDF is defined as the ratio of the change in bus voltage magnitude ΔV_i at any bus i to the change in power denoted by the p-th transaction, i.e., Δt_p, which is expressed as

$$VDF_{i,t_p} = \frac{\Delta V_i}{\Delta t_p} \tag{2.377}$$

where,

$$\Delta V_i = V_{i,t_p} - V_i^o \tag{2.378}$$

VDF is calculated by the same process used for PTDF calculation.

7. Line Outage Voltage Distribution Factors (LOVDF) LOVDF is defined as the change in the bus voltage magnitude during a line outage to the change in the transmitted real power flow in the line being taken out considering outage of a line l_o between the buses r and s, and is expressed as

$$LOVDF_{i,\{l_o\}} = \frac{\Delta V_{i,\{l_o\}}}{P_{rs}^o} \tag{2.379}$$

where

$$\Delta V_{i,\{l_o\}} = V_{i,\{l_o\}} - V_i^o \tag{2.380}$$

and P_{rs}^{o} is the preoutage real power flow in a line between bus-r and bus-s.

2.4.11 Contingency analysis

When the transmission system operates in steady state all the variables are within their corresponding limits. On the contrary, when transmission system operates beyond its constraints, concerning bus voltages, or its equipments are overloaded (not in the fault condition when transients occur) then the system is not static secure. It is clear that no overloading means securely transmitting the scheduled power. Since the system dynamics (swing dynamics) are not involved the overloading due to an abnormal condition is still a steady analysis problem. The above mentioned analysis is called the contingency analysis. In other words, contingency analysis is the process of identifying the consequences of potential components outages (contingencies) of the system. Contingency could be an outage of a line, transformer, breaker, generator or a combination of them.

Power flow study stands as the basis for contingency analysis [10] which is also a very crucial problem in power system analysis. Contingency analysis is concerned with the impacts of abnormal conditions in the steady-state operation of the network, leading to the security degree enhancement of the power system. Power system security has the task of evaluating a series of a-priori determined contingencies which have multiple form, of either a single outage of any system element (transmission line, generator, transformer, reactor) known as the N-1 contingency, or simultaneous outages of double lines or even the outage of the largest generator and the interconnections with the rest of the system.

A single outage can be simulated by simply removing the branch under consideration and at the same time solving the associated power flow problem. This is the simple case. Since multiple contingencies have to be evaluated, it is reasonable that multiple load flow studies have to performed one for each contingency in order to assess the network state after the outage of one or multiple elements.

Contingency analysis may be viewed as a load flow analysis for each a-priori specified abnormal condition. However, since the number of possible contingencies is large enough, increasing the computational burden, other methods than the conventional power flow are executing the task. These algorithms are usually the DC load flow analysis by the use of the different types of sensitivity analysis factors (distribution factors, line outage factors, etc), or the compensation method.

It must be mentioned that not all line outages cause system overloading. So, in order to reduce computational time, a procedure called contingency ranking is carried out

according to the probability of system overloading being caused by a line outage. Ranking indexes try to evaluate the loading of transmission lines or transformers after an outage by using proper distribution factors which are linear factors denoting the change of power flow in transmission lines and transformers after the outage of a generator or branch element.

Contingency ranking is followed by the next procedure called the contingency checking which performs the load flow contingency analysis first on the lines with higher probability of being overloaded. Lines with the lowest probability are not subject to contingency analysis, because a rationale assumption is being made that these lines will not cause any trouble in case of overloading.

Another used algorithm is based on load flows, used so as to face abnormal voltage analysis, which performs a check for overloads and voltage problems on the approximate state obtained after the end of the first step of the load flow analysis.

Most of the contingency analysis tools perform the following steps during operation

1. Calculate base power flow
2. Check all limiting elements for violations
3. Screen all the contingencies, that is, a process of simulating each contingency from a given set one by one by DC model based quick power flow analysis.
4. Check each for potential violation
5. Run all suspicious contingencies through the full AC power flow analysis
6. Report violations in base case and under contingencies.

2.4.12 Continuation Power Flow

One of the load flow applications is the so-called (CPF) employed in voltage stability analysis. Voltage stability is concerned with the voltage limits, beyond which abnormal system operation begins [37]. It is known that at voltage stability limit the Jacobian matrix of the load flow becomes singular. This problem can be overcome by the use of continuation power flow which performs load flow algorithm based on a load scenario. The conventional power flow model in polar coordinates is the basis for CPF analysis, and is expressed by the well known equations

$$P_i = \sum_{j=1}^{n} |V_i||V_j|(G_{ij}\cos\delta_{ij} + B_{ij}\sin\delta_{ij}) \tag{2.381}$$

$$Q_i = \sum_{j=1}^{n} |V_i||V_j|(G_{ij} \sin \delta_{ij} - B_{ij} \cos \delta_{ij}) \tag{2.382}$$

$$P_i = P_{Gi} - P_{Di} \tag{2.383}$$

$$Q_i = Q_{Gi} - Q_{Di} \tag{2.384}$$

The loading scenario is based on the introduction of a scalar load parameter λ inserted into demand load active and reactive power, that is

$$P_{Di} = P_{Dio} + \lambda(P_{\delta base}) \tag{2.385}$$

$$Q_{Di} = Q_{Dio} + \lambda(Q_{\delta base}) \tag{2.386}$$

where

P_{Dio} and Q_{Dio} are the original load demands (if conventional load flow was taken into account) while $P_{\delta base}$ and $Q_{\delta base}$ are quantities of powers that are chosen to scale the scalar λ appropriately.

Incorporating equations 2.385 and 2.386 into equations 2.381, 2.382, 2.383, 2.384, a new set of equations is expressed as,

$$F(\delta, V, \lambda) = 0 \tag{2.387}$$

where δ is the voltage phase angle state variable, V is the voltage magnitude phase state variable, and λ is the new state variable since it affects the controlled variables P and Q. If $\lambda = 0$ the above algorithm is turned to a conventional power flow problem.

CPF method engages predictor and corrector steps. The predictor step consists in estimating next solution for a specified loading scenario (a load pattern described by λ) by using a tangent prediction direction step, taking into account a base case power flow solution. The predictor analysis, starts by taking the derivatives of equation 2.387 w.r.t. all the state variables, which gives the next expression

$$\frac{\partial F}{\partial \delta} d\delta + \frac{\partial F}{\partial V} dV + \frac{\partial F}{\partial \lambda} d\lambda = 0 \tag{2.388}$$

which in a more compact form is expressed as,

$$F_\delta d\delta + F_V dV + F_\lambda d\lambda = 0 \tag{2.389}$$

which in matrix form is,

$$\begin{bmatrix} F_\delta & F_V & F_\lambda \end{bmatrix} \begin{bmatrix} d\delta \\ dV \\ d\lambda \end{bmatrix} = \begin{bmatrix} 0 \end{bmatrix} \tag{2.390}$$

The above equation has one more unknown than the number of equations, so it needs an additional equation. This can be done by introducing the so-called continuation parameter, that is, setting one of the tangent vector components to either $+1$ or -1, leading to a nonsingular Jacobian matrix at the critical point. Now, 2.390 takes the following form,

$$\begin{bmatrix} F_\delta & F_V & F_\lambda \\ e_k & & \end{bmatrix} \begin{bmatrix} d\delta \\ dV \\ d\lambda \end{bmatrix} = \begin{bmatrix} 0 \\ (+-)1 \end{bmatrix} \tag{2.391}$$

where e_k is a row vector with all elements zero, except the k^th element which is equal to 1. Equation 2.391 can be solved in order to find the tangent vector. The prediction step is the made as follows:

$$\begin{bmatrix} \delta \\ V \\ \lambda \end{bmatrix}^{p+1} = \begin{bmatrix} \delta \\ V \\ \lambda \end{bmatrix}^{p} \sigma \begin{bmatrix} d\delta \\ dV \\ d\lambda \end{bmatrix} \tag{2.392}$$

where superscript $p+1$ denotes the next step of prediction. σ is a step size chosen so that the predicted solution lies within the range of convergence of the corrector. In correction step, local parameterization is used so as to correct the predicted solution. One more equation is added to the original set of conventional power flow equations, so the new matrix form of power flow model is now given by,

$$\begin{bmatrix} F(\delta, V, \lambda) \\ x_k - \eta \end{bmatrix} = \begin{bmatrix} 0 \end{bmatrix} \tag{2.393}$$

where x_k is the chosen state variable playing the role of continuation parameter and η is the predicted value of this state variable. Equation 2.393 is a slightly modified power flow model which is solved by a consequent modified NRPF algorithm.

The two-step predictor-corrector CPF method is iteratively solved, which is done by new predictions made for changes in load pattern (described by λ) upon the new tangent vector, followed by the equivalent corrector steps. The process keeps going until a predefined critical point is reached. This critical point is the one where the tangent vector is zero.

2.4.13 Complementarity approach of Power Flow

A novel approach considering the power flow problem in an optimization framework introduced in [38]. The proposed method is the first in bibliography trying to examine and solve the power flow problem in a way that most usually is applied in optimal power flow problems. The authors claim that the main reasons for the need of a totally alternative approach method compared to almost all, more or less conventional power flow methods, are the convergence problems that come into surface for large scale systems when using a flat start (that is taking the voltage phase angle $\delta = 0$ and the voltage magnitude $|V| = 1$), or when exceeding the maximum loadability of the system, leading to a required initial solution close to the final solution, or when the conventional PF model requires iterative PV-PQ bus switching when the reactive power at a specified bus violates the limits. The proposed method uses the so-called complementarity constraints in order to describe properly the reactive power generation limits. The basic formulation of the optimization framework PF model is given by the following equations

$$minF(\epsilon_p, \epsilon_q) = \sum_i (\epsilon_{pi}^2 + \epsilon_{qi}^2) \tag{2.394}$$

$$\Delta P_i(\delta, P_s, |V_D|, |V_G|, Q_G) - \epsilon_{pi} = 0 \forall i \tag{2.395}$$

$$\Delta Q_i(\delta, P_s, |V_D|, |V_G|, Q_G) - \epsilon_{qi} = 0 \forall i \tag{2.396}$$

$$|V_{Gi}| = |V_{Gi0} + V_{Ga1} - V_{Gb1} \forall i \in gen \tag{2.397}$$

$$0 \leq (Q_{Gi} - Q_{Gi}^{min}) \perp V_{Ga_i} \geq 0 \forall i \in gen \tag{2.398}$$

$$0 \leq (Q_{Gi}^{max} - Q_{Gi}) \perp V_{Gb_i} \geq 0 \forall i \in gen \tag{2.399}$$

$$|V_{Gi}|, V_{Ga_i}, V_{Gb_i} \geq 0 \forall i \in gen \tag{2.400}$$

where symbol $\perp$ denotes the complementarity condition that is for $0 \leq a \perp b \geq 0$, $a = 0$, if $b \geq 0$ and $b = 0$ if $a \geq 0$ which can also be expressed as $ab = 0$, $a \geq 0$, $b \geq 0$.

The above set of equations contains the power balance equations describing the conventional power flow, that is, equations 2.395 and 2.396, while equations 2.398 and 2.399 are the complentarity equations with the appropriate constraints equations 2.397 and 2.400. The model includes two additional variables, namely V_{Ga} and V_{Gb} so as to regulate bus voltage magnitude variations at generator and slack bus when reactive power generation reaches limits.

By proper explanation of the complementarity conditions applied for reactive power generation limits modeling, the above set of equations can take the final form

$$minF(\epsilon_p, \epsilon_q) = \sum_i (\epsilon_{pi}^2 + \epsilon_{qi}^2) \tag{2.401}$$

$$\Delta P_i(\delta, P_s, |V_D|, |V_G|, Q_G) - \epsilon_{pi} = 0 \forall i \tag{2.402}$$

$$\Delta Q_i(\delta, P_s, |V_D|, |V_G|, Q_G) - \epsilon_{qi} = 0 \forall i \tag{2.403}$$

$$|V_{Gi}| - |V_{Gi0} - V_{Ga1} + V_{Gb1} = 0 \forall i \in gen \tag{2.404}$$

$$(Q_{Gi} - Q_{Gi}^{min}) V_{Ga_i} = 0 \forall i \in gen \tag{2.405}$$

$$(Q_{Gi}^{m} ax - Q_{Gi}) V_{Gb_i} = 0 \forall i \in gen \tag{2.406}$$

$$(Q_{Gi} - Q_{Gi}^{min}) \geq 0 \forall i \in gen \tag{2.407}$$

$$(Q_{Gi}^{m}ax - Q_{Gi}) \geq 0 \forall i \in gen \tag{2.408}$$

$$|V_{Gi}|, V_{Ga_i}, V_{Gb_i} \geq 0 \forall i \in gen \tag{2.409}$$

The objective function in both complementarity PF problem stands as the minimization of the power flow mismatches which is absolutely reasonable if one considers that in conventional power flow, the iteration steps are ended when power mismatches are below a prespecified tolerance limit. The proposed method relates the power flow problem to the predictor-corrector steps of a classical optimization method called the generalized reduced gradient (GRG) method, which is a solver of the so-called mixed complemntarity proble (MCP). By doing this it really creates an iterative method that results in the final solution of the state variables vector. The most encouraging issue about this method is that through simulation tests on real power system cases, it shows good convergence in cases when a robust NRPF algorithm fails to converge.

2.4.14 Optimal power flow

2.4.14.1 Optimal Power Flow theory

The importance of the load flow studies lies in the fact that it is the core of the optimal power flow algorithm [10] which is the base of the optimization procedure taking place in the so-called economic dispatch of the power system. The latter is the mechanism for scheduling the power generation in order to match the demand load by the customers of electric energy, in a technical as well as economic efficient and reliable way. Irrelevant of the type of the optimization algorithm that is to be solved, the power flow equations are the basic physical constraint of the system formulated in the already mentioned power mismatch balance equality constraint.

One of the major issues concerning the electric power system operation is economic dispatch. In its early form, economic dispatch of power market performs the allocation of total demand among various generating units, calculates the power flows all over the transmission network system, also the clearing prices of electricity sold to consumers while concurrently evaluates, through optimization techniques, the social welfare objective function related to consumer benefits and total system costs via their social surpluses. The load demand can be either inelastic or elastic. The aggregated algorithm that performs the operation of economic dispatch taking into account all of the network

physical and technical constraints, as well as the power flow balance equations is called optimal power flow problem (OPFP).

The objective of OPFP is to find the output levels for a set of generation resources that are distributed over a transmission network (and are already running and synchronized), so as to minimize total cost of serving specified loads (or maximize social welfare if loads are characterized by price sensitive loads), while accounting for losses and without violating transmission flow constraints. In other words the OPF procedure [8] consists of determining the optimal steady-state operation of a power system, which simultaneously minimizes the value of a chosen objective function and satisfies certain physical and operating constraints. Optimal power flow consists not only of the objective function that has to be evaluated but also, of system physical constraints that are responsible for its reliable and secure operation. These equality and inequality constraints that act as a safety margin for the power system take into consideration supply power and demand load limit ranges as long as transient and voltage stability limits.

The constraints of OPF include, [8] power flow equations constraints, upper and lower bounds on the generator active power outputs, upper and lower bounds on the generator reactive power outputs, capacity constraints on shunt capacitors and reactors, upper and lower bounds on the transformer or phase shifter tap positions, branch transfer capacity limits, node voltage limits, stability (small signal and transient) limits.

OPF algorithms are met in every kind of electric power system optimization model, namely, classical economic dispatch [39], power rescheduling or redispatching, generation unit commitment, stability constrained optimization (voltage stability [40], small signal stability [41] as well as transient stability [42]), ancillary services procurement [43], etc.

As already mentioned optimal power flow is an optimization problem. These kinds of problems are solved by either classical mathematical-based programming techniques or new evolutionary techniques [8]. In mathematical-based OPF expression a Lagrange function is formulated involving the mathematical components that describe the network operation. Each equality or inequality constraint takes a Lagrange multiplier associated with it [10]. More about that issue will follow on the subject relative to transmission pricing.

2.4.14.2 Optimal Power Flow Formulation

The optimal power flow problem can be expressed in many forms relative to the objective function to be optimized, the equality and inequality restrictions [10], [8]

The general mathematical expression of OPF is the following

$Minimize f(x,u)$
$subject h(x,u) = 0$
$g(x,u) \geq 0$

where $f(x,u)$ is the objective function to be minimized, $h(x,u)$ are the equality constraints and $g(x,u)$ are the inequality constraints, x is the vector of state variables and finally u is the vector of controlled variables.

In a more analytical description the OPF problem is stated as follows

Objective function

$$min \sum_{i \in S_G} C_i(P_{Gi}) = min \sum_{i \in S_G} (a + bP_{Gi} + cP_{Gi}^2) \tag{2.410}$$

where a,b,c,are the fuel cost coefficients of generating unit i S_G is the set of generating units in the system.

Equality Constraints

$$P_{Gi} - P_{Di} - V_i \sum_{j=1}^{n} V_j (G_{ij} \cos \delta_{ij} + B_{ij} \sin \delta_{ij}) = 0 \tag{2.411}$$

$$Q_{Gi} - Q_{Di} - V_i \sum_{j=1}^{n} V_j (G_{ij} \sin \delta_{ij} - B_{ij} \cos \delta_{ij}) = 0 \tag{2.412}$$

These two equations can be written in the form

$$P_{Gi} - P_{Di} = V_i \sum_{j=1}^{n} V_j (G_{ij} \cos \delta_{ij} + B_{ij} \sin \delta_{ij}) \tag{2.413}$$

$$Q_{Gi} - Q_{Di} = V_i \sum_{j=1}^{n} V_j (G_{ij} \sin \delta_{ij} - B_{ij} \cos \delta_{ij}) \tag{2.414}$$

the above equations being the well known AC power flow mismatch equations, the meaning of which is that calculating at specific iteration steps the right hand side of the two equations, the power balance between supply and demand must be kept constant, so the system operates normally.

So the above equations can be simplified to

$$f(P_{G,i}) = \sum_{i=1}^{m} P_{Gi} - \sum_{i=1}^{n} P_{Di} = 0 \tag{2.415}$$

If transmission system losses have to be considered then

$$f(P_{G,i}) = \sum_{i=1}^{m} P_{Gi} - \sum_{i=1}^{n} P_{Di} - P_{loss}(P_{G2}, P_{G3}, \cdots, P_{Gm} = 0. \tag{2.416}$$

Inequality constraints

$$P_{Gi}^{min} \leq P_{Gi} \leq P_{Gi}^{max} i \in S_G \tag{2.417}$$

$$Q_{Ri}^{min} \leq Q_{Ri} \leq Q_{Ri}^{max} i \in S_R \tag{2.418}$$

$$V_i^{min} \leq V_i \leq V_i^{max} \tag{2.419}$$

$$|P_i| = |P_{ij}| = |V_i V_j (G_{ij} \cos \delta_{ij} + B_{ij} \sin \delta_{ij}) - V_i^2 G_{ij}| \leq P_l^{max} \tag{2.420}$$

where ineq. 2.417 and 2.418 are the lower and upper limits of generation active and reactive power, ineq.2.419 is the voltage limit range and ineq.2.420 is the upper limit for the line power flow (transmission line capacity limit). The above formulation is the basic optimal power flow algorithm where the objective function handles the minimization of generation cost, while the inequality constraints are the most usually found in every type of OPF expression.

If voltage and reactive power issues are not of major importance, and in the case of simplification needed the DC power flow is the proper solution so the equality constraint has the expression

$$P_i = \sum_{j=1}^{n} \frac{\delta_{ij}}{x_{ij}}. \tag{2.421}$$

So far, the objective function characterizing the optimization procedure only dealt with generation cost minimization leading to the basic form of economic dispatch. If the consumer benefit is added, then the expression of the optimization of the so-called social welfare characterizes the OPF, that is

$$min \sum_{i \in S_G} C_i(P_{Gi}) - \sum_{i \in S_P} W_i(P_{Ei}) = min \sum_{i \in S_G} (a + bP_{Gi} + cP_{Gi}^2) - \sum_{i \in S_P} W_i(P_{Ei}). \quad (2.422)$$

The above is a more general form of the OPF model since it tries to find the most appropriate generation dispatch that minimizes generation cost having calculated the customer profit.

If stability issues have to considered, the basic constraint has the form

$$-\pi \leq \delta_{rot,i} \leq \pi \quad (2.423)$$

which is the consequence of the equal area criterion, where $\delta_{rot,i}$ is the rotor or torque angle describing the relative rotor position w.r.t. a reference machine stationary frame. This angle is connected to the phase angle of the bus connected at the output of generator under study.

To introduce the way electricity pricing is obtained we start with the simple form of economic dispatch concerning only the objective function of minimizing generation cost and the equality constraint, that is the power balance kept constant by utilizing the power flow algorithm.

From eq.2.422 and 2.415 a new function, expressed as a Lagrange formulation is obtained,

$$L(P_G)\lambda) = \sum_{i=1}^{m} C_i(P_{Gi}) - \lambda(\sum_{i=1}^{m} P_{Gi} - \sum_{i=1}^{n} P_{Di}). \quad (2.424)$$

By taking the first order partial derivatives, that constitute the necessary optimality conditions we can have

$$\frac{\partial L}{\partial P_{G,i}} = IC_i(P_{G,i}) - \lambda = 0, \qquad i = 1, \cdots, n \quad (2.425)$$

$$\frac{\partial L}{\partial \lambda} = \sum_{i=1}^{m} P_{Gi} - \sum_{i=1}^{n} P_{Di} = 0 \quad (2.426)$$

where

$$IC_i(P_{G,i}) = \frac{dC_i(P_{G,i})}{dP_{G,i}} \quad (2.427)$$

is the incremental cost for generating the next 1MW of supply power.

From eq.2.425 one can obtain

$$\lambda = IC_i(P_{G,i}) \tag{2.428}$$

which can be thought the definition of Lagrange multiplier λ as the incremental cost that has to be paid for the generation of the next increment of supply power, evidently in order to keep the supply-demand balance equation (power flow equation). A first intuitive thought of the above statement is the fact that multiplier λ multiplies the power balance equation, so it is closely related to it. This is an ideal definition of nodal price equal for all the nodes participating in a electricity power system in an unconstrained condition and without considering losses.

When considered inequality constraints, like generation active power limits, the Lagrangian function has the following form

$$L(P_G)\lambda) = \sum_{i=1}^{m} C_i(P_{Gi}) - \lambda(\sum_{i=1}^{m} P_{Gi} - \sum_{i=1}^{n} P_{Di}) - (\sum_{i=1}^{m} \mu_i^{max} P_{Gi} - P_{Gi}^{max}) - (\sum_{i=1}^{m} \mu_i^{max} P_{Gi} - PGi^{min}) \tag{2.429}$$

Taking the partial derivatives, i.e., the optimality conditions we have

$$\frac{\partial L}{\partial P_{G,i}} = IC_i(P_{G,i}) - \lambda - \mu_i^{max} - \mu_i^{min} = 0, \qquad i = 1, \cdots, n \tag{2.430}$$

$$\frac{\partial L}{\partial \lambda} = \sum_{i=1}^{m} P_{Gi} - \sum_{i=1}^{n} P_{Di} = 0 \tag{2.431}$$

The incremental cost can now be defined

$$IC_i(P_{G,i}) = \lambda + \mu_i^{min} \geq \lambda \qquad if \qquad P_{Gi} = P_{Gi}^{min} \tag{2.432}$$

$$IC_i(P_{G,i}) = \lambda \qquad if \qquad P_{Gi}^{min} \leq P_{Gi} \leq P_{Gi}^{max} \tag{2.433}$$

$$IC_i(P_{G,i}) = \lambda + \mu_i^{max} \leq \lambda \qquad if \qquad P_{Gi} = P_{Gi}^{max} \tag{2.434}$$

The above formulations show that in case of constraints the nodal price denoted by Lagrange multiplier λ is the same for all nodes only when generation operates between limits. In case limits are to be obtained additional prices denoted by μ modify the final nodal prices.

When losses are considered then the Lagrange function takes the form

$$L(P_G)\lambda) = \sum_{i=1}^{m} C_i(P_{Gi}) - \lambda(\sum_{i=1}^{m} P_{Gi} - \sum_{i=1}^{n} P_{Di} - P_{loss}(P_G, P_D) \tag{2.435}$$

The optimality condition are

$$\frac{\partial L}{\partial P_{G,i}} = IC_i(P_{G,i}) - \lambda(1 - \frac{\partial P_{loss}}{\partial P_{Gi}}) = 0, \qquad i = 1, \cdots, n \tag{2.436}$$

$$\frac{\partial L}{\partial \lambda} = -\sum_{i=1}^{m} P_{Gi} + \sum_{i=1}^{n} P_{Di} + P_{loss}(P_G, P_D) = 0 \tag{2.437}$$

From 2.436, by rearrangement one obtains

$$IC_i(P_{G,i}) = \lambda(1 - \frac{\partial P_{loss}}{\partial P_{Gi}}) \qquad i = 1, \cdots, n \tag{2.438}$$

the interpretation of which is that in case of losses an additional term is influencing the incremental power cost, leading to different values than the original nodal price.

Finally in case of transmission line constraints relative to line capacity limits the power flow through the whose capacity is limited can be expressed as,

$$P_f = \sum_{i=1}^{n} \beta_i(P_{Gi} - P_{Di} = \beta^T(P_G - P_D) \tag{2.439}$$

where the capacity limits have the form

$$-P_f^{max} \leq \beta^T(P_G - P_D) \leq P_f^{max} \tag{2.440}$$

After the Lagrange function formulation and the optimality conditions of it, the incremental cost is expressed as

$$IC_i(P_{G,i}) = \lambda + \gamma\beta_i \tag{2.441}$$

where γ is the additional Lagrange multiplier associated with the line capacity constraints of 2.440 when one of them is active. The meaning eq. 2.441 is that congestion (capacity constraint being active) adds one more price term in the original nodal price described by λ.

From the above analysis it is clear that the original nodal price in case of unconstrained and/or lossless network is the market clearing price, that is the price of active energy supplies to consumers. However, in any case of limit constraints or losses or both of them, additional terms affect the nodal price more or less. It is also evident that (although mentioned) the basis for nodal price computation is the Lagrange multiplier λ associated with the equality constraint, i.e., the power balance equation kept constant by the use of the power flow model. Nodal pricing is therefore, one more reason for investigating the power flow problem since it is already shown that a numerous algorithms are based on it, for their computation.

2.4.14.3 Distributed optimal Power Flow techniques

As already mentioned the classical power flow problem utilizes sparse matrix techniques and reordering after factorization to simplify the large dimension problem in case of very large-scale power networks. Since power flow is the core of the optimal power model, alternative equivalent methods for faster but reliable processing of the OPF algorithm in large scale systems have been proposed in the literature.

Some of these methods rely on the concept of parallel distributed modeling and processing of the OPF model. In [44] the authors propose a decomposition scheme of a large power system into geographically separate regions and perform computations for each region in parallel. Decomposition is suited to distributed computation where a separate processor is assigned to each regional calculation. The basic approach considers a division of geographically regions each one corresponding to an existing utility area. Any transmission line that crosses between two adjacent areas in conceptually divided in two lines by adding a dummy bus at the border between the two regions. The four power flow variables, namely active and reactive power flow, voltage magnitude and angle are assigned for each of the initially adjacent buses as well as for the dummy bus. For each dummy bus four equality constraints between duplicated variables must be added. This approach decomposes the overall optimization problem into a set of regional optimization problems. The solution of the regional optimization problem is alternated with an update of the Lagrangian multipliers on the equality constraints. The objective for each regional optimization problem is very similar to the objective of a standard OPF problem for the region alone, neglecting the rest of the system. The authors use

the interior point method for the OPF problem and an appropriate system to run the distributed OPF algorithm. The proposed method shows good results concerning the computational speed as well as the efficiency.

Alternative large-scale power system reduction methods have been presented as in [45], where the PTDF matrix is utilized for that purpose. The reduced PTDF matrix has the same structural properties as the original networks PTDF does. The method is tested and compared to other reduction methods, yielding satisfactory results. Since the method is independent of the operation set point it is a precise representation of the transmission network so it can be used for large system OPF algorithms.

2.4.15 Power Flow and Machine Stability

As it was mentioned at the beginning of this chapter power flow analysis is the basis for power systems analysis since it is engaged with system dynamics. Consequently the ordinary differential equations describing the generator (machine) internal dynamics are transformed to a set of differential-algebraic equations (DAE) due to the power flow equations involved. The connection of power flow to system dynamics, which is the basis for stability analysis, especially transient stability, is achieved by the multimachine stability analysis

The concept is the following. It is known that generators are interconnected by the transmission system, in which the generator output power is delivered before passing to distribution system and the final end-user. It is also known that in normal operating conditions, that is the steady-state the power flow is the tool for calculating all the transmission network variables injected to buses. The important difference in stability analysis, when electromechanical behavior occurs, is that, during transient phenomena, the complex power injected into the same transmission network nodes varies. So, it is necessary for the bus voltages to be calculated again leading to a new power flow analysis. That is why, as we shall see, when transient phenomena are examined, the prefault and postfault and during fault periods are being studied. Another important issue is load modelling. Load models involve a combination of constant impedance, constant power and constant current.

Before proceeding with the expression of MMS it is important to mention that for MMS studies a generator is connected to the output bus (the well known infinite bus) by a mediate bus which can be thought as an internal generator bus where the internal machine voltage is applied, instead of the terminal voltage that is applied at infinite bus.

The mathematical formulation of multimachine stability contains the following equations: The machine currents prior to disturbance are

$$I_{m,i} = \frac{S^*_{m,i}}{V^*_{m,i}} \tag{2.442}$$

The internal voltage of the machine can be described in phasor format as $E'_i = |E'_i|\angle\delta_{m,i}$ and the terminal voltage as $V_i = |V_i|\angle\delta_i$. Then the rotor angle of the machine which is responsible for stability is given by

$$\delta_{i,0} = \delta_{m,i} + \delta_i \tag{2.443}$$

which skows the angle difference between internal and external sides of the machine.

The voltages behind the transient reactances X'_d, that is, the internal machine voltage applied to the internal bus is given by

$$E'_{m,i} = V_{m,i} + jX'_d I_{m,i} \tag{2.444}$$

The loads are converted to equivalent admittances by

$$y_{i0} = \frac{S^*_i}{|V_i|^2} = \frac{P_i - jQ_i}{|V_i|^2} \tag{2.445}$$

Speaking for the bus admittance matrix, it is constructed in an augmented form containing the buses loads transformed to load admittances and the internal reactances also transformed to admittances. So the bus admittance matrix has the following form involved in the equation $I = YV$

$$\begin{bmatrix} I_1 \\ I_2 \\ \vdots \\ I_n \\ I_{n+1} \\ \vdots \\ I_{n+m} \end{bmatrix} = \begin{bmatrix} Y_{11} & \cdots & Y_{1,n} & Y_{1,n+1} & \cdots & Y_{1,n+m} \\ Y_{21} & \cdots & Y_{2,n} & Y_{2,n+1} & \cdots & Y_{2,n+m} \\ \vdots & \cdots & \vdots & \vdots & \cdots & \vdots \\ Y_{n1} & \cdots & Y_{n,n} & Y_{n,n+1} & \cdots & Y_{n,n+m} \\ Y_{n+1,1} & \cdots & Y_{n+1,n} & Y_{n+1,n+1} & \cdots & Y_{n+1,n+m} \\ \vdots & \cdots & \vdots & \vdots & \cdots & \vdots \\ Y_{n+m,1} & \cdots & Y_{n+m,n} & Y_{n+m,n+1} & \cdots & Y_{n+m,n+m} \end{bmatrix} \begin{bmatrix} V_1 \\ V_2 \\ \vdots \\ V_n \\ E'_{n+1} \\ \vdots \\ E'_{n+m} \end{bmatrix} \tag{2.446}$$

which in a more compact form is

$$\begin{bmatrix} I_n \\ I_m \end{bmatrix} = \begin{bmatrix} Y_{n,n} & Y_{n,m} \\ Y_{m,n} & Y_{m,m} \end{bmatrix} \begin{bmatrix} V_n \\ E'_m \end{bmatrix} \tag{2.447}$$

in which proper ordering is made in order to place the n terminal buses in the upper rows while the machine internal buses are places at the bottom rows. In this matrix expression $Y_{n,n}$ represents the bus admittance submatrix involving the terminal buses and additional load buses admittances, $Y_{n,m}$ and $Y_{m,n}$ are the submatrices containing the admittances that are constructed by the interconnection of terminal as well as internal buses (involving the machine internal reactance term transformed to admittance) and $Y_{m,m}$ is the bus admittance submatrix handling only the internal machine buses.

Since no current enters or leaves the load buses, currents in the first n rows are zero so the above matrix equation takes the form

$$\begin{bmatrix} 0 \\ I_m \end{bmatrix} = \begin{bmatrix} Y_{n,n} & Y_{n,m} \\ Y_{m,n} & Y_{m,m} \end{bmatrix} \begin{bmatrix} V_n \\ E'_m \end{bmatrix} \tag{2.448}$$

The above matrix equation can be expanded into the following equations

$$0 = Y_{n,n}V_n + Y_{n,m}E'_m \tag{2.449}$$

$$I_m = Y_{m,n}V_n + Y_{m,m}E'_m \tag{2.450}$$

Solving 2.449 for V_n and substituting in 2.450 the following are obtained

$$V_n = -Y_{n,n}^{-1}V_nY_{n,m}E'_m \tag{2.451}$$

$$I_m = [Y_{m,m} - Y_{m,n}Y_{n,m}^{-1}Y_{n,n}]E'_m = Y_{bus}^{red}E'_m \tag{2.452}$$

where the modified, by utilizing Kron reduction, bus admittance matrix is obtained

$$Y_{bus}^{red} = [Y_{m,m} - Y_{m,n}Y_{n,m}^{-1}Y_{n,n}] \tag{2.453}$$

The interesting about the new bus admittance matrix is that it contains only the internal machines buses and not the external terminal buses.

The electrical output of the generator is the well-known active power that forms the first of two power flow equations and is obtained as follows

The complex power produced by the generator, that is, the output complex power is

$$S^*_{1,e,i} = E'_{m,i} I_{m,i} \tag{2.454}$$

where complex power is expressed in terms of the internal excitation machine voltage

The active power is

$$P^*_{1,e,i} = Re(E'_{m,i} I_{m,i}) \tag{2.455}$$

$$I^*_{1,e,i} = \sum_{j=1}^{m} E'_{m,i} Y_{1,i,j} \tag{2.456}$$

Eq. 2.455 can be written in the form (in terms of internal voltages)

$$P^*_{1,e,i} = \sum_{j=1}^{m} |E'_{m,i}||E'_{m,j}||Y_{1,i,j}| \cos(\theta_{i,j} - \delta_i + \delta_j) \tag{2.457}$$

where $Y_{1,i,j}$ represents the bus admittance element describing the pre-fault condition (normal operation).

The above equation has the same form as the classical power flow equation with the difference that instead of bus terminal voltages describing transmission system, internal machine voltages are used, that represent the machine steady-state. The above equation constitutes the initial pre-fault condition of the machine power output. This means that prior to any disturbance, in normal operation, there is an equilibrium between electrical power output and mechanical power input which is expressed as

$$P^*_{1,m,i} = \sum_{j=1}^{m} |E'_{m,i}||E'_{m,j}||Y_{1,i,j}| \cos(\theta_{i,j} - \delta_i + \delta_j) \tag{2.458}$$

where $P_{1,m,i}$ is the mechanical input power and $P_{1,e,i}$ is the electrical output power of machine i, for the pre-fault condition.

For the faulted case, which is described by V_i=0 a new admittance matrix is obtained by setting the row and column corresponding to the faulted node to zero. The new power output is given by

$$P^{*}_{2,e,i} = \sum_{j=1}^{m} |E'_{m,i}||E'_{m,j}||Y_{2,i,j}| \cos(\theta_{i,j} - \delta_i + \delta_j) \tag{2.459}$$

where $Y_{2,i,j}$ is the bus admittance element describing the fault case (during fault is happening), while the post-fault power output is given by

$$P^{*}_{3,e,i} = \sum_{j=1}^{m} |E'_{m,i}||E_{m,j'}||Y_{3,i,j}| \cos(\theta_{i,j} - \delta_i + \delta_j) \tag{2.460}$$

where $Y_{3,i,j}$ is the bus admittance element describing the post-fault case (after fault is has happened), while the post-fault power output. It must mentioned that the post-fault bus admittance matrix is obtained by removing the line that would have been switched following the protective switch operation. It is also worth mentioning that the internal excitation voltages remain constant, during the fault and post-fault conditions.

The internal machine dynamics are described by the well-known swing equations that relate the machine rotor angle to the power balance between mechanical and electrical power. When the system is balanced there is rate of change and the system is stable (operates in normal condition). When a disturbance, in the form of a fault, line outage, generator outage or even abrupt increase in demand load, occurs the internal machine balance is no more valid, since one of the two parts of machine power exceeds to other, meaning that machine starts accelerating or decelerating. This rate of change is described by the swing equations, in which rotor angle is responsible for stability as well as synchronism of the interconnected machines.

The equations describing the swing phenomenon inside the machine are

$$\frac{d\delta_{m,i}}{dt} = \omega_i \tag{2.461}$$

$$\frac{d\omega_{m,i}}{dt} = \frac{\pi f_0}{H_i}(P_{m,i} - P_{e,i}) \tag{2.462}$$

Substituting equation2.459 to the above equations one can obtain

$$\frac{d\omega_{m,i}}{dt} = \frac{\pi f_0}{H_i}(P_{m,i} - \sum_{j=1}^{m} |E'_{m,i}||E'_{m,j}||Y_{2,i,j}| \cos(\theta_{i,j} - \delta_i + \delta_j)) \tag{2.463}$$

for the faulted case, while for the post-fault

$$\frac{d\omega_{m,i}}{dt} = \frac{\pi f_0}{H_i}(P_{m,i} - \sum_{j=1}^{m} |E'_{m,i}||E'_{m,j}||Y_{3,i,j}| \cos(\theta_{i,j} - \delta_i + \delta_j)) \tag{2.464}$$

The swing equation given as a second order differential equation has the final form

$$\frac{d^2\delta_{m,i}}{dt^2} = \frac{\pi f_0}{H_i}(P_{m,i} - \sum_{j=1}^{m} |E'_{m,i}||E'_{m,j}||Y_{2,i,j}| \cos(\theta_{i,j} - \delta_i + \delta_j)) \tag{2.465}$$

and

$$\frac{d^2\delta_{m,i}}{dt^2} = \frac{\pi f_0}{H_i}(P_{m,i} - \sum_{j=1}^{m} |E'_{m,i}||E'_{m,j}||Y_{2,i,j}| \cos(\theta_{i,j} - \delta_i + \delta_j)) \tag{2.466}$$

for the fault and post-fault conditions respectively, where H_i is the inertia constant of machine i on a common system power base and is given by

$$H_i = \frac{S_{G,i}}{S_B} H_{G,i} \tag{2.467}$$

where $H_{G,i}$ is the inertia constant of machine i expressed on the machine rated MVA $S_{G,i}$.

From the above analysis by eq.2.442 to 2.467 it is clear that system dynamics are closely related to power flow problem, so the first significantly influences the second.

Chapter 3

Motivation and Challenges

3.1 Introduction

The Power Flow Problem exists for about half of the last century and still seems to incentivize researchers all over the world to keep studying it trying to find improvements, since it is clearly the backbone of the electric power grid operation. In recent years, many new challenges have come into surface concerning the new structure of the electrical power systems and mainly the need for restructuring power grids so as to give financial incentives to customers and generators for selling and buying electrical energy. The new deregulated electricity power markets will play a dominant role in the future years generation, transmission and distribution of electrical energy. In the next sections a brief introduction of future challenges relative to the power flow problem will be presented.

We should point out here that, to the best of our knowledge, the first review similar, at least in the principles, to the one presented in the rest of this paper can be found in [46]. It is also interesting to mention that recently several other review efforts have been published [46] with each one focusing on different aspects.

3.1 Size

PJM is a regional transmission organization (RTO) that coordinates of wholesale electricity in 14 states in the USA. In Figure 3.1 we present the graph of the actual regional prices as those were observed at 01.00 on 06 September 2014.

In recent years electric power industry structure changes its form radically by the need to involve distributed and renewable generation sources as well as new types of demand response [Albadi2008] by the customers. Distributed generation [47] is any kind of locally

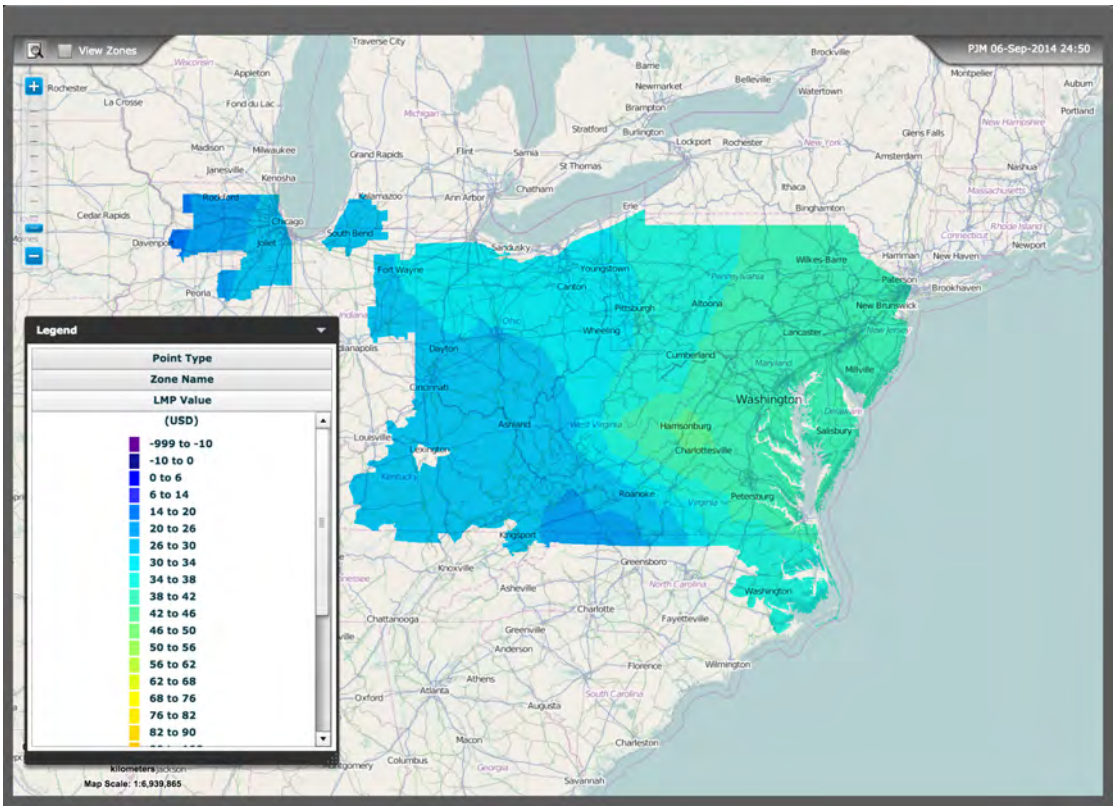

FIGURE 3.1: A three bus system

based generation units that can provide a source of active electric power. The location of the distributed generation is defined as the installation and operation of electric power generation units connected directly to the distribution network or connected to the network on the customer side of the electric power meter. Renewable generation is a form of distributed generation with the difference that it is produced by physical resources, namely wind generation, solar power generation (photovoltaics), etc. Large scale penetration of intermittent renewable sources, especially the fluctuating features of wind power that will increase the uncertainties, is expected to have significant impacts in many aspects of power system planning, operation and control as well as on regulation. There will be an uncontrollable power flow governed by Ohms and Kirchhoffs law which may cause bottlenecks in the power system such as angle and voltage instability.

In the existing power grid which is mostly a water-fall system from power generation, to transmission system, to substation networks and eventually delivery to the customer, the power plants have limited real time information about end-users. Therefore, the grid has to maintain maximum expected peak demand capacity across the aggregated load since electricity cannot be economically stored. As this peak demand occurs infrequently the grid is inherently inefficient. Studies and engineering experience show that 20% of power generation capacity exists to maintain peak demand which is used in only 5% of

the time. Furthermore, since there is a significant issue with legacy components of the electricity grid and the gap between increasing power demand and lagging investments, there has been deterioration in system reliability.

To overcome this inefficiency between supply and time-uncertain peak demand that leads the entire power grid to expensive electric energy costs, demand response (DR) [48] is designed to reduce peak demand and encourage electric consumption when renewable energy is available in response to market price and/or availability over time. A more general definition is that demand response [49] is defined as the changes in electric usage by end-use customers from their normal consumption patterns in response to changes in the price of electricity over time. Further DR can be defined as the incentive payments designed to induce lower electricity use at times of high wholesale market prices or when system reliability is jeopardized. The consumption patterns modified by the use of DR are the level of instantaneous demand, timing alteration and total electricity consumption. DR provides a variety of financial and operational benefits to electricity customers, load-serving entities and grid operators.

3.1.1 Distribution Systems and Power Flow

Distribution systems which constitute the last part of the electric grid, delivering energy to end-users, also play a significant role in power systems operation. The power flow analysis presented so far, was targeted on transmission system, because of its inherent, unique characteristics, involving stability analysis, too. However, distribution systems have different characteristics from transmission systems and these briefly are:

1. Distribution are almost totally radial and only in some cases weakly meshed networks, unlike transmission which are meshed by their nature (loop flows is a proof for that)
2. They have high R/X ratios
3. They are always multi-phase, and have unbalanced operation.
4. They handle unbalanced distributed load
5. They must handle distributed generation which seems the most challenging issue for the next generation distributed systems

Distribution systems work on medium to low voltage, unlike transmission systems that operate in high to very high voltage. The three-phase representetion and unbalanced operation is due to unbalanced loads, radial topology and untransposed conductors.

For all the above reasons distribution systems fall in the category of ill-conditioned systems, in which conventional power flow methods are usually not applicable. For that reasons, three phase power flow analysis is necessary for distribution systems. This analysis is carried out in two different reference frames, the phase frame and the sequence frame. Phase frame handles directly the unbalance quantities. Sequence frame handles seperately each of the three phases and then superposes them to give the total unbalanced three phase circuit.

Several methods have been proposed for load flow analysis of distribution systems following the basic seperation into frame and sequence methods

1. Phase frame power flow
   (a) Forward and Backward sweep algorithm
      i. Current summation methods
      ii. Power summation methods
      iii. Admittance summation methods
   (b) Compensation methods
   (c) Implicit Z_{bus} Gauss Method
   (d) Modified Newton/Newton like methods
   (e) Miscellaneous Power Flow methods
      i. Direct method (BIBC/BCBV matrix method)
      ii. Loop impedance matrix method
2. Sequence Frame Power Flow Analysis

3.1.1.1 Forward-Backward Sweep method

The current summation method from the above mentioned methods, maybe the most popular and consequently used, is always the benchmark among all methods when comparative analyses are being attempted between different methods. As its name says, the method performs backward and forward sweeps through the entire network involving Kirchhoff's current and voltage laws. The backward sweep starts from the last node of the network and ends at the source node utilizing Kirchhoff's current law through current summation updating voltages. The forward sweep starts from the source node and ends at the last network node utilizing Kirchhoff's voltage law updating currents. Sweeps are executed on the opposite direction with each other "scanning" the network and computing the basic variables, current and voltage, through which all other can

also be calculated. Although a very popular method for radial balanced or unbalanced networks it has the drawback of not being usable for meshed or even weakly meshed networks. Several methods extending or improving the basic current summation method have been presented in the literature during last two decades.

Since the method concerns three-phase balanced or unbalanced systems and involves basic features characterizing the network the following figure 3.2 is illustrative for better understanding

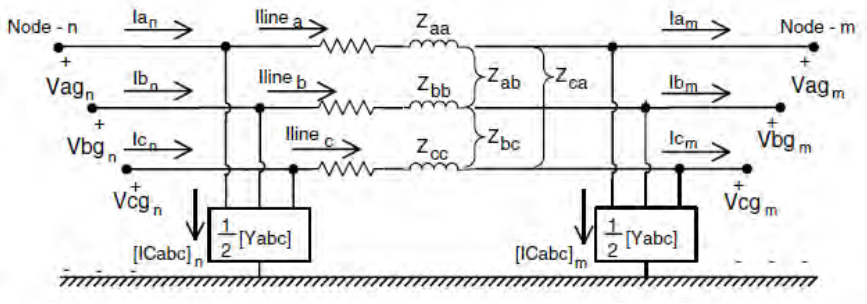

FIGURE 3.2: Three-phase line segment model

A more compact form instead of the above analytical schematic representation of a network line is shown in fig. 3.3

FIGURE 3.3: Three-phase line segment model

Considering the above figures 3.2 and 3.3 and applying the KCL and KVL the following matrix equations between voltage, current and impedance(admittance) between the input (node n) and output (node m) are obtained

$$[V_{abc}]_n = [a][V_{abc}]_m + [b][I_{abc}]_m \tag{3.1}$$

$$[I_{abc}]_n = [c][V_{abc}]_m + [d][I_{abc}]_m \tag{3.2}$$

while the general equation relating the output (node m) and input (node n) voltages is given by:

$$[V_{abc}]_m = [A][V_{abc}]_n - [B][I_{abc}]_m \tag{3.3}$$

where the matrices $[a], [b], [c], [d], [A], [B]$ are calculated as follows

$$[a] = [U] + \frac{1}{2}[Z_{abc}][Y_{abc}] \tag{3.4}$$

$$[b] = [Z_{abc}] \tag{3.5}$$

$$[c] = [Y_{abc}] + \frac{1}{4}[Y_{abc}][Z_{abc}][Y_{abc}] \tag{3.6}$$

$$[d] = [U] + \frac{1}{2}[Z_{abc}][Y_{abc}] \tag{3.7}$$

$$[A] = [a]^{-1} \tag{3.8}$$

$$[B] = [a]^{-1}[b] \tag{3.9}$$

in which

$$\left[Y_{abc}\right] = \begin{bmatrix} Y_{aa} & Y_{ab} & Y_{ac} \\ Y_{ba} & Y_{bb} & Y_{bc} \\ Y_{ca} & Y_{cb} & Y_{cc} \end{bmatrix} \tag{3.10}$$

$$\left[Z_{abc}\right] = \begin{bmatrix} Z_{aa} & Z_{ab} & Z_{ac} \\ Z_{ba} & Z_{bb} & Z_{bc} \\ Z_{ca} & Z_{cb} & Z_{cc} \end{bmatrix} \tag{3.11}$$

are the admittance and impedance matrix in three-phase coordinates, and finally

$$\left[U\right] = \begin{bmatrix} 1 & 0 & 0 \\ 0 & 1 & 0 \\ 0 & 0 & 1 \end{bmatrix} \tag{3.12}$$

is the identity matrix.

The FBS method also known as the improved ladder network technique is analytically explained in [Kersting]. The basic features of the algorithm in the referred book will be given next. The algorithm is given exactly as presented in the specific textbook and to understand it the following figure 3.4 is representative, while figures 3.5 and 3.6 best explain the FBS method from Kersting.

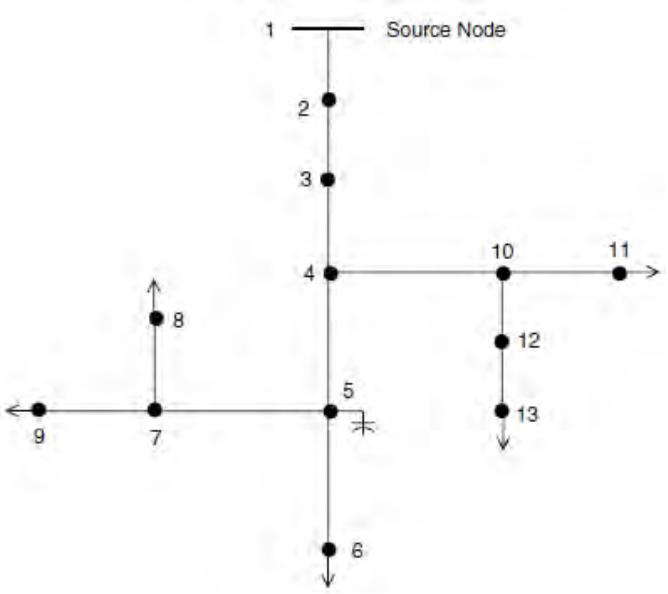

FIGURE 3.4: Typical distribution feeder

1. Assume three-phase voltages at the end nodes (6,8,9,11, and 13). The usual assumption is to use the nominal voltages.
2. Starting at Node 13, compute the node current (load current plus capacitor current if present).
3. With this current, apply Kirchhoff's voltage law (KVL) to calculate the node voltages at 12 and 10.
4. Node 10 is referred to as a "junction" node since laterals branch in two directions from the node. For this feeder, go to Node 11 and compute the node current. Use that current to compute the voltage at Node 10. This will be referred to as "the most recent voltage at Node 10."
5. Using the most recent value of the voltage at Node 10, the node current at Node 10 (if any) is computed.
6. Apply Kirchhoff's current law (KCL) to determine the current flowing from Node 4 toward Node 10.
7. Compute the voltage at Node 4.
8. Node 4 is a junction node. An end node downstream from Node 4 is selected to start the forward sweep toward Node 4.
9. Select Node 6, compute the node current, and then compute the voltage at Junction Node 5.
10. Go to downstream end Node 8. Compute the node current and then the voltage at Junction Node 7.
11. Go to downstream end Node 9. Compute the node current and then the voltage at Junction Node 7.
12. Compute the node current at Node 7 using the most recent value of the Node 7 voltage.
13. Apply KCL at Node 7 to compute the current flowing on the line segment from Node 5 to Node 7.
14. Compute the voltage at Node 5.
15. Compute the node current at Node 5.
16. Apply KCL at Node 5 to determine the current flowing from Node 4 toward Node 5.
17. Compute the voltage at Node 4.
18. Compute the node current at Node 4.
19. Apply KCL at Node 4 to compute the current flowing from Node 3 to Node 4.
20. Calculate the voltage at Node 3.
21. Compute the node current at Node 3.
22. Apply KCL at Node 3 to compute the current flowing from Node 2 to Node 3.

FIGURE 3.5: Forward-Backward Sweep algorithm for a typical distribution feeder

3.1.1.2 Alternative forms of the Forward-Backward Sweep method

Case1 According to [50], the FBS algorithm consists of four district steps which are described below.

23. Calculate the voltage at Node 2.
24. Compute the node current at Node 2.
25. Apply KCL at Node 2.
26. Calculate the voltage at Node 1.
27. Compare the calculated voltage at Node 1 to the specified source voltage.
28. If not within tolerance, use the specified source voltage and the forward sweep current flowing from Node 1 to Node 2, and compute the new voltage at Node 2.
29. The backward sweep continues, using the new upstream voltage and line segment current from the forward sweep to compute the new downstream voltage.
30. The backward sweep is completed when new voltages at all end nodes have been completed.
31. This completes the first iteration.
32. Repeat the forward sweep, only now using the new end voltages rather than the assumed voltages as was done in the first iteration.
33. Continue the forward and backward sweeps until the calculated voltage at the source is within a specified tolerance of the source voltage.
34. At this point the voltages are known at all nodes, and the currents flowing in all line segments are known. An output report can be produced giving all desired results.

FIGURE 3.6: Forward-Backward Sweep algorithm for a typical distribution feeder

1. The first step is the identification of the different layers in the radial or weakly meshed power system as shown in figure 3.7.

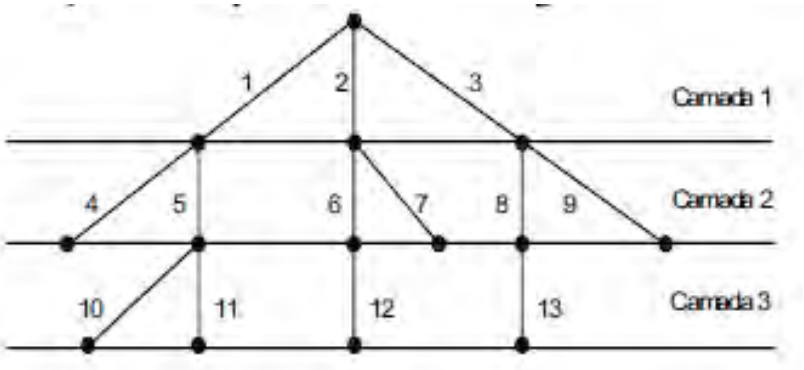

FIGURE 3.7: Layers in a radial distribution system

2. The second step of the algorithm consists in the calculation of nodal current injections, assuming a flat voltage profile, as shown in the next equation 3.13.

$$I_k^s = (\frac{S_k^s}{V_k^s})* \tag{3.13}$$

3. This is the backward sweep step. Beginning from the last layer node and working a way up towards the first layer node a summation of the branch currents is calculated as shown in the following equation 3.14. This is the so-called backward sweep starting calculations from the lower layer last nodes and ending at the higher layer initial node.

$$J_k^s = -I_k^s + \sum_{m \in \omega_M} J_m^s \tag{3.14}$$

where J_k^s is the total phase s current at branch k and ω_M is the set of branches adjacantly connected to branch k, in the lower layer.

The above equation is simply the application of KCL which states that the current flowing out of a node towards the branch k equals the current injections plus the currents of the branches directly connected to branch k.

4. The next step is the Forward sweep step in which a correction of voltages is performed, following the opposite direction, that is beginning from the first layer node towards the bottom layer nodes, as,

$$V_m^s = V_k^s - Z_{km}^{st} J_k^s \tag{3.15}$$

The above steps are executed repeatedly until the currents calculated by 3.14 are below a given precision.

Case II In [51] a modified backward/forward sweep is presented, based on the linear proportional principal. The basic steps are the two known backward and forward sweeps. As long as it concerns the backward sweep KCL and KVL are applied to find the currents from downstream towards upstream and the voltages for each upstream bus of a line or a transformer branch. It is the conventional backward sweep as it is already applied to distribution power systems. At the end of the backward sweep step the voltage at the higher level node (i.e. the transformer bus) is calculated and the equivalent mismatch between the initially specified and the recently computed voltage is calculated. The ratio of the specified to the calculated voltage at the source node is then utilized in order to correct the bus voltages towards downstream nodes performing a decomposed forward sweep based on the linear proportional principle.

As it is already mentioned the basic equations for voltage and current between sending and receiving ends can be described by the equations

$$V_S = AV_R + BI_R \tag{3.16}$$

$$I_S = DI_R \tag{3.17}$$

The above equations can easily be decomposed into real and imaginary parts as follows

$$V_S^r = AV_R^r + B^r I_R^r - B^i I_R^i \tag{3.18}$$

$$V_S^i = AV_R^i + B^i I_R^r + B^r I_R^i \tag{3.19}$$

The ratio of the specified to calculated voltage at the source node is given

$$\gamma = \frac{V_S}{V_1} \tag{3.20}$$

After executing the backward sweep and having found the value of the source node the feeder network is decomposed for every phase into a real and imaginary part as shown with equations 3.18 and 3.19. In this decomposed network the forward sweep is then executed utilizing the voltage ratio from eq. 3.20 to correct the bus voltages from upstream to downstream nodes. The proposed method has been tested against the conventional FBS as well as the ladder network technique and has proved its superiority in terms of computational efficiency and solution accuracy.

The power summation method performs power flow summation in backward and forward sweeps, instead of current summation, and can handle various DG sources modeling. In improved form it can also handle radial as well as meshed networks by introducing the terms of Generator Break Points (GBP) and Loop Break Points (LBP) respectively, which can be created by proper network manipulation through injected real and reactive power with opposite signs, and by doing power summation in backward sequence. Reference [52] presents the proposed method analytically.

The admittance summation method is used only when active and reactive load nodes are of constant admittance. In this case the method is non-iterative and thus much faster than the other methods.

Compensation iterative methods are based on a mix of backward/forward sweep method with breaking points for meshed networks to be transformed to radial. DG's are modeled as PQ and PV nodes.

Implicit Z_bus method uses optimal triangularization of the explicit Y_{bus} solution method, which means that it performs LU factorization on sparse admittance matrix and equivalent current injections. The method uses an appropriate controlled bus as the only swing bus, thus it is suitable for systems with many PQ nodes and one PV node.

Modified Newton methods are based on conventional Newton-Raphson power flow methods involving the Jacobian matrix. The methods try to explore and take advantage of the topological structure in order to form the Jacobian matrix, by using matrix computational techniques like UDU^T, where D is a diagonal matrix expressing the radial structure of the distribution system and U is the upper triangular matrix depending on on system topology. Other similar Newton like methods are performing some kind of LU factorization where the U matrix (upper triangular) is decomposed to an identity matrix and a diagonal matrix. The method is fast and robust for radial networks but no so effective for meshed networks. Other researchers [14], [15] have proposed the current mismatch NR power flow algorithm in rectangular coordinates, modifying the conventional power mismatch load flow model. The method is suitable for 3ph unbalanced radial networks, so each Jacobian submatrix element is an $6x6$ matrix in order to accommodate the 3ph model. The off-diagonal elements are constant equal to the nodal admittance matrix elements, but not for PV buses. The diagonal elements are updated during iteration steps, resulting in a reduced computational burden. Without DG sources the Jacobian matrix is almost constant. Several other formulation of the NRPF model have also been presented in the literature during the last years.

BIBC/BCBV matrix method is a direct method which incorporates the use of two matrices, namely the Bus Injection Branch current (BIBC) and Branch Current Bus Voltage (BCBV) each one representing the corresponding relationship between the variables introduced. The advantage of this method is that is makes the computation faster since it eliminates the time consuming procedures such as the LU factorization and forward/backward substitution of the Jacobian matrix, based on the two matrices topology being upper and lower triangular. It is efficient both for radial and weakly meshed networks, and can also be used for different DG sources included.

For the interested reader [53] has a descriptive review of all these methods and many more references in literature.

Recently a hybrid method involving direct and iterative techniques for solving power flow problems for distributed systems is presented in [54]. The methods utilizes the FDLF method (mentioned in previous chapter) to solve the problem. It also uses the direct method, based on LU factorization with partial pivoting to handle the active power mismatch, while the reactive power mismatch is computed by the use of the iterative restarted generalized minimal residual method (restarted GMRES) with incomplete LU

pre-conditioner. The method is compared to other methods like GS, NR, BX and XB of fast decoupled and shows encouraging results.

A comparison analysis between the Backward/Forward Sweep method and the three-phase current injection method (TCIM) is presented in [50], concerning only radial distribution systems. Figure 3.8 presents a comparison between the main characteristics of the two methods

CHARACTERISTICS OF TCIM X FBS

	FBS	TCIM
Methodology	Simple	Complex
Implementation	Simple	Complex
Extension to 4/5 wires	Simple	Complex
Robust	Average	High
convergence	Many iterations	Few iterations Quadratic
Controls	Complex Implementation	Simple Implementation
Radial Systems	Yes	Yes
Mesh Systems	No	Yes
Total time	Low	Low
Iteration time	Very low	Low

FIGURE 3.8: Characteristics of the two compared methods

A summary of the test cases is shown in figure 3.9

TEST CASES

Case	Busbars	Load levels	Controls
1	503	3	No
2	4981	3	No
3	10103	1 (Medium)	No
4	232	1 (Medium)	Yes

FIGURE 3.9: Test cases for the two compared methods

In the following figures, in pairs, a comparison of the methods is illustrated. In each pair the first figure shows the comparison concerning computation time in seconds, while the second figure shows comparison in terms of time ratios.

503 BUSBARS SYSTEM, TIME IN SECONDS

	FBS		TCIM	
Load	Iterations number	Total time	Iterations number	Total time
Light	8	0.032	3	0.0525
Medium	17	0.062	4	0.0647
Heavy	-----	-----	5	0.0769
	Average time for iteration			
	0.004		0.0173	

FIGURE 3.10: Comparison of two methods concerning computation time for 503 busbars

TIME RATIOS TCIM /FBS, 503 BUSBARS SYSTEM

Load	Total time ratios	Average iteration time ratios
Light	1.64	4.32
Average	1.04	4.32
Heavy	----	----

FIGURE 3.11: Comparison of two methods concerning time ratios for 503 busbars

4981 BUSBARS SYSTEM, TIME IN SECONDS

	FBS		TCIM	
Load	Iterations number	Total time	Iterations number	Total time
Light	10	0.375	2	0.378
Medium	17	0.632	3	0.556
Heavy	----	-----	5	0.906
	Average time for iteration			
	0.0375		0.1812	

FIGURE 3.12: Comparison of two methods concerning computation time for 4981 busbars

TIME RATIOS TCIM /FBS, 4981 BUSBARS SYSTEM

Load	Total time ratios	Average iteration time ratios
Light	1.008	4.89
Medium	0.879	4.89
Heavy	----	----

FIGURE 3.13: Comparison of two methods concerning time ratios for 4981 busbars

From simulation tests, the results show that FBS method is generally faster than the TCIM method, in case of light loading conditions. However, for heavy loading conditions, it is apparent that TCIM is more efficient because it requires less iterations.

10103 BUSBARS SYSTEM, TIME IN SECONDS

	FBS		TCIM	
Load	Iterations number	Total time	Iterations number	Total time
Medium	18	1.31	3	1.10
	Average time for iteration			
	0.0727		0.3666	

FIGURE 3.14: Comparison of two methods concerning computation time for 10103 busbars

TIME RATIOS TCIM/FBS, 4981 BUSBARS SYSTEM

Load	Total time ratios	Average iteration time ratios
Medium	0.84	5.04

FIGURE 3.15: Comparison of two methods concerning time ratios for 10103 busbars

232 BUSBARS SYSTEM, TIME IN SECONDS

	FBS		TCIM	
Load	Iterations number	Total time	Iterations number	Total time
Medium	42	0.074	4	0.029
	Average time for iteration			
	0.00176		0.00725	

FIGURE 3.16: Comparison of two methods concerning computation time for 232 busbars

TIME RATIOS TCIM/FBS, 232 BUSBARS SYSTEM

Load	Total time ratios	Average iteration time ratios
Medium	0.39	4.11

FIGURE 3.17: Comparison of two methods concerning time ratios for 232 busbars

3.1.2 Microgrids and Power Flow

Distribution networks are going to be transformed into active network clusters the so-called microgrids consisting of loads and local generation and will also play a dominant role in the electric power industry management. The microgrid [55] can be described as a cluster of loads, distributed generation (DG) units and energy storage systems (ESS) operated in coordination to reliably supply electricity, connected to the central power grid at the distribution level, at a single point of connection, the point of common coupling. This point may be at the low-voltage bus of the substation transformer. A general schematic diagram of a microgrid is given in the following figure 3.18

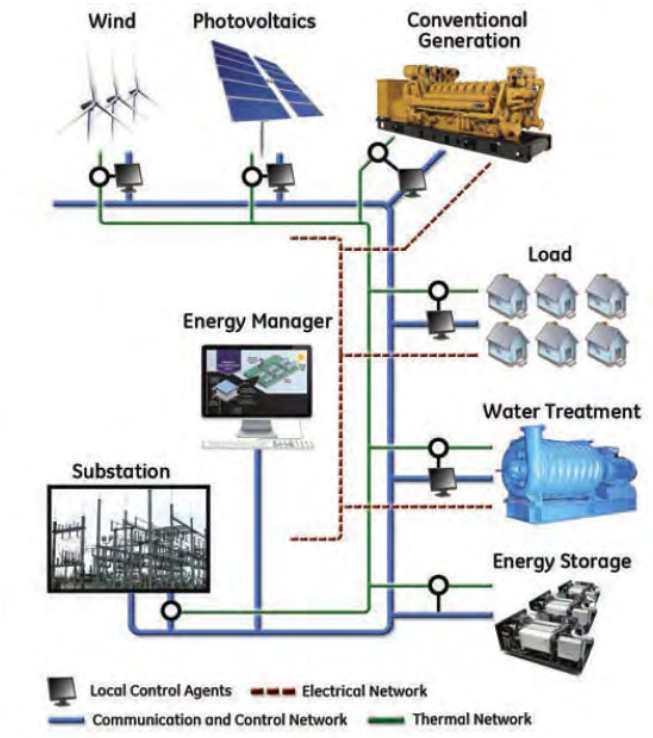

FIGURE 3.18: Microgrid power system

while a more analytical form of a microgrid interconnected to the central electrical grid is illustrated in figure 3.19

A microgrid is designed to be able to separate from the main grid when problems in the utility grid arise, reconnecting again once the problems are resolved. In grid connected mode, the sources of the microgrid, the so-called microsources, act as constant power sources, which are controlled to supply all the demanded power into the network. Islanding means that the microgrid is completely isolated from the main electrical grid, completely independent without any electrical or magnetic connection to the central grid, but at the same time having the ability and the sources to satisfy all the nominal frequency and voltage regulations. In autonomous mode, the same microsources are controlled to supply all the power needed by the local loads while maintaining the voltage and frequency within acceptable operating limits. In other words, the adoption of microgrids as the integration of distributed energy resources (DERS) will allow technical problems to be solved in a decentralized fashion reducing the need for a complex central coordination and facilitating the realization of the smart grid. An important characteristic of the microgrids is that the microsources are generally connected to the network through appropriate electronic control devices like Voltage Source Inverters (VSI) which allows through its flexibility the microgrid to operate either grid-connected or islanded. More information on the microgrid concept can be found on [56].

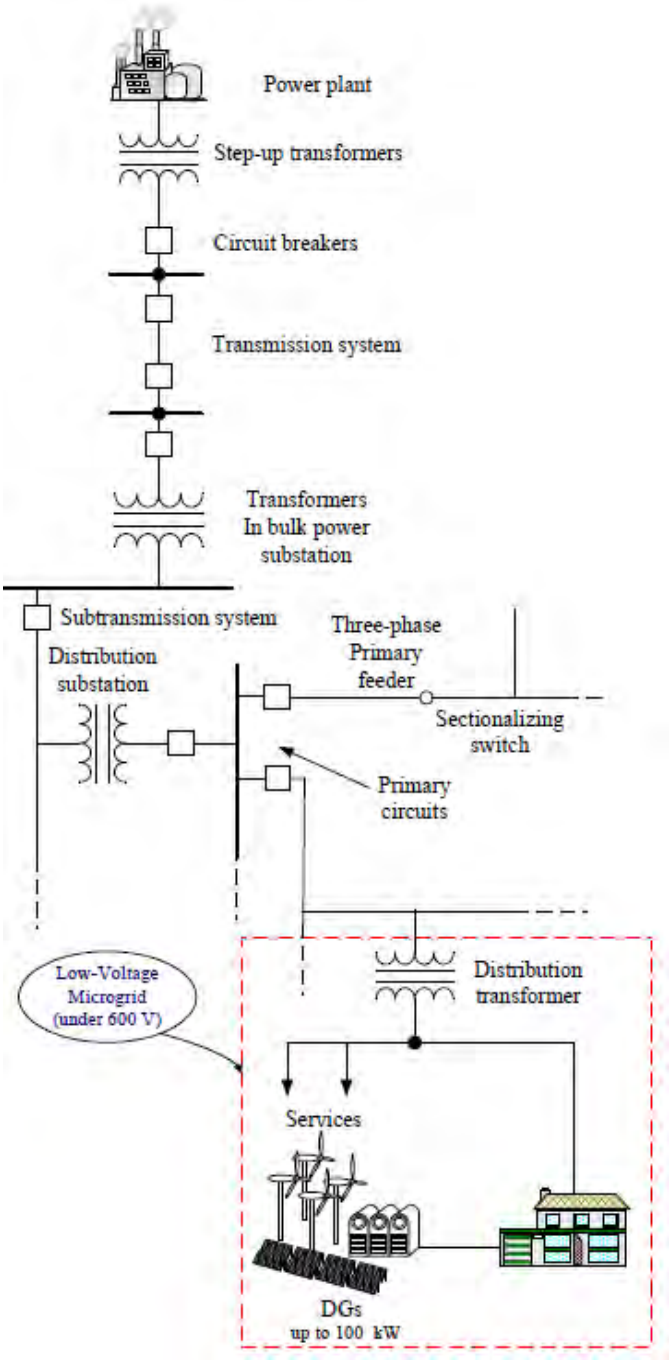

FIGURE 3.19: Schematic diagram of the low-voltage microgrid system

Since microgrids constitute the future local generation plants they must be always ready to an islanded operation, so they must always be in a position to keep supply from DGs in a stable condition without compromising the voltage profile and to determine the state of the system. The meaning of this is that load flow analysis is more than necessary to evaluate the microgrid condition in real time operation. Microgrid load flow analysis follows the basic principles of the distributed systems operation, so the methods that are encountered to solve the power flow problem, as stated in literature,

are classified into three categories,that is, direct methods, Newton-Raphson methods and backward/forward sweep based methods. Direct methods involve impedance matrix calculations but suffer from tedious computations. The well-known NR methods come from transmission load flow analysis but are now in a compatible form to match the unbalanced 3ph nature of DS. The drawback of NR methods is that they fail to exploit the system topology. The backward/forward sweep is the basic method for DS and thus it appears as an attractive approach for microgrid operation.

When microgrids operated in grid-connected mode, a microsource controller regulates the interconnection with the central electrical grid. The power mismatch between generation supply and load demand is given by the main grid. Microsource controllers can be modelled as PQ-load buses with negative load, that is they act as aggregators of load demand from lower levels of the distribution system. The main medium voltage grid can then be represented as a slack bus. In that sense, in grid connected mode the number of microgrids is approximated as the familiar transmission system with the well-known bus types, so power flow can be solved by the use of well-established conventional power flow algorithms like NRPF methods. When microgrids operate in islanded mode, several reasons make conventional load flow algorithms not viable. The main reason is the absence of the main grid securing the normal operation in the sense of voltage and frequency. Microsources are not able to provide sufficient capacity for the load imbalance which arises from the disconnection from the main grid. In that way, modified load flow algorithms that take into account the steady state behavior of the microsource controllers is necessary. Such a method is presented in [57]. The basic idea of the proposed method is that the steady-state of a microsource controller (enabling the connection of the microgrid to the bulk power system) is expressed by the P-f and Q-V droop characteristics as shown in the following figure 3.20.

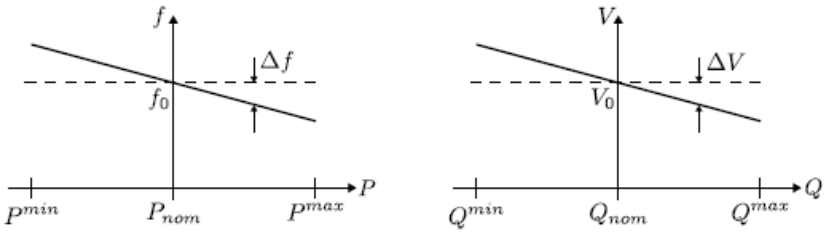

FIGURE 3.20: P-f and Q-V droop characteristics

As is already known in traditional power flow algorithms the power balance equations are given by

$$\Delta P_k = P_{gk} - P_{dk} - P_k(V, \delta) \tag{3.21}$$

$$\Delta Q_k = Q_{gk} - Q_{dk} - Q_k(V, \delta) \tag{3.22}$$

where $\Delta P_k, \Delta Q_k$ are the active and reactive power mismatches, P_{gk}, Q_{gk} are the active and reactive power generation, P_{dk}, Q_{dk} are the active and reactive load demand and $P_k(V, \delta), Q_k(V, \delta)$ are the non linear functions representing active and reactive power flows of the branches connected to bus k.

The main features of the proposed method are the following. The load flow method does not consider a slack bus and consists in a different expression of the active and reactive generation power outputs by depending them on the microsource controller steady state characteristics by introducing new variables to the load flow problem, that is, the system frequency for the representation of P-f droop characteristics and voltage magnitudes of buses for the representation of the Q-V droop characteristic.

Two types of controller are also introduced:

1. A controller of type 1 based on the definition of P-f and Q-V droop characteristics. Then the active and reactive power generation is given by the following equations

$$P_{gk} = -K_{\omega_k}(\omega - \omega_0) + P^0_{gk} \tag{3.23}$$

$$Q_{gk} = -K_{V_k}(V_k - V_{0k}) + Q^0_{gk} \tag{3.24}$$

   where K_{ω_k} is the inverse of $P - f$ droop characteristic value, K_{V_k} is the inverse of $Q - V$ droop characteristic, ω is the grid frequency, ω_0 is the initial grid frequency, V_k is the voltage magnitude, V_{0k} is the initial voltage magnitude, P^0_{gk}, Q^0_{gk} are the active and reactive power generation, all variables concerning bus k.

2. A controller of type 2 which uses P-f droop characteristic for active power, while reactive power is controlled in order to regulate the terminal voltage according to a preset value. Thus, the reactive power balance equation is not necessary since the voltage magnitude is known. This is a situation similar to a PV-generation bus in which active power and voltage magnitude are the known variables, while reactive power and voltage phase angle are the unknown variables. For this type of controller only one equation needs to solved and this is 3.23.

Based on the controllers definitions proper bus definitions are also introduced, and have the following performance

1. Type 1 bus: is the bus where a controller type 1 is connected. The power balance equations now have the form

$$\Delta P_k = -K_{\omega_k}(\omega - \omega_0) + P_{gk}^0 - P_{dk} - P_k(V, \delta) \tag{3.25}$$

$$\Delta Q_k = -K_{V_k}(V_k - V_{0k}) + Q_{gk}^0 - Q_{dk} - Q_k(V, \delta) \tag{3.26}$$

2. Type 2 bus: is the bus where a controller of type 2 is connected. The power balance equations are now given by

$$\Delta P_k = -K_{\omega_k}(\omega - \omega_0) + P_{gk}^0 - P_{dk} - P_k(V, \delta) \tag{3.27}$$

3. PQ-load bus: is the bus of the conventional load type since no microsource controller is connected to it. The power balance equations are now

$$\Delta P_k = P_{dk} - P_k(V, \delta) \tag{3.28}$$

$$\Delta Q_k = Q_{dk} - Q_k(V, \delta) \tag{3.29}$$

It is then almost clear that the linearization of the load flow equations by utilizing the NR method leads to a new formulation of the Jacobian matrix as a $2x3$ matrix while the state variables are not only the bus voltage magnitude and angle, but the system frequency too. It is worth mentioning that the definition of nodal voltage angle reference is still necessary for the modified power flow solution. This solution leads to immediate calculation of not only the basic state variables of the problem but of the grid frequency too.

Just for comparison to other NR formulations we present the modified version of the load flow algorithm, as it follows

$$\begin{bmatrix} \Delta P \\ \Delta Q \end{bmatrix} = - \begin{bmatrix} \frac{\partial \Delta P}{\partial \delta} & \frac{\partial \Delta P}{\partial V} & \frac{\partial \Delta P}{\partial \omega} \\ \frac{\partial \Delta Q}{\partial \delta} & \frac{\partial \Delta Q}{\partial V} & \frac{\partial \Delta Q}{\partial \omega} \end{bmatrix} \begin{bmatrix} \Delta \delta \\ \Delta V \\ \Delta \omega \end{bmatrix} \tag{3.30}$$

which can take the compact form

$$\begin{bmatrix} \Delta P \\ \Delta Q \end{bmatrix} = - \begin{bmatrix} H & N & E \\ M & L & F \end{bmatrix} \begin{bmatrix} \Delta \delta \\ \Delta V \\ \Delta \omega \end{bmatrix} \tag{3.31}$$

where

$H = \frac{\partial \Delta P}{\partial \delta}$, $N = \frac{\partial \Delta P}{\partial V}$, $M = \frac{\partial \Delta Q}{\partial \delta}$, $N = \frac{\partial \Delta Q}{\partial V}$, $E = \frac{\partial \Delta P}{\partial \omega}$ and $F = \frac{\partial \Delta Q}{\partial \omega}$.

The partial derivatives described by the matrices H, N, M, L are the already well-known from previous chaprters of the conventional power flow solution procedure. The matrices E, F are calculated by

$$E_i = \begin{cases} -K_{\omega_i} & \text{if } bus \;\; i \;\; is \;\; of \;\; type \;\; 1 \;\; or \;\; type \;\; 2 \\ 0 & \text{if} \quad otherwise. \end{cases} \tag{3.32}$$

$$F_i = 0 \tag{3.33}$$

According to the paper authors, the proposed method is validated by comparison with steady-state values obtained through non-linear time domain simulations of a microgrid test-case system.

A similar, to the above, method of handling isolated microgrid operation, without defining a unique slack bus is presented in [58]. This approach has the same already mentioned main features, that is, it expresses the generation power outputs dependent on the system frequency (coordinated by the microsource controllers), and extends the NRPF matrix formulation by incorporating system frequency as the additional state variable leading to two additional sensitivity terms in the Jacobian matrix. The main difference between methods is that it uses a load model formulation for both active and reactive power expressed in terms of constant power, constant current and constant admittance, also dependent on system frequency. In other words both generation and demand load are dependent on system frequency. The regulation ability of the DG's is given by the equations

$$P_{Gi} = P_{Gi0}(1 - k_{Gi,p}(f - f_0) \tag{3.34}$$

$$Q_{Gi} = Q_{Gi0}(1 - k_{Gi,q}(V_{Gi} - V_{Gi,0}) \tag{3.35}$$

where

P_{Gi}, Q_{Gi} are the active and reactive power generated by the i^{th} generator,
P_{Gi0}, Q_{Gi0} are the initial values of active and reactive power generated by the i^{th} generator,
$k_{Gi,p}, k_{Gi,q}$ are the equivalent regulation coefficients of active and reactive power generated by the i^{th} generator,
f, f_0 are the frequency and initial value of frequency,
$V_{Gi}, V_{Gi,0}$ are the voltage magnitude and its initial value.

The power equations of the load are based on a polynomial type of a static load model, and are

$$P_{Li} = P_{Li0}(A_{i,p}(\frac{V_i}{V_{i0}})^2 + B_{i,p}(\frac{V_i}{V_{i0}}) + C_{i,p})(1 + k_{Li,p}(f - f_0)) \tag{3.36}$$

$$Q_{Li} = Q_{Li0}(A_{i,q}(\frac{V_i}{V_{i0}})^2 + B_{i,q}(\frac{V_i}{V_{i0}}) + C_{i,q})(1 + k_{Li,q}(f - f_0)) \tag{3.37}$$

Finally the two additional terms concerning the partial derivatives of active and reactive power w.r.t. to microgrid frequency (that must be kept constant and equal to the main grid frequency) are

$$E_i = \frac{\partial \Delta Q_i}{\partial f} = \begin{cases} -Q_{Li0}(A_{i,q}(\frac{V_i}{V_{i0}})^2 + B_{i,q}(\frac{V_i}{V_{i0}}) + C_{i,q})k_{Li,q} & \text{for} \quad i = 1, \dots m \\ 0 & \text{for} \quad i = m+1 \dots n. \end{cases} \tag{3.38}$$

$$F_i = \frac{\partial \Delta P_i}{\partial f} = \begin{cases} -P_{Li0}(A_{i,q}(\frac{V_i}{V_{i0}})^2 + B_{i,q}(\frac{V_i}{V_{i0}}) + C_{i,q})k_{Li,p} & \text{for} \quad i = 1, \dots m \\ -P_{Gi0}K_{Gi,p} & \text{for} \quad i = m+1 \dots n. \end{cases} \tag{3.39}$$

So, the conclusion concerning the two above presented islanded microgrid PF methods is that they succeed not only steady state operation but control as well in islanded mode.

A totally different approach of power flow solution for autonomous microgrids is given is [59]. In this paper two load flow models are proposed, both based on the forward/backward sweep method applied to radial distribution systems. The first methods adopts the unique slack bus definition (the largest generator plays the role of slack bus) while all other distributed generators (DG's) are considered as purely PQ buses. The FBS

method is modified in order to capture the main characteristics of islanded microgrids. In order to understand the first proposed method the following bus-branch schematic diagram in figure 3.21 is representative.

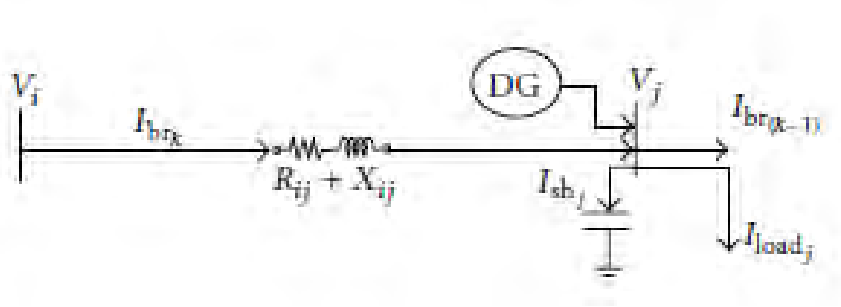

FIGURE 3.21: Steady-state representation of a branch k between i^{th} and j^{th} buses of a microgrid

The Forward/Backward Sweep is modified and involves the following steps

1. Backward Sweep: the k branch current is calculated by the equation

$$I_{br_k} = I_{br_{k-1}} - I_j \tag{3.40}$$

where

$$I_j = I_{g_j} - (I_{sh_j} + I_{load_j}) \tag{3.41}$$

$$I_{load_j} = conj(\frac{S_{load_j}}{V_j}) = (\frac{S_{load_j}}{V_j})^* \tag{3.42}$$

The node as well as branch currents are computed iteratively by utilizing the above three equations. Equation 3.41 incorporates the DG into the proposed method with a positive polarity, unlike the negative polarity assigned in load currents.

2. Forward Sweep: this step follows the well-established conventional approach where the bus voltages are calculated beginning from the higher to the lower level of the radial layout, by the equation

$$V_i = V_j + I_{br_k}(R_{ij} + X_{ij}) \tag{3.43}$$

It must be noted that the bus with the largest generator connected to it, is considered as the slack-reference bus and hence its voltage is maintained at $1 + j0$. The rest of the voltages are computed by 3.43.

The above procedure is iterative and terminates only when a tolerance criterion of the form

$$V_i^k - V_i^{k-1} < tolerance \tag{3.44}$$

where k denotes the iteration count. The advantages of the first proposed method are the exploitation of the radial topology of the system, the simplicity since the method deals only KCL and KVL avoiding complex matrix manipulations as well as formulation of bus admittance matrix, and finally the convergence rate which is very high, the algorithm terminates in two or three iterations. The only drawback is that the method requires performing a NR algorithm in order to calculate an initial guess for active and reactive power injections that are essential for the calculation of current injections during the backward sweep.

The second method is based on the concept of the distributed slack bus model, where all generators are modelled as slack buses, meaning that each one of them participates in loss as well as in loads contribution in order to update real and reactive power generations. The idea of distributed slack bus employs the techniques of domains, commons and contribution factors, first introduced in [63], and will be further discussed later on. The method is almost similar to the first single slack bus method, the main difference is that each generator, acting as a slack bus has a flat voltage profile $1 + j0$. This is utilized not only in backward sweep, but also in when performing forward sweeps which are as many as the number of generators. After identifying "commons" and "domains" the participation factors of each generator to share the loads and losses in a common are determined. According to them the active and reactive powers to be generated by each generator are calculated by the equations

$$P_{g_i} = P_{g_{i_{loss}}} + P_{g_{i_{load}}} \tag{3.45}$$

$$Q_{g_i} = Q_{g_{i_{loss}}} + Q_{g_{i_{load}}} \tag{3.46}$$

where

$$P_{g_{i_{load}}} = \sum_{n=1}^{nc} K_{g_{i_{load_{act}}}} P_{load} \tag{3.47}$$

$$P_{g_{i_{loss}}} = \sum_{n=1}^{nc} K_{g_{i_{loss_{act}}}} P_{loss} \tag{3.48}$$

$$Q_{g_{i_{load}}} = \sum_{n=1}^{nc} K_{g_{i_{load_{react}}}} Q_{load} \tag{3.49}$$

$$Q_{g_{i_{loss}}} = \sum_{n=1}^{nc} K_{g_{i_{loss_{react}}}} Q_{loss} \tag{3.50}$$

where

P_{g_i} is the total active power generated by generator i^{th} generator,
Q_{g_i} is the total reactive power generated by generator i^{th} generator,
$P_{g_{i_{load}}}$ is the total active power of the i^{th} generator supplied to load,
$P_{g_{i_{loss}}}$ is the total active power of the i^{th} generator supplied to losses,
$Q_{g_{i_{load}}}$ is the total reactive power of the i^{th} generator supplied to load,
$Q_{g_{i_{loss}}}$ is the total active power of the i^{th} generator supplied to losses,
$K_{g_{i_{load_{act}}}}$ is the participation factor of the active generated power by the i^{th} generator to the load,
$K_{g_{i_{loss_{act}}}}$, is the participation factor of the active generated power by the i^{th} generator to the losses,
$K_{g_{i_{load_{react}}}}$ is the participation factor of the reactive generated power by the i^{th} generator to the load,
$K_{g_{i_{loss_{react}}}}$ is the participation factor of the reactive generated power by the i^{th} generator to the losses,
P_{load} is the total active power load,
P_{loss} is the total active power loss,
Q_{load} is the total reactive power load,
Q_{loss} is the total reactive power loss.

The proposed load flow methods are examined on a 33-bus autonomous microgrid, in which the results show similar convergence and accuracy properties compared to the standard NRPF model for distribution systems. Test results are illustrated in the two figures below

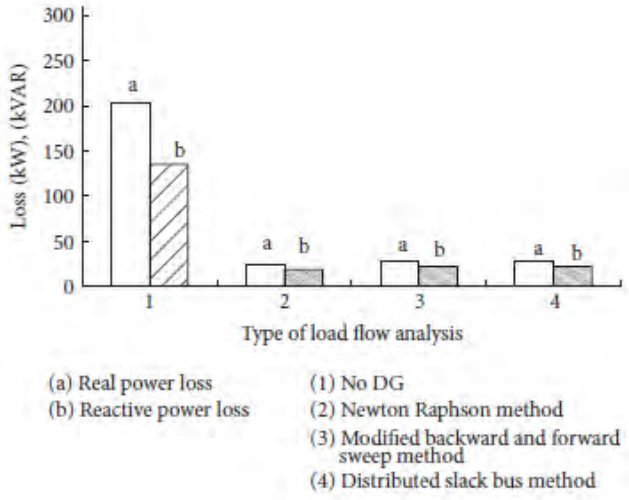

FIGURE 3.22: Comparison of losses for summer demand of the 33-bus microgrid

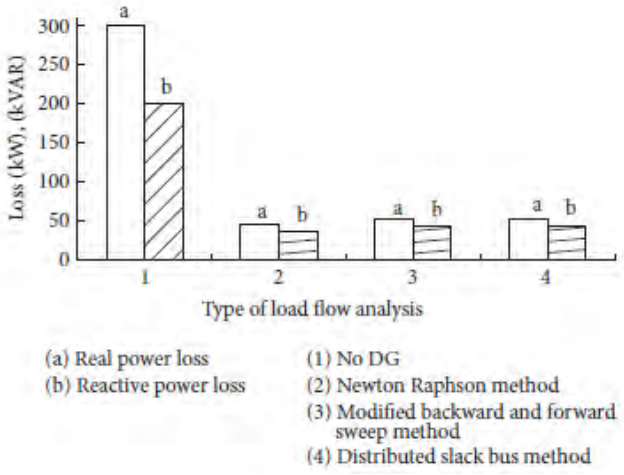

FIGURE 3.23: Comparison of losses for winter demand of the 33-bus microgrid

3.1.3 Smart Grids and Power Flow

The integration of renewable generation sources and distributed generation as well as the demand response management into the conventional grid will allow the development of the new restructured form the so-called smart grid. Smart grid is [60] the enhancement of the 20th century conventional power grid, capable of delivering power in more efficient ways and responding to wide ranging conditions and events. More generally speaking the smart grid can be regarded as a reformulated electric system that uses two-way information, cyber-secure communication technologies and computational intelligence in an integrated fashion across electricity generation, transmission, substations, distribution and consumption to achieve a system that is clean, safe, secure, reliable, resilient, efficient and sustainable. A SG can respond to any change that can occur anywhere in

the grid such as generation, transmission or distribution and consumption and adopt the proper corresponding strategies. For example once a medium voltage transformer failure event occurs in the distribution grid the SG could automatically change the power flow and recover the power delivery service.

The above mentioned changes towards a reformed electric power grid, are intentionally been briefly described in order to emphasize that the expansion of the electric network transmission and distribution lines leading to a size increase, is unavoidable in order to transport renewable and distributed energy from distant areas and enable the coupling of power markets. Power flow calculations [1] are generally performed on the transmission network and the distribution network is thus aggregated at buses in the power system model. This model is no more suitable, since distribution networks become more and more operationally complex. The consequence is that power flow calculations will probably need to include distribution networks resulting in very large-scale electric power systems consisting of thousands or even millions of buses incorporated. Apart from that, the forthcoming coupling of different national electric systems in a centralized form in order to enhance the deregulated competitive power market will also lead to a huge increase in system size.

The new reformed electric power system structure is a challenge for power flow calculation algorithms. The increased size and complexity of the future electric networks dictate the need for improved power flow analysis tools concerning the computational speed in order to be able to respond in real time situations.

3.2 Multipe swing - Distributed slack bus method

So far, recalling what mentioned in the previous chapter 1.3., the power flow problem has been well established by coding the system area buses into three categories, namely the load (PQ) buses, the generation (PV) buses, and the one and only swing or slack bus which is considered as a generation bus with slightly different characteristics, that is, voltage control through the internal excitation of the machine. The slack bus is a "special purpose" bus since it accomplishes two main tasks: first it serves as a reference bus for the other system buses with its voltage magnitude equal to 1.0 p.u. and its voltage phase angle equal to zero degrees. By this referenced bus all the other buses are being expressed with one equation for PV buses and two equations for PQ buses, which are being solved by the iterative NR method (or the GS method) suitable for linear systems, by formulating the well-known Jacobian matrix. The second purpose is of acting like a "swing" trying to balance possible power imbalances as well as dumping for the unaccounted power system losses. This reference bus is not involved in the power

flow equations, nor at the Jacobian matrix formulation, and its controlled variables, namely active and reactive power are calculated after the iterative procedure is ended.

It is also known the vital role that power flow plays for the optimal power flow modeling since it is one of its basic features. If we consider that the OPF calculates nodal prices based on the idea of economic dispatch that is delivering energy to consumers by the producers ascertaining the minimum fuel generation cost, it is evident that the slack bus is not participating in what is called the incremental fuel cost that has to be kept equal on all buses, since it is responsible for carrying all the losses. So it is clear that the so-called optimum solution is not optimum for the slack bus.

Based on these technical and economical features of the electric grid as well as on the role of the slack bus, a number of researchers [61], [62] have been proposed an idea of "liberating" the slack bus from its burden carrying the system losses, by introducing the idea of distributed bus, which simply means distributing the entire loss effect in many more buses than the one slack bus, where every generator bus absorbs an amount of loss evaluated by an appropriate factor called the participation factor. In other words the distributed slack bus technique aims at distributing loads and losses to all of the system generators. In that sense, to determine the active as well as reactive generation power of each generator, the contribution of each generator to the active and reactive power flows, loads and losses must be evaluated. For this evaluation the authors of [Strbach, Kirchnen] introduce the definitions of "domains" and "commons". A "domain" is defined as the set of buses and interconnection branches that are supplied by the generator. The "domain" is determined after identifying the positive power flow directions on the system. The "common" is defined as the set of buses supplied by the same generators. Concerning the "commons" the proportionality principle is applied, meaning that the proportion of loss and loads supplied by different generators to a "common" is the same as the proportion of positive active power injected by the generators to this "common". In that sense, the proportion of loads and loss of a "common" is assigned to the corresponding generator "domain". Based on the proportionality principle the following equations describe the contributions of generators to "commons" that finally lead contribution factors.

The contribution of a generator "m" to a common "n" is calculated as follows

$$C_{mn} = \frac{\sum_{n=1}^{nc} F_{mpn}}{I_n} \tag{3.51}$$

where

$$F_{mpn} = C_{mp} x F_{pn} \tag{3.52}$$

$$I_n = \sum_{p=1}^{nln} F_{pn} \tag{3.53}$$

where

C_{mn} is the contribution of m_{th} generator towards n_{th} common,
C_{mp} is the contribution of n_{th} generator towards p_{th} link,
F_{mpn} is the contribution of m_{th} generator through p_{th} link to n_{th} common,
F_{pn} is the power flow contributed by p_{th} link to n_{th} common,
I_n is the total power inflow into the n_{th} common.

After calculating the above contributions of the generators to the "commons" the participation factors of a generator to active and reactive power loads and losses in every "common" are calculated by the following equations

$$K_{g_{mn-loss_{act}}} = \frac{\sum_{n=1}^{nc} C_{mn} P_{com_{n_{loss_{act}}}}}{P_{loss}} \tag{3.54}$$

$$K_{g_{mn-load_{act}}} = \frac{\sum_{n=1}^{nc} C_{mn} P_{com_{n_{load_{act}}}}}{P_{loss}} \tag{3.55}$$

$$K_{g_{mn-loss_{react}}} = \frac{\sum_{n=1}^{nc} C_{mn} P_{com_{n_{loss_{react}}}}}{P_{loss}} \tag{3.56}$$

$$K_{g_{mn-load_{react}}} = \frac{\sum_{n=1}^{nc} C_{mn} P_{com_{n_{load_{react}}}}}{P_{loss}} \tag{3.57}$$

where

$K_{g_{mn-loss_{act}}}$ is participation factor of m_{th} generator for active power loss in n_{th} "common",
$K_{g_{mn-load_{act}}}$ is the participation factor of m_{th} generator for active power load in n_{th} "common",
$K_{g_{mn-loss_{react}}}$ is participation factor of m_{th} generator for reactive power loss in n_{th} "common",
$K_{g_{mn-load_{react}}}$ is the participation factor of m_{th} generator for reactive power load in n_{th} "common",

$P_{com_{n_{loss_{act}}}}$ is the active power loss in n_{th} "common",
$P_{com_{n_{load_{act}}}}$ is the active power load in n_{th} "common",
$P_{com_{n_{loss_{react}}}}$ is the reactive power loss in n_{th} "common",
$P_{com_{n_{load_{react}}}}$ is the reactive power load in n_{th} "common",

The participation factor is dependent on system parameters like the distance of generators from one another, etc. The whole concept can be viewed as creation on multiple swing buses system, or modifying the unique swing bus to a PV bus with similar characteristics.

The participation factor is a simple algebraic ratio resulting in a scalar. The multiplication of this factor by the unaccounted system loss power gives a weight of the amount of power that shall be distributed to a bus. In other words the participation factor defines the amount of division of power system losses among the buses. It is obvious that the participation factors have values < 1 and the summation of all of them gives unity.

One of the most used participation factors is based on the instantaneous active power generation of the generators in the system.

Recalling the power flow equations of the classic model

$$P_i = |V_i| \sum_{j=0}^{n} |V_j|(G_{ij} \cos \delta_{ij} + B_{ij} \sin \delta_{ij}) \tag{3.58}$$

$$Q_i = |V_i| \sum_{j=0}^{n} |V_j|(G_{ij} \sin \delta_{ij} - B_{ij} \cos \delta_{ij}) \tag{3.59}$$

as well as the power mismatch equations

$$\Delta P_i = P_{is} - |V_i| \sum_{j=0}^{n} |V_j|(G_{ij} \cos \delta_{ij} + B_{ij} \sin \delta_{ij}) = 0 \tag{3.60}$$

$$\Delta Q_i = Q_{is} - |V_i| \sum_{j=0}^{n} |V_j|(G_{ij} \sin \delta_{ij} - B_{ij} \cos \delta_{ij}) = 0 \tag{3.61}$$

the new power flow equations considering the distributed loss effect on generation power gives

$$P_i = |V_i| \sum_{j=0}^{n} |V_j|(G_{ij} \cos \delta_{ij} + B_{ij} \sin \delta_{ij}) + K_i P_B \tag{3.62}$$

where K_i is the participation factor which can take different expressions dependent on the sensitivity of corresponding variables. So, if network sensitivity factors are engaged their definition is as follows

$$K_i = \frac{L_i P_{Gi}^{load}}{\sum_{i=0}^{m} L_i P_{Gi}^{load}} \tag{3.63}$$

where

$$L_i = \frac{1}{1 - \frac{\partial P_L}{\partial P_n}} \tag{3.64}$$

is the weighting parameter of the distance involved and hence the extra losses.

If generator domain participation factors are involved, then parameter K_i can be calculated based on the concept of generator domains and commons. Domains are the set of buses and branches that take power flows of a generator only (meaning that some buses and branches are the domain field of an individual generator). Commons are the set of buses and branches whose power is supplied by the same generators (meaning that some generator supply some buses and branches in common). These participation factors can explicitly describe network parameters, load distribution and generator capacities. For more information about generator domains and commons as well as the participating factors the interested reader may refer to [63], in which the authors introduce these terms and the appropriate technique for involving them in power system analysis.

In this way the participation factor is defined as,

$$K_i = \frac{P_{Gi}^{loss}}{P_{Loss}} \tag{3.65}$$

which explicitly distributes the entire network loss into each individual generator i.

The active power that is then included in power flow study contains not only the scheduled power but the participating power loss component into the load flow calculations. So,

$$P_{Gi} = P_{Gi,scheduled} + K_i P_{loss} \tag{3.66}$$

A new modified power flow algorithm based on the above observations is about to be formulated. The facts for this algorithm is that each PV bus is represented again by the equation of the active generation power only, with the additional participation term,

while for each PQ bus the well-known and unchanged equations for both active and reactive power are still valid.

If there is a total number of n buses and m is the number of PV buses, then there is a number of $n-1$ equations for active power and $n-m-1$ equations for reactive power. The size of the Jacobian matrix is therefore $(2n-m-2)$ x $(2n-m-2)$, in which the slack bus is not included, when dealing with the conventional power flow algorithm.

The main differences between the two NR formulations is that in the new modified form the slack bus can be included, as well as a new term representing the participation effect of power losses for each generation bus, which is the P_B term in eq. 3.62. Moreover, a new term must be added in the state variable vector, that is the term ΔP_B which denotes the change of distributed power w.r.t. the participation factor. The above observations are expressed in the new NR power flow algorithm which, in matrix form, is as follows

$$\begin{bmatrix} \Delta P_1 \\ \vdots \\ \Delta P_n \\ \Delta Q_1 \\ \vdots \\ \Delta Q_{n-m} \end{bmatrix} = \begin{bmatrix} \frac{\partial \Delta P_1}{\partial \delta_1} & \cdots & \frac{\partial \Delta P_1}{\partial \delta_n} & \frac{\partial \Delta P_1}{\partial |V_1|} & \cdots & \frac{\partial \Delta P_1}{\partial |V_{n-1}|} & K_i \\ \vdots & \vdots & \vdots & \vdots & \vdots & \vdots & \vdots \\ \frac{\partial \Delta P_n}{\partial \delta_1} & \cdots & \frac{\partial \Delta P_n}{\partial \delta_n} & \frac{\partial \Delta P_n}{\partial |V_n|} & \cdots & \frac{\partial \Delta P_n}{\partial |V_{n-m}|} & K_n \\ \frac{\partial \Delta Q_1}{\partial \delta_1} & \cdots & \frac{\partial \Delta Q_1}{\partial \delta_n} & \frac{\partial \Delta Q_1}{\partial |V_1|} & \cdots & \frac{\partial \Delta Q_1}{\partial |V_{n-m}|} & \frac{\partial Q_1}{\partial P_B} \\ \vdots & \vdots & \vdots & \vdots & \vdots & \vdots & \vdots \\ \frac{\partial \Delta Q_{n-m}}{\partial \delta_1} & \cdots & \frac{\partial \Delta Q_{n-m}}{\partial \delta_n} & \frac{\partial \Delta Q_{n-m}}{\partial |V_1|} & \cdots & \frac{\partial \Delta Q_{n-m}}{\partial |V_{n-m}|} & \frac{\partial Q_{n-m}}{\partial P_B} \end{bmatrix} \begin{bmatrix} \Delta \delta_1 \\ \vdots \\ \Delta \delta_n \\ \Delta |V_1| \\ \vdots \\ \Delta |V_{n-m}| \\ \Delta P_B \end{bmatrix} \tag{3.67}$$

A more compact form of the modified matrix power flow equation is the following

$$\Big[J\Big] = \begin{bmatrix} J_1 & J_2 & J_5 \\ J_3 & J_4 & J_6 \end{bmatrix} \tag{3.68}$$

J is the Jacobian matrix of the modified Newton-Raphson power flow model,

$$\Big[x\Big] = \begin{bmatrix} \Delta \delta \\ \Delta |V| \\ \Delta P_B \end{bmatrix} \tag{3.69}$$

is the state variable (voltage vector or phasor), and

$$\Big[B\Big] = \begin{bmatrix} \Delta P \\ \Delta Q \end{bmatrix} \tag{3.70}$$

The main differences of matrix forms 3.68, 3.69 and 3.70, with the corresponding matrix forms of the conventional power flow are the additional vectors J_5 and J_6 in the Jacobian

matrix, the additional term ΔP_B representing the change of P_B, and finally the inclusion of the slack bus.

The sub-matrices J_1, J_2, J_3 and J_4 are computed the same way as for the conventional power flow problem and are described by the equations described in a previous chapter.

The new submatrices (vectors) J_5 and J_6 are computed as follows:

For the J_5, concerning the participation effect for active power of PQ,PV buses, one can obtain

$$\frac{\partial P_i}{\partial P_B} = K_i \tag{3.71}$$

for a PV bus (where the participation effect is valid), and

$$\frac{\partial P_i}{\partial P_B} = 0 \tag{3.72}$$

for a PQ bus (where the participation effect is not valid)

For the J_6 concerning the participation effect for reactive power of PQ bus one then obtains

$$\frac{\partial Q_i}{\partial P_B} = 0 \tag{3.73}$$

Since the participation effect is valid only for the first m buses out of the n total number of buses the matrix equation 3.67, is now

$$\begin{bmatrix} \Delta P_1 \\ \vdots \\ \Delta P_n \\ \Delta Q_1 \\ \vdots \\ \Delta Q_{n-m} \end{bmatrix} = \begin{bmatrix} \frac{\partial \Delta P_1}{\partial \delta_1} & \cdots & \frac{\partial \Delta P_1}{\partial \delta_n} & \frac{\partial \Delta P_1}{\partial |V_1|} & \cdots & \frac{\partial \Delta P_1}{\partial |V_{n-1}|} & K_i \\ \vdots & \vdots & \vdots & \vdots & \vdots & \vdots & \vdots \\ \vdots & \vdots & \vdots & \vdots & \vdots & \vdots & K_m \\ \vdots & \vdots & \vdots & \vdots & \vdots & \vdots & \vdots \\ \frac{\partial \Delta P_n}{\partial \delta_1} & \cdots & \frac{\partial \Delta P_n}{\partial \delta_n} & \frac{\partial \Delta P_n}{\partial |V_n|} & \cdots & \frac{\partial \Delta P_n}{\partial |V_{n-m}|} & 0 \\ \frac{\partial \Delta Q_1}{\partial \delta_1} & \cdots & \frac{\partial \Delta Q_1}{\partial \delta_n} & \frac{\partial \Delta Q_1}{\partial |V_1|} & \cdots & \frac{\partial \Delta Q_1}{\partial |V_{n-m}|} & 0 \\ \vdots & \vdots & \vdots & \vdots & \vdots & \vdots & \vdots \\ \frac{\partial \Delta Q_{n-m}}{\partial \delta_1} & \cdots & \frac{\partial \Delta Q_{n-m}}{\partial \delta_n} & \frac{\partial \Delta Q_{n-m}}{\partial |V_1|} & \cdots & \frac{\partial \Delta Q_{n-m}}{\partial |V_{n-m}|} & 0 \end{bmatrix} \begin{bmatrix} \Delta \delta_1 \\ \vdots \\ \Delta \delta_n \\ \Delta |V_1| \\ \vdots \\ \Delta |V_{n-m}| \\ \Delta P_B \end{bmatrix} \tag{3.74}$$

The last matrix equation constitutes the modified NRPF algorithm of the distributed slack bus model.

It is worth mentioning some interesting approaches based on the distributed slack bus model, as applied in order to improve the system performance and operation. In [61] the

author utilizes the distributed slack bus theory so as to reform the OPF model and solve the economic dispatch algorithm in a poolco environment. In order to do this, several definitions are given. The most important are the following: First, the participants benefits obtained after joining the poolco operation defined as

$$B_i = F_i^{after} - F_i^{before} + \rho T_i \tag{3.75}$$

where

F_i^{after} is the total generation cost after the transaction defined by ISO for participant i
F_i^{before} is the total generation cost before the transaction ρ is the spot price of electricity defined as the minimum price offering to the market that satisfies load and generation constraints T is the transaction in terms of interchange power.

The benefit obtained by poolco operation is calculated as

$$DF_{total} = \sum_{i=1}^{GN} F_i^{before} - \sum_{i=1}^{GN} F_i^{after} \tag{3.76}$$

This difference is divided among participants, so now each participants benefit takes the form

$$B_i = -\Delta F_i + \rho T_i + K_i DF_{total} \tag{3.77}$$

where

K_i is the participation factor defined by the ISO, and $\sum_i K_i = 1$.

In distributed slack bus theory, the initially specified unique slack bus takes the form of each other participant changing its operation, since now it is concerned, like other participants, with its own benefit.

The proposed method takes as an assumption that the cost difference DF_{total} is caused by a net imbalance power during transactions operation and due to losses, and is the consequence over the whole transactions performance. By redistributing it to the participants by the use of the participation factors, a balance can be achieved between system performance and economic transactions. In that sense, every generation unit acting towards load frequency control (LFC) takes a participating term, leading to a new formulation of the generation scheduling equations as well as to a new modified load flow algorithm. The generation equation is now expressed as

$$P_{Gi} = P_{Gi}^{0} + K_i \Delta DF_{total}, \quad i = 1, 2, \cdots, GN \tag{3.78}$$

The above equation modifies the active power mismatch equation involved in the load flow algorithm, leaving the reactive power mismatch unchanged. Now the real power part of the system Jacobian in matrix form, is written as,

$$\begin{bmatrix} \Delta P_1 \\ \vdots \\ \Delta P_n \end{bmatrix} = \begin{bmatrix} \frac{\partial \Delta P_1}{\partial \delta_1} & \cdots & \frac{\partial \Delta P_1}{\partial \delta_{n-1}} & \frac{\partial \Delta P_1}{\partial DP_{total}} \\ \vdots & \vdots & \vdots & \vdots \\ \vdots & \vdots & \vdots & \vdots \\ \frac{\partial \Delta P_n}{\partial \delta_1} & \cdots & \frac{\partial \Delta P_n}{\partial \delta_{n-1}} & \frac{\partial \Delta P_n}{\partial DP_{total}} \end{bmatrix} \begin{bmatrix} \Delta \delta_1 \\ \vdots \\ \Delta \delta_{n-1} \\ \Delta DP_{total} \end{bmatrix} \tag{3.79}$$

where $\frac{\partial P_i}{\partial DP_{total}} = K_i$ is the participation factor at bus i.

The modification of the distributed slack bus formulation compared to the conventional NRPF model is that it involves not only voltage magnitude and phase angle but also active power generation participating in economic dispatch as an additional state variable that gets updated after each iteration. The generation units are updated as,

$$P_{Gi}^{t+1} = P_{Gi}^{t} + K_i \Delta DF_{total}^{t}, \quad i = 1, 2, \cdots, GN \tag{3.80}$$

The next step is the formulation of the OPF algorithm involving both equality and inequality constraints. By using the Lagrange functions optimality conditions, by defining the incremental cost as well as the incremental transmission loss, and using fast decoupled load flow formulation, the final equations of the partial derivatives (sensitivity terms) of the slack bus contribution to the other buses as well as the total transmission loss at economic dispatch are obtained.

In [62] the distributed slack bus theory is utilized for the locational marginal price calculations. Since, only PV (generation) buses are involved a new power balance equation is formulated as

$$f_i(\theta) - P_i - a_i \delta = 0 \quad for \quad i = 1, 2, \cdots, N \tag{3.81}$$

where $\theta = [\theta_1, \theta_2, \cdots, \theta_{n-1}]$ defines the voltage phase angle vector, f_i is the active power flow injections into the network which includes the contribution of power δ according to the participation factor a_i and P_i denotes the active power injection at bus i. From the above equation one easily realizes that the term $f_i(\theta)$ is the active power flow equation

that is solved iteratively with NR algorithm, while the term $P_i + a_i\delta$ is the new scheduled power including the power contribution term. By taking the Taylor series expansion the matrix form of the above equation is as follows:

$$\begin{bmatrix} \Delta p'_1 \\ \Delta p_n \end{bmatrix} = \begin{bmatrix} \frac{\partial \Delta f'}{\partial \theta} & -a' \\ \frac{\partial \Delta f'_N}{\partial \theta} & -a_N \end{bmatrix} \begin{bmatrix} \Delta\theta \\ \Delta\delta \end{bmatrix} = \begin{bmatrix} \Delta p \end{bmatrix} \tag{3.82}$$

where

$f' = [f_1, f_2, \cdots, f_{N-1}]^T$ $a' = [a_1, a_2, \cdots, a_{N-1}]^T$ $p' = [P_1, P_2, \cdots, P_{N-1}]^T$ $p = [P_1, P_2, \cdots, P_N]^T$

By defining the transmission constraints as

$$g(\theta) - g^{max} \leq 0 \tag{3.83}$$

where $g(\theta)$ is the active power flow (equality constraint) and g^{max} is its upper limit (when is binding congestion occurs

By defining the well known power transfer distribution factor (PTDF) representing the sensitivity of a power flow on a transmission line k with respect to the power injection at bus i as,

$$T = \frac{\partial g}{\partial p} = \frac{\partial g}{\partial \theta}\frac{\partial \theta}{\partial p} \tag{3.84}$$

where the phase angle sensitivities w.r.t. power injections are obtained from the inverse Jacobian matrix from equation 3.82

A modified expression of the OPF problem involving the modified power balance equation involving the participation factors and the remaining network and active power constraints is being formulated, and the Karush-Kuhn-Tucker optimality conditions result in the new form of the LMP equation,

$$\lambda_i = \lambda_0 - \lambda_0 \frac{\partial P_{loss}}{\partial P_i} - \sum_k \mu_k T_k i \tag{3.85}$$

where $T_k i$ is taken from 3.84.

The above distributed slack bus analysis is so far applied to transmission systems from where it was started. This theory can also be applied to distribution systems by simply involving all the three phases so as to capture the unbalanced nature of these distribution

network operation. References [64], [59] are among the most representative describing the distributed slack bus model for distribution networks.

3.3 Transmission and Congestion

Competitive electricity markets are based on the concept of open access transmission network, that is, a network free for all the participants, operating in a fair and equitable manner without discriminations. Since the basic participants are generation producers and load consumers, it becomes apparent that an independent system operator must play the role of the mediate in the forthcoming transactions. The ISO is responsible for ensuring the normal, secure and efficient operation of an open access transmission network. Among other things ISO has to deal with transmission congestion, transmission losses and ancillary services. Each one of the above terms defines a specific operation in the network that has impacts on electricity prices.

The physics of electric power systems [3], namely the Kirchhoffs current and voltage laws are used to solve the problem of how much electric power being moved from one node to another, flows over each of the network branches. Several factors can create limits over the transfer of power between two nodes in a transmission network, such as thermal limits, capacity limits, voltage limits and stability limits. These limits refer both to normal as well as abnormal conditions, the latter also known as contingencies.

When consumers and producers of electric energy desire to consume and produce in amounts that would cause the transmission system to operate at or beyond one or more of its abovementioned transfer limits the system is said to be congested [65]. Congestion occurs when the transmission network [66] is unable to accommodate all of the desired transactions due to a violation of system operating limits. A more analytical description of congestion is that congestion occurs whenever the system state of the grid is characterized by one or more violations of the physical, operational, or policy constraints under which the grid operates in the normal state or under any one of the contingency cases in a set of specified contingencies. Congestion may also be caused [10] by generation or power grid outages, increase in demand, or loop flow problems. Congestion is associated with a specified point in time. As such, the problem of congestion may arise during the day-ahead dispatch, in the day-ahead market, the hourahead dispatch, in the hour-ahead market or the real time operations of the system, in the balancing market.

An evident impact of congestion to the market participants is the additional cost resulting from all the restrictions that have to be taken into account. In an uncongested

electricity market the auction-based market clearing price is unique among all the participants, is the same for all transmission nodes either it is a generator or load node therefore it is the price that consumers pay to the producers. On the contrary in a congested system this equilibrium condition is no more valid, so prices are completely different from node to node, depending on how congested is the network. Those additional costs result in a new network condition where consumers pay more money to the network than the money paid back to the producers, resulting in a net income or surplus for the system operator.

Congestion management [10] is one of the critical operations the ISO has to handle, that is, to control the transmission system so that transfer limits are observed. This means setting a set of rules accepted by all participants in order to ensure sufficient control over generation suppliers and load consumers so as to maintain an acceptable level of security and reliability in both the short-term (real-time operation) as well as the long term (transmission and generation construction) while maximizing market efficiency. One can say that congestion management is the process that ensures the delivery of all the power transactions between sellers and buyers without any violation on the operating limits of the transmission system. Since congestion management is a critical set of operations performed by the ISO, it must be solved in real-time operation of an electricity market.

Several methods have been proposed over the years in order to handle congestion and provide congestion relief. Numerous papers can be found in the literature for each one of the following congestion management methods. These methods have been surveyed in [67] and are classified into the following general categories

1. Sensitivity factors based methods
2. Auction based congestion management
3. Pricing based methods
4. Re-dispatch and willingness-to-pay methods
5. Congestion cost allocation methods

Several algorithms have been presented for congestion management in literature papers like in [34] and [68] where three methods are the most commonly used, namely 1. Use of available resources such as operation of FACTS controllers, rescheduling of generation etc. 2. Providing the timely information regarding the probability of having a particular line congested and economic incentives to system users to adjust their requests

and remain within the system constraints. 3. Physically curtailing the transactions. The authors of this paper propose the second method as the basis of a simple method for congestion management based on an idea of the so-called congestion zones/clusters, obtained with a set of transmission congestion distribution factors (TCDFs), which are described as the change in real and/or reactive power flow in a transmission line connected between two buses when a unity (1MW) power is injected at the first bus the so-called sending bus. The meaning is that when a new incremental injection of unity power is produced in a generator connected to a bus this power is going to be distributed through all the lines connecting the particular bus with their adjacent buses. This distribution is then characterized by proper factors defining the percentage of this unity injected power among the connecting lines power flows. This mechanism is quite useful when a line is congested and thus outaged, since then, the necessary redistribution of the unity injected power is described by reformulation of the TCDFs. The TCDFs are calculated by defining the real and/or reactive AC power flow in a line connecting two buses , and taking, using the Taylors series approximation (ignoring the higher order terms), the partial derivatives of the power with respect to the state variables, namely the voltage magnitude and angle of the connected buses. A Newton-Raphson Jacobian relationship is formulated by the equations of the sensitivities and either in full AC or decoupled form the TCDFs expressions are derived. The proposed AC load flow sensitivity based methods are more accurate compared to the DC load flow based methods. The determination of the TCDFs is utilized for identifying different congestion zones/-clusters for a given system. This clustering technique provides a suitable congestion management scheme since not all connecting lines contribute the same to the congestion occurrence (dependent on the TCDFs values). An optimization algorithm can, therefore, be formulated in order to redispatch the congestion management in the form of changing the generation scheduling as well as the load demand timing. In other words, the market administrator can post the information of congested zones/clusters so that the market participants can bid and adjust their outputs for congestion management, accordingly.

As already mentioned electricity pricing is a very important task the ISO has to deal with, since the energy prices computed reflect the final end-user prices that consumers have to pay on retailers, distributors or even generators, according to the contracts made (pool market contracts, or bilateral). A power flow techniques have been used for transmission cost calculation and allocation, among them, AC flow sensitivity, Full AC Power Flow Solution and Power flow Decomposition are the most representative. In AC Flow sensitivity method [], the sensitivities (partial derivatives) of transmission line flows w.r.t. to the bus power injections are computed from AC power flow models using the same logic as in the DC power flow derivation of distribution factors. In Full AC

power flow solution [] two cases are examined. One is the base case with no transaction included, the other is when all transactions are included. Each case is evaluated by the proper AC load flow algorithm. Concerning each transaction separately, a two power flow algorithm is also used. One for the transaction itself, and the second when all other transaction except the one mentioned before, are included. The results of each simulation are compared with the base case (no transactions) and safe conclusions can be obtained relative to the impacts of each transaction case on the system operation, concerning both marginal and incremental prices. From these results, a distribution of the MW/MVAR line flows for each transactions is being performed. Finally, in Power Flow Decomposition [], the network flows are decomposed into components that are related to individual transactions and one more interaction component is added to account for the non-linearity of power flow models. One such component associated with transactions is the voltage phase angle which can be closely related to line flow transactions by utilizing the DC load flow model [69].

The congestion modeling and analysis lies in the optimal power flow study which as an optimization procedure is capable of solving multiple tasks. Among others the OPF algorithm calculates the prices of energy [70] over all the nodes of the system. A mathematical formulation of a Lagrange function consisting of the original objective function plus all the equality and inequality binding/active constraints, including the power flow balance equation, multiplied with appropriate multipliers called the Lagrange multipliers is the tool for calculating prices. It is crucial for every active constraint to have a Lagrange multiplier associated with it.

Applying the Karush-Kuhn-Tucker optimality conditions in the form of the derivatives of the Lagrange function with respect to variable terms, the prices for the various network operations are computed. Essentially the Lagrange multiplier is the negative of the derivative of the function that is being optimized with respect to the enforced constraint. The Lagrangian multipliers provide economic signals to either enforcing a constraint or relieving it. The greater impact a constraint has on the objective function the greater the potential improvement on generation costs or social welfare will be. Especially for the power flow balance equality constraint, the Lagrange multiplier can be computed either as the derivative of the total cost with respect to an increase in zonal/locational load or, as the derivative of the Lagrange function with respect to the generation power.

If the system is uncongested the relevant Lagrange multiplier can be defined as the instantaneous price of the next small increment of load or simply the market clearing unique price equal for all zones or locations in the form of buses/nodes of the system. Consequently this price is, in a generic way, the locational marginal price. This is the price that clears the market auction negotiations. In other words, in an uncongested

electricity market the auction-based market clearing price is unique among all the participants, its the same for all transmission nodes either if it is a generator or load node therefore it is the price that consumers pay to the producers. In a full AC power flow, even in the case of no congestion, the locational marginal prices throughout the network may be different due to transmission losses. The difference between zone/location prices equals the value of marginal losses between zones/locations.

However, if the system is congested with respect to every active constraint the Lagrange multiplier of the equality power flow constraint is no more, the unique market marginal clearing price. By applying the same optimality conditions it results that the Lagrange multipliers for the inequality constraints participate additionally in the formulation of the locational marginal price. In simple words, when congestion is faced during system operation the prices vary throughout the entire network dependent on the original marginal price plus the price associated with congestion. The binding constraints price associated to congestion is also called the shadow and can be defined as the maximum dispatch cost savings, under optimal dispatch that can be achieved due to an incremental unit increase in the lines flow capacity constraint without violating any of the binding transmission constraints. Clearly only lines operating at the limit have positive shadow prices. Under the locational marginal pricing approach the independent system operator (ISO) calculates power dispatch schedules by maximizing the social welfare function within the available network capacity. The price of energy at a location is determined by the rate of decrease of optimal social welfare with respect to the fixed load increase at that location.

3.3.1 Transmission pricing

Since the power flow is inherent to the optimal power model, it is evident that it plays a significant role in the calculation of electricity transmission pricing. Several publications are dealing with comparative analyses of AC and DC power flow models and their impacts on the derivation of locational marginal pricing. To mention some of them, [71] is a former paper that proposes a DC power flow algorithm, due to its linearity approximation to calculate transmission congestion and pricing, in order to offer a congestion management pricing method, falling in the third category from the above mentioned.

In [72] the authors are presenting an analytical formulation of the whole transmission pricing aspect by deriving equations, cost functions, Lagrange functions, physical constraints concerning the basic transfer limits (neglecting stability constraints) and finally through the appropriate Lagrange multipliers, the locational marginal prices for three different models of power flow, namely the full structured AC power flow, derivation of

the full structured DC power flow and finally derivation of the reduced form DC power flow. Apart from that, an attempt is made towards derivation of LMP and LMP components based on OPF models, the LMP definition and the envelope theorem. Finally the LMP decomposition formulas (neglecting power losses) are derived and explained. As already mentioned the OPF model handles only the simple economic dispatch problem with the generation cost function as the objective function to be minimized. The analysis shows the involvement of generation shift factors in LMP calculation and concludes with the results of congestion impacts on LMP derivation (additional costs). By analyzing the three OPF formulas, also presenting them with examples, illustrates that LMP solution values derived for the full-structured DC OPF model are the same as those derived for the reduced-form DC OPF model.

A comparison between a DCOPF and a ACOPF are presented in [36]. A DCOPF including transmission losses is proposed where the losses computation and congestion price calculation involve the proper sensitivity factors, namely delivery factors and generation shift factors. The DCOPF is compared to an ACOPF model including the well known active and reactive power balance equations as equality constraints and the line flow, generation real and reactive power limits as inequality constraints. Simulation results show that although, the iterative DCOPF may generate LMP very close to the LMP from the ACOPF representing the real-time dispatch, for most of the cases in various loading levels, significant errors of DCOPF may be caused due to its inherent linearization that could lead to a step change at a particular loading level. The change may switch the marginal units and hence cause significant LMP errors. DCOPF can also generate errors when the line resistance to reactance ratio grows especially in the generation dispatch.

The difference between the LMPs of two adjacent nodes is the congestion cost or rent. This is why the consumer pays more money than the generator is paid. The congestion leads to a net surplus for the system operator. In the case of congestion the increase in load in a location may not come from the lowest cost generator due to the fact that a contingency or a transfer limit prevents the generation from increasing.

3.3.2 Loop Flows

The power flow in a meshed grid distributes in such a way that every change in generation, load or transmission capacity affects the flow of the entire network. This phenomenon is known as loop flows. Loop flow [73] occurs when some portions of a scheduled power are distributed into other branches adjacently connected. It is a consequence of the electric system physical behavior that is basically governed by Kirchhoffs law and

not by financial contractual arrangements between the electricity market participants. It is mathematically defined as the difference between the scheduled transaction and actual loading of the line connecting two adjacent buses. The loop flow behavior of a system mainly depends on the network topology. Loop flow is the consequence of the transmission pricing performed by the use of optimal power flow economic dispatch. It means that power flows from a high price bus to a low price bus. Loop flows describe in general, the benefit or cost imposed on other market players when one market player changes supply or demand or the transmission capacity of a line. Locational marginal pricing and transmission congestion are the main aspects that are responsible for the loop flow impacts on the transmission network. Loop flow analysis is carried out by using the linear DC load flow model due to its simplification without loosing accuracy, compared to the nonlinear AC model. The amount of loop flow along a line depends on the physical parameters of the network which are the line impedances. The line impedance between two buses is determined by its length, number of parallel paths, voltage level and number of series elements like transformers. The paper also deals with the operational impacts of loop flow control devices such as power electronics thyristor controlled series capacitors on financial transmission rights congestion rentals. In short, the paper concludes that loop flow always occur in interconnected loop networks. As long as there is a constrained line, nodes within the loop could experience volatile nodal prices (LMP), thus creating different congestion charges and FTR allocations.

3.3.3 Transmission Rights

As already mentioned transmission nodal pricing gives different locational prices over the nodes if the system is congested. The adjusted nodal prices are higher at consumer locations than at resources locations. That is, the bus nodal differences lead to increased payments from buyers to the ISO, more than the money paid by the ISO to suppliers. In [74], Hogan suggests that this extra net income to the ISO can be the source of a system of contract network rights. The idea behind contract network rights is to provide a mechanism to control the financial risks of congestion-induced price variations. In other words, a contract right is intended to provide the right holder with access from one node in the network to another, that is, it is the right to inject power at one node and withdraw it at another. That is the most usual FTRs are also called point to point transmission rights. The specific paper by Hogan is the most representative of the auction-based congestion management schemes.

Since this may not be physically possible, due to Kirchhoffs physical laws restrictions, the right holder may be paid in a form of a compensation rent due to the inability to use the entire right. Furthermore, since the right holder has already purchased the right to

transmit power from one bus to another, he is paid back for expense for any congestion charges he must pay under nodal pricing. The concept behind this is, that right holders should not pay congestion charges because they have paid in advance by purchasing the contract right, and that right holders are indifferent between physical delivery and financial compensation. In other words, an FTR generates payments to the right holder that in effect refund some of, all of, or more than the users congestion expenses. In that sense, financial rights have the advantage of enabling complete decoupling between the actual dispatch and the settlement of congestion charges.

Chapter 4

Synopsis

4.1 Synopsis

The present thesis is focused on the power flow problem which constitutes one of the most well established, however, quite challenging research topic of the power system analysis. This is reasonable, since it is the most widely used identification tool for solving the physical variables which via Kirchhoff's and Ohm's law, characterize the normal steady-state electric system operation. Based on the above fact, this thesis attempts a literature review of the power flow model and related algorithms, found for almost 20-30 years period. The power flow problem is presented in its conventional polar formulation as well as in its rectangular one, both concerning the power mismatch Newton-Raphson iterative method utilized for solving it. Alternative forms, like the current mismatch NRPF and its combinations, simplified forms like the Fast-Decoupled Load Flow and DC Load Flow, combinations of both power and current mismatch methods, several forms of attractive extensions or modifications, are, in our belief, been explained and analyzed in a thorough manner. Moreover, new attractive research fields like microgrids and smartgrids closely related to the distribution systems power flow model are also presented. Finally, recently proposed methods for modifying the power flow problem making it more easier to be solved are also presented

4.1.1 Highlights

A literature review, always offers the ability for the interested reader, to focus on specific issues, that in his opinion are the most interesting in terms of challenge for future research.

In that sense, several aspects can arise by the reading of a power flow review. Considering the power flow engagement in other types of models and algorithms, (optimal power flow, sensitivity analysis, contingency analysis, machine stability and so on), it is almost evident that it is a highlight by itself.

A quite interesting point is the evolution of the method through decades, in which, the basic power flow model initially introduced for small to medium sized networks, has resulted to a powerfull tool for large scale electric grids steady state analysis. The method has passed from the conventional form, to many other simplified, modified, augmented, extended forms, all aiming at making it the most efficient and effective. The presentation of such methods, in this thesis, can not be viewed terminated, since a lot other interesting aspects will be discussed in the future. In our opinion the most appealing topics that, at one hand might offer valuable solutions, while at the other are designated for future research and development, are:

- The distributed slack bus model, which already seems to gain research attention, since European projects are focused on that. This thesis, only presented the basic idea of the method, its source of development, but in no sense, has made a very insightfull view to it. However, in our opinion, the brief description of the method and the presentation of only a few of its applications, is quite indicative of the future prospects that might offer. It is a belief that distributed slack bus method can be incorporated in solving local power flow problems. This method could potentially be utilized for solving boundary conditions where transmission interacts with distribution systems, especially in the form of microgrids operating interchangeably.

- The different kinds of combinations of the AC and DC load flow especially for problems that need a complex management, like the new electricity market configuration, where new variables affecting grid performance must be evaluated. High dimensionality of the new reformed electric power grid may unavoidably impose mixed power flow solvers for complex power flow problems. Mixed AC and DC power flow solvers could also be used for integration of transmission to distribution systems.

- The combination of direct plus iterative techniques for solving distribution systems power flow seems also encouraging results. This may be considered as a mix of the advantages of both methods for effective solving.

- Augmented forms of power flow that have already been utilized so as to provide a solution to different kind of problems, like islanded microgrid operation, generation redispatch, power control device incorporation, among others, can be viewed as

quite promising alternatives of involving other parameters for different problems configuration, like price control models.

- Despite the fact that microgrids and smartgrids have not been discussed analytically so far, their importance is indisputable, if one considers that they are the core of the reformed electrical grid. This reformed grid, based on the electricity market deregulation, has made distribution systems quite more attractive than transmission systems which had gained more attention so far. Although not fully analyzed, distribution systems power flow, has already become a state-of-the-art for deregulated electricity power grids. Electric grid reform is responsible for distribution systems modification from a radial to a meshed, initially weakly meshed, network. In that sense traditional and modern power flow algorithms can be included in power systems analysis projects.

4.1.2 Future Research

It is already mentioned, in this thesis main body, that the power flow problem could not possibly be covered in great extent during this literature review. Specific topics are selected for future analysis, although a brief description is already presented.

The power flow problem has been solved by iterative methods like the Newton-Raphson or the Gauss-Seidel. However, in terms of numerical analysis, the problem utilized so far, direct methods based on Gauss elimination processes, like LU triangular factorization, or UDU^T factorization to give appropriate solutions. Additionally matrix reordering techniques, and other similar methods were also utilized for cost savings in terms of computational burden. However, high dimensionality of the reformed electric grid, has led to network topologies (especially in distribution systems) approximated with millions of nodes, lines and elements. In such a network high dimensionality, the aforementioned direct techniques seem to face severe convergence problems. This imposed the use of other techniques, with strong iterative characteristics able to handle such systems. These kinds of techniques will be analyzed in future research.

From the numerical analysis viewpoint, one of the major aspects for future research consists of the Krylov subspace iterative methods for solving real world large to huge scale electric power systems containing thousands to million of nodes. Although Krylov methods have a long history in computational analysis starting from the introduction of steepest descent method and its consequent, conjugate gradient method (CG), the most recently developed methods like generalized minimal residual (GMRES) and improvements of the aforementioned ones, like BiCG, MinREs and others have gained a remarkable attention since they proved to be ideal candidates for solving power flow

problems, while simultaneously offering convergence, computation time reduction and accuracy.

The most promising of Krylov methods, namely the Conjugate-Gradient (CG) and the Generalized Minimal REsidual (GMRES) either in conventional or in extended form, have already offered good results, tested in high dimensional electric power systems, numbering millions of nodes. However, there is an open field of study and research. The design and implementation of more effective matrix preconditioners that allow improved computational performance of the linearized Jacobian matrix power flow is a quite interested area of numerical analysis of electric power systems. Preconditioners that take advantage of the network topology characteristics may provide effective as well as accurate solution with computation cost reduction, and this is an appealing area for our future research. New preconditioner design could offer valuable algorithms for commercial power flow software implementation, since most of the existing software tools are still working based on already well-established but not robust numerical techniques.

From the electrical engineering viewpoint, the extension of the power flow problem to the lowest voltage level, that is, inside the building aiming at the appliance, a possible combination of the building power flow with the electrical installation, and the possible engagement of price control model in an augmented power flow formulation, can be viewed as challenging approaches.

Distributed generation in terms of renewable resources will unavoidably bring uncertainty in power system analysis. Stochastic load flow analysis involving renewable sources, microgrid structures and uncertain load demand due to variation in consumer profile, changing almost in real time, is a good candidate for searching robust power flow solvers, capable to react flexibly when provocative conditions may occur, especially in a case scenario where nearby microgrids operate either in islanded mode or in an interchangeable mode sending/receiving energy with each other.

The integration of transmission and distribution systems is one more challenging aspect for future study. Until now, independent system operators (ISO's) typically handle this integration in terms of single loads aggregating distribution networks and microgrids. A slack bus models the highest level of a distribution system where all the loads are aggregated. A reasonable question arises then, of how these possible large number of slack buses interact with the transmission buses, namely the different kinds of PQ or PV buses. In our knowledge, so far, none of the open source or commercially software tools solving power systems, are incorporating both transmission and distribution systems. Many ISOs have indicated the need for more analytical modelling tools of the interaction between thw two subsystems with a simulation tool that could evaluate in real time operation. The engagement of transmssion to the conventional distribution system is

more or less knwon and tested for a long period of time. However, the deployment of distributed energy resources with stochasticity (wind energy), will increase systems complexity and consequently the error in load forecasting. Additionally, there are issues that limit the transmission/distribution integration,namely single phase modelling of transmission versus three phase modelling for distribution system, transmission balanced versus distribution unbalanced network nature, and so on. All these can potentially affect the power flow problem, addressing either new power flow solvers, or different power flow forms for the distribution and transmission systems, even new bus identification for the boundaries between the two subystems.

Finally, local solution of the power flow problem, that is, calculation of only a few buses voltages among the entire set of nodes, that is a local limited power flow via the random walk algorithms already implemented and tested in electronic power grids, and the consequent Monte-Carlo simulation, can become promising in high voltages electric networks, offering computation time reduction, while simultaneously offering locality in power flow calculations. Random walk algorithm, inspired by statistics and the theory of large numbers, seems quite attractive for solving problems in terms of locality, that is, it offers the opportunity to solve for small portions even an individual node instead of the large even huge networks globally. Building power flow, causing only small changes to the nearest substation buses, or more generally certain load demand changes at certain buses, could potentially require such local power flow analysis. This leads to fast and, even approximate, yet accurate solutions in terms of accuracy-runtime tradeoff, and computational time. Test cases based on the circuit DC analysis give encouraging results. However, there seems to be an open field for research and implementation of random walk algorithms in full AC system analysis. Finally random walk algorithms are capable of operating in parallel computing. The computations for different nodes or even random walks for the same node can be carried out independently on different processors. Since random walk algorithms are based on the concept of nodes with known voltage values, that is the slack bus for conventional power flow problems, it is our belief that the distributed slack bus model developed for distribution systems initially, and transmission system on the following, could become a very helpful assistance.

As a conclusion, the high dimensionality inherent to the new form of electric power grid, is enough reason for searching new patterns of the power flow problem, new and more efficient power flow solution methods for faster and more accurate computation almost in real time.

Appendix A

Appendix Title Here

Write your Appendix content here.

Bibliography

[1] R. Idema. Newton-krylov methods in power flow and contingency analysis, November 2012.

[2] Arthur R. Bergen and Vijay Vittal. *Power Systems Analysis 2nd ed.* Prentice Hall, 2000. ISBN 978-0136919902.

[3] John Grainger and William D. Stevenson. *Power System Analysis.* Mc-Graw Hill, 1994. ISBN 978-0070612938.

[4] Prabha Kundur. *Power System Stability and Control.* Mc-Graw Hill, 1994. ISBN 978-0070359581.

[5] Goran Andersson. Modelling and analysis of electric power systems. Technical report, ITET ETH Zurich, 2012.

[6] Hadi Saadat. *Power System Analysis.* PSA Publishing; THIRD EDITION, 2010. ISBN 978-0984543809.

[7] John J. Grainger and William D. Stevenson. *Power System Analysis.* Mc-Graw Hill, 1994. ISBN 978-0070612938.

[8] Xi-Fan Wang, Yonghua Song, and Malcolm Irving. *Modern Power Systems Ananysis.* Springer, 2009. ISBN 978-0387728520.

[9] J Duncan Glover and Mulukutla S Sarma. *Power System Analysis and Design.* Brooks/Cole Publishing Co., Pacific Grove, CA, USA, 3rd edition, 2001. ISBN 0534953670.

[10] Antonio Gomez-Exposito, Antonio Conejo, and Claudio Canizares. *Electric Energy Systems Analysis and Operation.* Taylor & Francis Group, 2009. ISBN 978-0-8493-7365-7.

[11] Jizhong Zhu. *Optimization of Power System Operation.* John Wiley & Sons, Inc., Hoboken, NJ, USA, July .

[12] A.G. Exposito and E.R. Ramos. Augmented rectangular load flow model. *IEEE Transactions on Power Systems*, 17(2):271–276, May 2002. ISSN 0885-8950.

[13] Rainer Bacher and Eric Bullinger. Application of non-stationary iterative methods to an exact newton-raphson solution process for power flow equations. In *Power Systems Computation Conference*, pages 453–459.

[14] V.M. da Costa, N. Martins, and J.L.R. Pereira. Developments in the newton raphson power flow formulation based on current injections. *IEEE Transactions on Power Systems*, 14(4):1320–1326, 1999. ISSN 08858950.

[15] P.A.N. Garcia, J.L.R. Pereira, S. Carneiro, V.M. da Costa, and N. Martins. Three-phase power flow calculations using the current injection method. *IEEE Transactions on Power Systems*, 15(2):508–514, May 2000. ISSN 08858950.

[16] V.M. da Costa, J.L.R. Pereira, and N. Martins. An augmented newtonraphson power flow formulation based on current injections. *International Journal of Electrical Power & Energy Systems*, 23(4):305–312, May 2001. ISSN 01420615.

[17] V. M. da Costa and A. L. S. Rosa. A comparative analysis of different power flow methodologies. In *2008 IEEE/PES Transmission and Distribution Conference and Exposition: Latin America*, pages 1–7. IEEE, August 2008.

[18] S. Kamel, M. Abdel-Akher, and F. Jurado. Improved NR current injection load flow using power mismatch representation of PV bus. *International Journal of Electrical Power and Energy Systems*, 53(1):64–68, December 2013. ISSN 01420615. doi: 10.1016/j.ijepes.2013.03.039. URL http://www.scopus.com/inward/record.url?eid=2-s2.0-84877771061&partnerID=tZOtx3y1.

[19] Shrirang Abhyankar, Qiushi Cui, and Alexander J. Flueck. Fast power flow analysis using a hybrid current-power balance formulation in rectangular coordinates. In *IEEE Transmission and Distribution Conference and Exposition*, Chicago IL,, 2014. IEEE.

[20] Thanatchai Kulworawanichpong. Simplified newtonraphson power-flow solution method. *International Journal of Electrical Power & Energy Systems*, (6):551–558, July . ISSN 01420615.

[21] Sourav Mallick, D.V. Rajan, S.S. Thakur, P. Acharjee, and S.P. Ghoshal. Development of a new algorithm for power flow analysis. *International Journal of Electrical Power & Energy Systems*, (8):1479–1488, October . ISSN 01420615.

[22] Mevludin Glavic and Fernando L. Alvarado. An extension of newtonraphson power flow problem. *Applied Mathematics and Computation*, 186(2):1192–1204, March 2007. ISSN 00963003.

[23] Ramiah Jegatheesan, Nursyarizal Mohd Nor, and Mohd Fakhizan Romlie. Newton-raphson power flow solution employing systematically constructed jacobian matrix. In *2008 IEEE 2nd International Power and Energy Conference*, pages 180–185. IEEE, December .

[24] L. Wang and X.R. Lin. Robust fast decoupled power flow. *IEEE Transactions on Power Systems*, (1):208–215. ISSN 08858950.

[25] S.C Lee and K.B Park. Flexible alternatives to decoupled load flows at minimal computational costs. *International Journal of Electrical Power & Energy Systems*, (4):319–326, May . ISSN 01420615.

[26] E. Chandrasekharan, M.S.N. Potti, R. Sreeramakumar, and K.P. Mohandas. Improved general purpose fast decoupled load flow. *International Journal of Electrical Power & Energy Systems*, (6):481–488, August . ISSN 01420615.

[27] Adriano Aron F. de Moura and Ailson P. de Moura. Newton-raphson decoupled load flow with constant matrices of condutance and susceptance. In *2010 9th IEEE/IAS International Conference on Industry Applications - INDUSCON 2010*, pages 1–6. IEEE, November 2010.

[28] B. Stott, J. Jardim, and O. Alsac. Dc power flow revisited. *IEEE Transactions on Power Systems*, (3):1290–1300, August . ISSN 0885-8950.

[29] Shuai Lu, Ning Zhou, Nirupama Kumar, Nader Samaan, and Bhujanga Chakrabarti. Improved DC power flow method based on empirical knowledge of the system. *IEEE PES Transmission and Distribution Conference and Exposition: Smart Solutions for a changing world*, pages 1–6, 2010.

[30] Thomas J. Overbye, Xu Cheng, and Yan Sun. A comparison of the ac and dc power flow models for lmp calculations. In *Proceedings of the Hawaii International Conference on System Sciences*, pages 725–734.

[31] R. Korab and G. Tomasik. Ac or dc opf based lmp's in a competitive electricity market? In *International Symposium CIGRE/IEEE PES, 2005.*, pages 61–68. IEEE.

[32] Soobae Kim and Thomas J. Overbye. Hybrid power flow analysis: Combination of ac and dc models. In *2011 IEEE Power and Energy Conference at Illinois*, pages 1–4. IEEE, February .

[33] Amir SAFDARIAN, Mahmud FOTUHI-FIRUZABAD, and Farrokh AMINIFAR. A novel efficient model for the power flow analysis of power systems. *Turkish Journal of Electrical Engineering & Computer Sciences*, 10.3906/el, 2014.

[34] Ashwani Kumar, S.C. Srivastava, and S.N. Singh. A zonal congestion management approach using ac transmission congestion distribution factors. *Electric Power Systems Research*, (1):85–93, November . ISSN 03787796.

[35] Power system analysis: Hadi saadat: 9780984543809: Amazon.com: Books.

[36] Fangxing Li, Rui Bo, and Wenjuan Zhang. Comparison of different lmp calculations in power market simulation. In *2006 International Conference on Power System Technology*, pages 1–6. IEEE, October .

[37] F. Milano. Continuous newton's method for power flow analysis. *IEEE Transactions on Power Systems*, (1):50–57, February . ISSN 0885-8950.

[38] Mehrdad Pirnia, Claudio A. Cañizares, and Kankar Bhattacharya. Revisiting the power flow problem based on a mixed complementarity formulation approach. *IET Generation, Transmission & Distribution*, (11):1194–1201, November . ISSN 1751-8687.

[39] D Chattopadhyay and D Gan. Market dispatch incorporating stability constraints. *International Journal of Electrical Power & Energy Systems*, 23(6):459–469, August 2001. ISSN 01420615.

[40] A.J. Conejo, F. Milano, and R. Garcia-Bertrand. Congestion management ensuring voltage stability. *IEEE Transactions on Power Systems*, 21(1):357–364, February 2006. ISSN 0885-8950.

[41] Rafael Zarate-Minano, Federico Milano, and Antonio J. Conejo. An opf methodology to ensure small-signal stability. *IEEE Transactions on Power Systems*, (3): 1050–1061, August . ISSN 0885-8950.

[42] R. Zarate-Minano, T. Van Cutsem, F. Milano, and A.J. Conejo. Securing transient stability using time-domain simulations within an optimal power flow. *IEEE Transactions on Power Systems*, (1):243–253, February . ISSN 0885-8950.

[43] J.M. Arroyo and F.D. Galiana. Energy and reserve pricing in security and network-constrained electricity markets. *IEEE Transactions on Power Systems*, 20(2):634–643, May 2005. ISSN 0885-8950.

[44] R. Baldick, B.H. Kim, and C. Chase. A fast distributed implementation of optimal power flow. *IEEE Transactions on Power Systems*, 14(3):858–864, 1999. ISSN 08858950.

[45] HyungSeon Oh. A new network reduction methodology for power system planning studies. *IEEE Transactions on Power Systems*, (2):677–684, May . ISSN 0885-8950.

[46] Brian Stott. Review of load-flow calculation methods. In *Proceedings of the IEEE*, volume 62, pages 916–929, 1974.

[47] Thomas Ackermann, Göran Andersson, and Lennart Söder. Distributed generation: a definition. *Electric Power Systems Research*, 57(3):195–204, April 2001. ISSN 03787796.

[48] Zhanle Wang, Raman Paranjape, Asha Sadanand, and Zhikun Chen. Residential demand response: An overview of recent simulation and modeling applications. In *2013 26th IEEE Canadian Conference on Electrical and Computer Engineering (CCECE)*, pages 1–6. IEEE, May .

[49] M.H. Albadi and E.F. El-Saadany. A summary of demand response in electricity markets. *Electric Power Systems Research*, 78(11):1989–1996, November 2008. ISSN 03787796.

[50] L.R. Araujo, D.R.R. Penido, S. Carneiro, J.L.R. Pereira, and P.A.N. Garcia. A comparative study on the performance of tcim full newton versus backward-forward power flow methods for large distribution systems. In *2006 IEEE PES Power Systems Conference and Exposition*, pages 522–526. IEEE, 2006.

[51] G.W Chang, S.Y Chu, and H.L. Wang. An Improved Backward/Forward Sweep Load Flow Algorithm for Radial Distribution Systems. *IEEE Transactions on Power Systems*, 22(2):882–884, 2007.

[52] M.H. Haque. A general load flow method for distribution systems. *Electric Power Systems Research*, (1):47–54, April . ISSN 03787796.

[53] K. Balamurugan and Dipti Srinivasan. Review of power flow studies on distribution network with distributed generation. In *2011 IEEE Ninth International Conference on Power Electronics and Drive Systems*, pages 411–417. IEEE, December 2011.

[54] Hongbo Sun, Daniel Nikovski, Tetsufumi Ohno, Tomihiro Takano, and Yasuhiro Kojima. A Fast and Robust Load Flow Method for Distribution Systems with Distributed Generations. *Energy Procedia*, 12:236–244, 2011. ISSN 18766102. URL http://www.scopus.com/inward/record.url?eid=2-s2.0-84555206580&partnerID=tZOtx3y1.

[55] Daniel E. Olivares, Ali Mehrizi-Sani, Amir H. Etemadi, Claudio A. Canizares, Reza Iravani, Mehrdad Kazerani, Amir H. Hajimiragha, Oriol Gomis-Bellmunt, Maryam Saeedifard, Rodrigo Palma-Behnke, Guillermo A. Jimenez-Estevez, and Nikos D. Hatziargyriou. Trends in microgrid control. *IEEE Transactions on Smart Grid*, (4):1905–1919, July . ISSN 1949-3053.

[56] Farid Katiraei, Reza Iravani, Nikos Hatziargyriou, and Aris Dimeas. Microgrids management. *IEEE Power and Energy Magazine*, (3):54–65, May . ISSN 1540-7977.

[57] Leonardo Rese, Antonio Simoes Costa, and Aguinaldo S. e Silva. A modified load flow algorithm for microgrids operating in islanded mode. In *2013 IEEE PES Conference on Innovative Smart Grid Technologies (ISGT Latin America)*, pages 1–7. IEEE, April .

[58] Y.H. Liu, Z.Q. Wu, S.J. Lin, and N.P. Brandon. Application of the power flow calculation method to islanding micro grids. In *2009 International Conference on Sustainable Power Generation and Supply*, pages 1–6. IEEE, April .

[59] M. Venkata Kirthiga and S. Arul Daniel. Compuational techniques for autonomous microgrid load flow analysis. *ISRN Power Engineering*, 2014:12, 2014.

[60] Xi Fang, Satyajayant Misra, Guoliang Xue, and Dejun Yang. Smart grid the new and improved power grid: A survey. *IEEE Communications Surveys & Tutorials*, 14(4):944–980, 2012. ISSN 1553-877X.

[61] Ping Yan. Modified distributed slack bus load flow algorithm for determining economic dispatch in deregulated power systems. In *Proceedings of the IEEE Power Engineering Society Transmission and Distribution Conference*, number WINTER MEETING, pages 1226–1231.

[62] T. Wu, M. Rothleder, Z. Alaywan, and A.D. Papalexopoulos. Pricing energy and ancillary services in integrated market systems by an optimal power flow. *IEEE Transactions on Power Systems*, (1):339–347, February . ISSN 0885-8950.

[63] D. Kirschen, R. Allan, and G. Strbac. Contributions of individual generators to loads and flows. *IEEE Transactions on Power Systems*, (1):52–60. ISSN 08858950.

[64] Shiqiong Tong and Karen Nan Miu. A participation factor model for slack buses in distribution systems with dgs. In *Proceedings of the IEEE Power Engineering Society Transmission and Distribution Conference*, pages 242–244.

[65] R.D. Christie, B.F. Wollenberg, and I. Wangensteen. Transmission management in the deregulated environment. *Proceedings of the IEEE*, 88(2):170–195, February 2000. ISSN 0018-9219.

[66] F. Hussin, M. Y. Hassan, and K. L. Lo. Transmission congestion management assessment in deregulated electricity market. In *2006 4th Student Conference on Research and Development*, pages 250–255. IEEE, June .

[67] Ashwani Kumar, S.C. Srivastava, and S.N. Singh. Congestion management in competitive power market: A bibliographical survey. *Electric Power Systems Research*, (1-3):153–164, September . ISSN 03787796.

[68] A. Kumar, S.C. Srivastava, and S.N. Singh. A zonal congestion management approach using real and reactive power rescheduling. *IEEE Transactions on Power Systems*, (1):554–562, February . ISSN 0885-8950.

[69] M. Oloomi-Buygi and M. Reza Salehizadeh. Considering system non-linearity in transmission pricing. *International Journal of Electrical Power & Energy Systems*, (8):455–461, October . ISSN 01420615.

[70] H. Suzuki, T. Wachi, and Y. Shimura. Components of nodal prices for electric power systems. *IEEE Transactions on Power Systems*, (1):41–49. ISSN 08858950.

[71] T.W. Gedra. On transmission congestion and pricing. *IEEE Transactions on Power Systems*, 14(1):241–248, 1999. ISSN 08858950.

[72] Haifeng Liu, Leigh Tesfatsion, and A. A. Chowdhury. Locational marginal pricing basics for restructured wholesale power markets. In *2009 IEEE Power & Energy Society General Meeting*, pages 1–8. IEEE, July .

[73] Chin Choo, Nirmal-kumar Nair, and Bhujanga Chakrabarti. Impacts of loop flow on electricity market design. In *2006 International Conference on Power System Technology*, pages 1–8. IEEE, October 2006.

[74] William W. Hogan. Contract networks for electric power transmission. Technical report, MIT.